AD-A154 128 ONE DIMENSIONAL MODEL HINDCASTS OF WARM ANOMALIES IN TH NORTH PACIFIC OCEAN(U) NAVAL POSTGRADUATE SCHOOL MONTEREY CA B J JARAMILLO DEC 84 1/1

UNCLASSIFIED F/G 8/10 NL

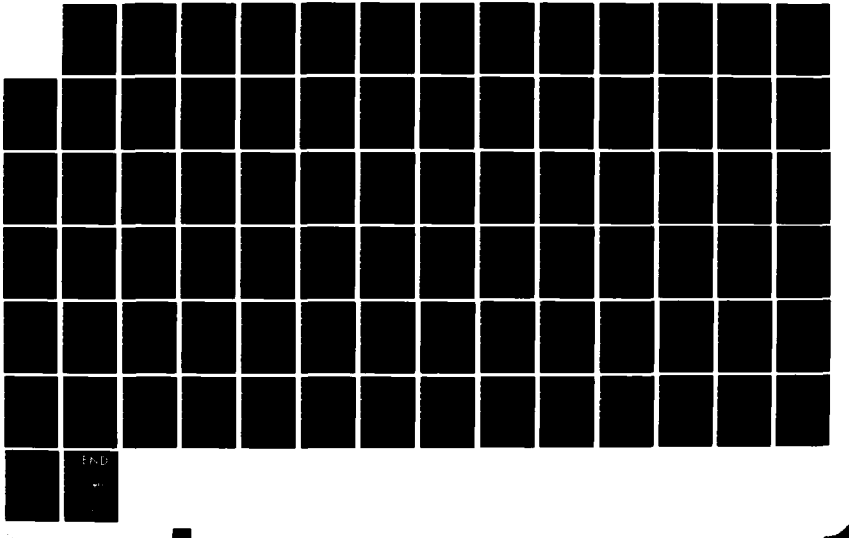

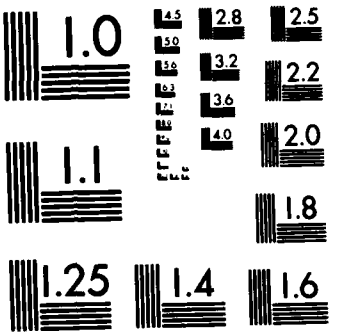

NAVAL POSTGRADUATE SCHOOL
Monterey, California

THESIS

ONE DIMENSIONAL MODEL HINDCASTS OF WARM ANOMALIES IN THE NORTH PACIFIC OCEAN

by

Bernardino J. Jaramillo

December 1984

Thesis Advisor: R.W. Garwood

Approved for public release; distribution unlimited

UNCLASSIFIED

SECURITY CLASSIFICATION OF THIS PAGE *(When Data Entered)*

REPORT DOCUMENTATION PAGE	READ INSTRUCTIONS BEFORE COMPLETING FORM
1. REPORT NUMBER	2. GOVT ACCESSION NO. AD-A154128	3. RECIPIENT'S CATALOG NUMBER
4. TITLE *(and Subtitle)* One Dimensional Model Hindcasts of Warm Anomalies in the North Pacific Ocean	5. TYPE OF REPORT & PERIOD COVERED Master's Thesis December 1984 6. PERFORMING ORG. REPORT NUMBER
7. AUTHOR(s) Bernardino J. Jaramillo	8. CONTRACT OR GRANT NUMBER(s)
9. PERFORMING ORGANIZATION NAME AND ADDRESS Naval Postgraduate School Monterey, CA 93943	10. PROGRAM ELEMENT, PROJECT, TASK AREA & WORK UNIT NUMBERS
11. CONTROLLING OFFICE NAME AND ADDRESS Naval Postgraduate School Monterey, CA 93943	12. REPORT DATE December 1984 13. NUMBER OF PAGES 82
14. MONITORING AGENCY NAME & ADDRESS(if different from Controlling Office)	15. SECURITY CLASS. (of this report) Unclassified 15a. DECLASSIFICATION/DOWNGRADING SCHEDULE

16. DISTRIBUTION STATEMENT *(of this Report)*

Approved for public release; distirubition unlimited

17. DISTRIBUTION STATEMENT *(of the abstract entered in Block 20, if different from Report)*

18. SUPPLEMENTARY NOTES

19. KEY WORDS *(Continue on reverse side if necessary and identify by block number)*

North Pacific Ocean
Warm Anomalies
One-Dimensional Model Hindcasts
TRANSPAC

20. ABSTRACT *(Continue on reverse side if necessary and identify by block number)*

Hindcasts of the development, maintenance and decay of warm anomalies in the North Pacific Ocean are attempted with the Garwood one-dimensional ocean mixed layer model. Monthly temperature analyses from the North Pacific Ocean Experiment (NORPAX) provide the initial and verifying fields, and the atmospheric forcing is derived from FNOC archived analyses.

DD FORM 1 JAN 73 1473 EDITION OF 1 NOV 65 IS OBSOLETE
S N 0102-LF-014-6601

UNCLASSIFIED
SECURITY CLASSIFICATION OF THIS PAGE *(When Data Entered)*

Large systematic errors in the anomaly hindcasts during the early summer are apparently due to erroneous surface heat flux specifications. Variations of the heat flux corrections proposed by Elsberry et al. (1982) are extensively tested for one warm anomaly development period. The climatology of Wyrtki (1967) is the heat flux specification most successful in simulating the observed anomaly patterns. The hindcasts demonstrate the importance of an accurate heat flux specification for correct prediction of warm anomalies.

Approved for public release; distribution is unlimited.

One Dimensional Model Hindcasts of Warm Anomalies in the North Pacific Ocean

by

Bernardino J. Jaramillo
Lieutenant Commander, United States Navy
B.S., University of Utah, 1975

Submitted in partial fulfillment of the
requirements for the degree of

MASTER OF SCIENCE IN METEOROLOGY AND OCEANOGRAPHY

from the

NAVAL POSTGRADUATE SCHOOL
December 1984

Author: Bernardino J. Jaramillo

Approved by: R.W. Garwood, Thesis Advisor

R.L. Elsberry, Second Reader

C.N.K. Mooers, Chairman,
Department of Oceanography

John N. Dyer,
Dean of Science and Engineering

ABSTRACT

Hindcasts of the development, maintenance and decay of warm anomalies in the North Pacific Ocean are attempted with the Garwcod one-dimensional ocean mixed layer model. Monthly temperature analyses from the North Pacific Ocean Experiment (NORPAX) provide the initial and verifying fields, and the atmospheric forcing is derived from FNOC archived analyses. Large systematic errors in the anomaly hindcasts during the early summer are apparently due to erroneous surface heat flux specifications. Variations of the heat flux corrections proposed by Elsberry et al. (1982) are extensively tested for one warm anomaly development period. The climatology of Wyrtki (1967) is the heat flux specification most successful in simulating the observed anomaly patterns. The hindcasts demonstrate the importance of an accurate heat flux specification for correct prediction of warm anomalies.

TABLE OF CONTENTS

LIST OF FIGURES

I. INTRODUCTION

A. PURPOSE AND HYPOTHESIS

The purpose of this study is to test the applicability of the Garwood (1977) one-dimensional bulk mixed layer model for hindcasting the warm ocean thermal anomalies found in the Anamoly Dynamics Study (ADS) domain. Descriptions of several warm anomalies suitable for this study are found in Elsberry (1984).

Stringer (1983) conducted a similar study which involved cold anomalies in the ADS domain. He found that the Garwood model does a good job of hindcasting cold anomalies in the fall-winter period but experiences larger errors in the spring-summer period. Stringer suggests that uncertainties in the heat flux correction fields are fairly large in the spring and summer and limit the ability of the model to hindcast anomalous ocean conditions during those seasons. Therefore, a second purpose for this study is to further examine the heat flux correction fields and to uncover factors which may affect the ability of the model to hindcast in the spring and summer.

Three warm anomalies have been chosen for this study that should satisfactorily test the Garwood model for the spring and summer conditions. The first case involves a warm anomaly starting in January 1976 and ending in July 1976. The next two anomalies extend from June 1977 to December 1977 and June 1978 to November 1978. The time periods of these anomalies should adequately test all aspects of the Garwood model for the spring and summer hindcasts.

B. STUDY DESCRIPTION

The North Pacific Ocean Experiment (NORPAX) ADS area (Figure 1.1) is the region examined in this study. The

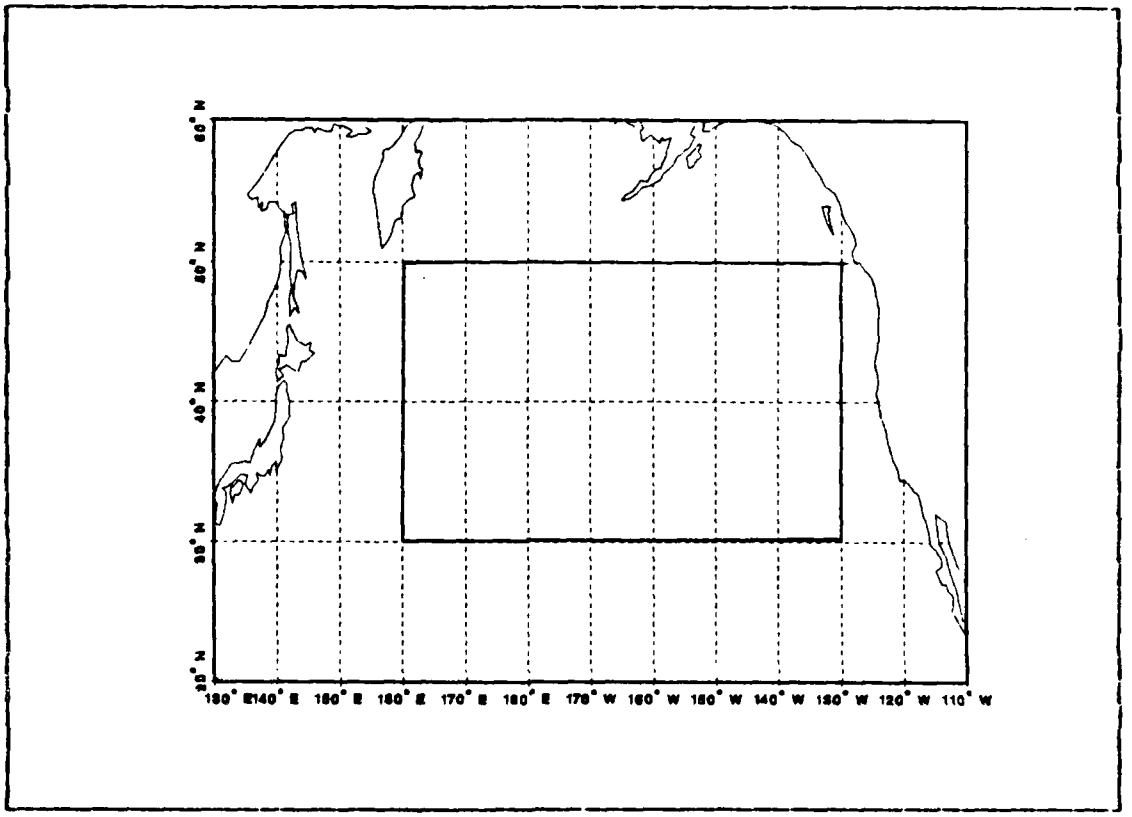

Figure 1.1 ADS REGION.

region is bounded by 30N-50N and 130W-160E. Analyses of ships-of-opportunity expendable bathythermographs (XBT) provide ocean thermal structure fields on space scales of thousands of kilometers and time scales of one month (White and Bernstein, 1979). The TRANSPAC analyses provide the initial data for the ocean prediction model and also serve as validation fields.

As briefly described in section A, three warm anomaly periods are examined in this study. The first set of warm

anomalies (WA 1/2) occurs during winter (January 1976) and continues through July 1976. The second set of warm anomalies (WA 12/13/15) are part of a large-scale pattern which developed during the summer (June 1977 to December 1977). The third set from June 1978 to November 1978 contains an extreme, near-surface warm anomaly (WA 23) that forms near the western boundary of the domain. All three anomaly cases provide excellent examples for the model hindcast studies recommended by Stringer (1983).

II. DATA SOURCES AND PREPARATION

A. DATA SOURCES

Fleet Numerical Oceanography Center (FNOC) atmospheric forcing and TRANSPAC monthly temperature analyses over the ADS domain provide the data for this study. The resolution is two degrees latitude and five degrees longitude over the area bounded by 30N-50N and 130W-160E.

Atmospheric forcing data were obtained from the archived FNOC Northern Hemisphere analyses and short-term predictions. The archived data include wind speed and direction at six-hour intervals and solar flux and total surface flux at 12-hour intervals. The forcing fields are interpolated to one-hour intervals for use in the Garwood model. This interval is required to adequately resolve the oceanic response to the diurnal heating cycle. A complete description of the interpolation procedure can be found in Gallacher (1979).

Initialization and verification TRANSPAC data sources were described by White and Bernstein (1979). Ships-of-opportunity XBT observations were made along the shipping tracks between Japan and the west coast of the United States. A seasonal and "fair weather" bias, due to ships avoiding bad weather, is evident in the northern portion of the domain, where the data coverage is good in the summer and generally poor in the winter. Elsberry (1984) also found that the northwest and southwest corners were not well sampled and these areas will be excluded in this study. These areas will be cross-hatched on appropriate figures.

Objectively analyzed XBT profiles at depths of 0,30,60,90,120,150 and 200m are used for model

initialization. These values are vertically interpolated to a 5m spacing between 0 and 200m to produce the gridded monthly oceanic temperature fields.

Some observational and physical considerations must be kept in mind when studying the subsequent analyses. Elsberry (1984) points out that regions north of 45N and south of 35N are less reliable due to seasonal variations in the data coverage. The baseline study conducted by White and Bernstein (1979) indicated that the region west of 175W was dominated by strong mesoscale (300 km) baroclinic eddies or waves, whereas east of 175W the larger scale variability dominated.

B. PREDICTION MODEL

The model used for this study is the Garwood (1977) second-order closure, bulk model. Advection is not included in the model. The Garwood model is initialized with TRANSPAC objectively analyzed temperature fields, which are assumed to apply on the 15th of the month. Model output consists of vertical temperature profile predictions in 5m increments to 200m over the entire grid every hour. These hourly temperature profiles are averaged over five days centered on the 15th of each month. An additional output is the mixed layer temperature at the time of maximum mixed layer depth for each day. Model anomaly fields are formed by subtracting the four-year mean (climatological) fields from the predicted fields at 0, 60 and 120m.

III. WARM ANOMALY DESCRIPTION

A. WARM ANOMALY 1/2

The warm anomalies (WA) described in this section were initially designated and described by Elsberry (1984) as WA1 and WA2. This case persisted for approximately six months, as shown in Figures 3.1 through 3.6.

WA1 is evident to a depth of 60m during the first month of the period (Figure 3.1) in the southeast portion of the region. The warm anomaly intensifies to maximum amplitude (2.02 C at 34N, 150W) at the surface in February (Figure 3.2). It decreases in intensity as the period progresses (Figure 3.3 and 3.4). In May, WA1 (Figure 3.5) disappears at the surface, but it is still evident at 60m. In June(Figure 3.6), a warm anomaly again appears at the surface in relatively the same position, but it is unclear whether this is still part of WA1 or is an entirely new feature.

WA2 is barely evident at approximately 38N,170E during January (Figure 3.1). It continues to intensify during the period. In March (Figure 3.3), it has become a significant warm anomaly extending to 120m. In April and May (Figures 3.4 and 3.5), WA2 appears to move north and elongate while losing some of its structure at depth. Toward the end of the period (Figure 3.6), WA2 becomes disorganized at the surface but maintains some structure at depths of 60 and 120m.

B. WARM ANOMALY 12/13/15

Warm anomalies 12/13/15 were initially designated and described by Elsberry (1984). This case continued for approximately six months (Figures 3.7 through 3.12).

WA 12 develops in July 1977 in the eastern part (38N,150W) of the region and reaches an anomaly magnitude of +1.7C (Figure 3.7). Development continues in August (Figure 3.8) and appears to have reached a depth of approximately 120m, although the anomaly center is shifted slightly eastward at 60 and 120m. During September and October, WA 12 weakens and disappears (Figures 3.9 and 3.10).

WA 13 also develops in July 1977 in the region around 48N, 170W (Figure 3.7). In August 1977, its position and movement appear to be influenced by a large cold anomaly at approximately 40N, 170W. This cold anomaly seems to cause WA 13 to merge with another warm anomaly to the southeast of the initial position of WA 13 (Figure 3.8). Evidence of the merging in September (Figure 3.9) is indicated by the large broad warm anomaly in the northeast portion of the region. The large anomaly diminishes in size in October and November, and it is no longer evident in December (Figures 3.10 and 3.11).

WA 15 is evident in July 1977 (Figure 3.7) along the extreme western boundary at 40N, 160E. It continues to develop and reaches maximum imtensity of +3.63C in August at 42N, 170E (Figure 3.8). At this time it also appears to have merged with WA 13, which contributes to a large warm anomaly area along the northern border. The anomalously high temperatures persist through November and disappear in December (Figures 3.11 and 3.12).

C. WARM ANOMALY 23

Warm anomaly 23 was initially designated and described by Elsberry (1984). This case persisted for approximately four months as seen in Figures 3.13 through 3.16.

During June 1978 (Figure 3.13), a general warm area at the surface has developed on the southwestern boundary of the region. By July (Figure 3.14), this area shows a strong (approximately +2.5C) surface anomaly at the boundary region. A slight shift northward is evident in August (Figure 3.15), and the temperature anomaly decreases by approximately 1.5C. By September (Figure 3.16), WA 23 has disappeared.

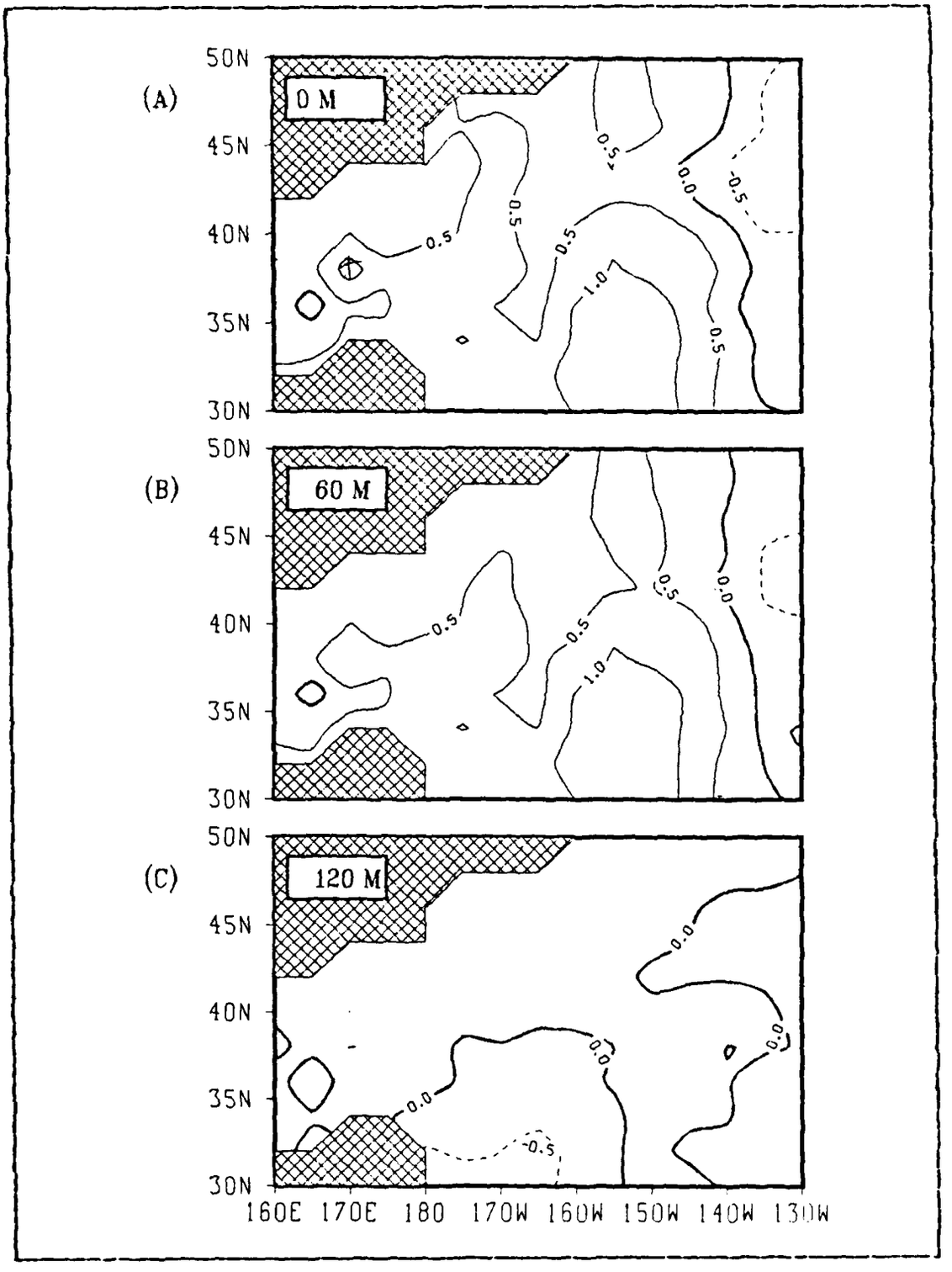

Figure 3.1 Temperature (C) anomaly WA 1/2 during January 1976 at (A) surface, (B) 60m and (C) 120m.

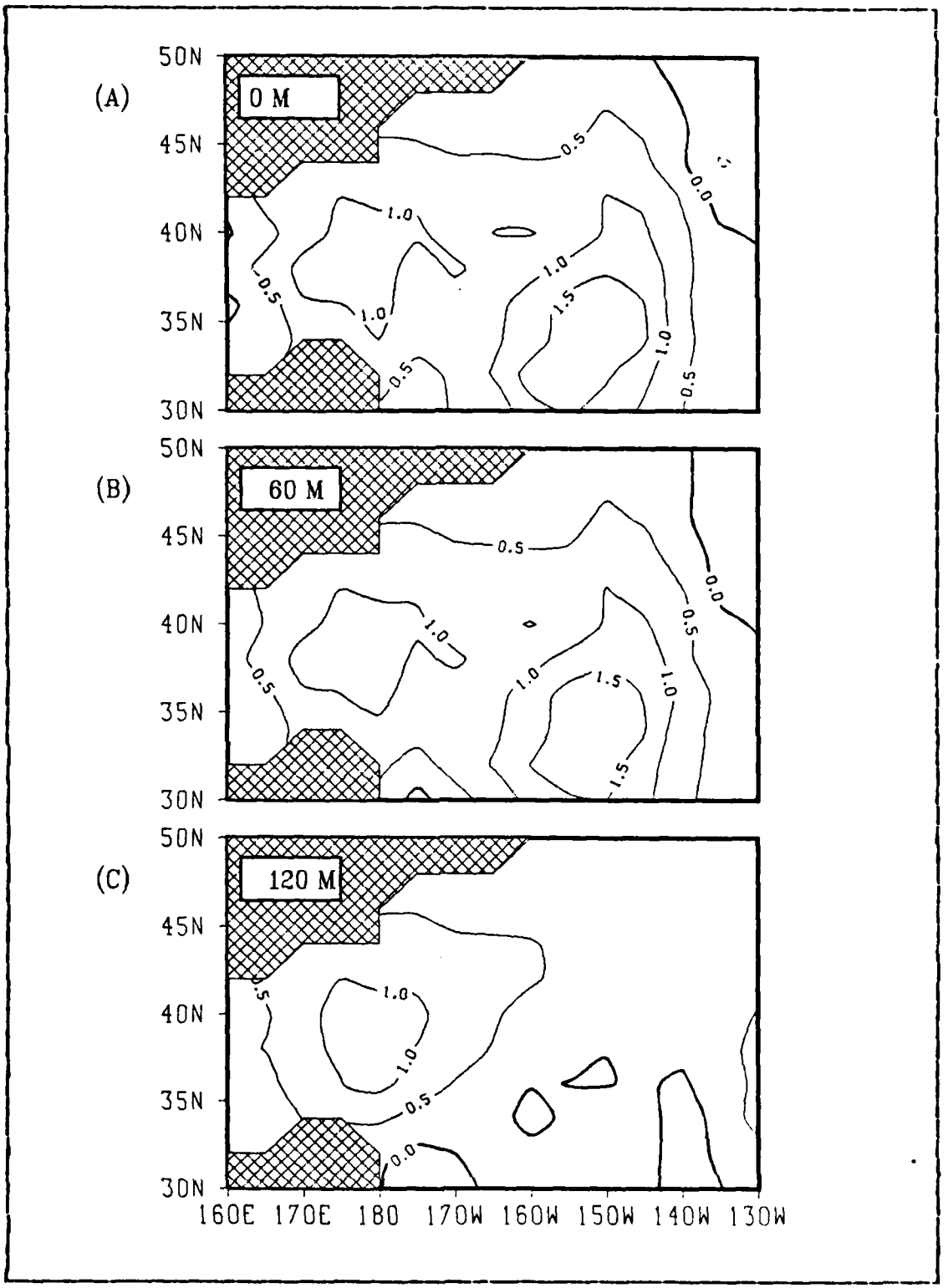

Figure 3.2 Similar to Figure 3.1 except for February 1976.

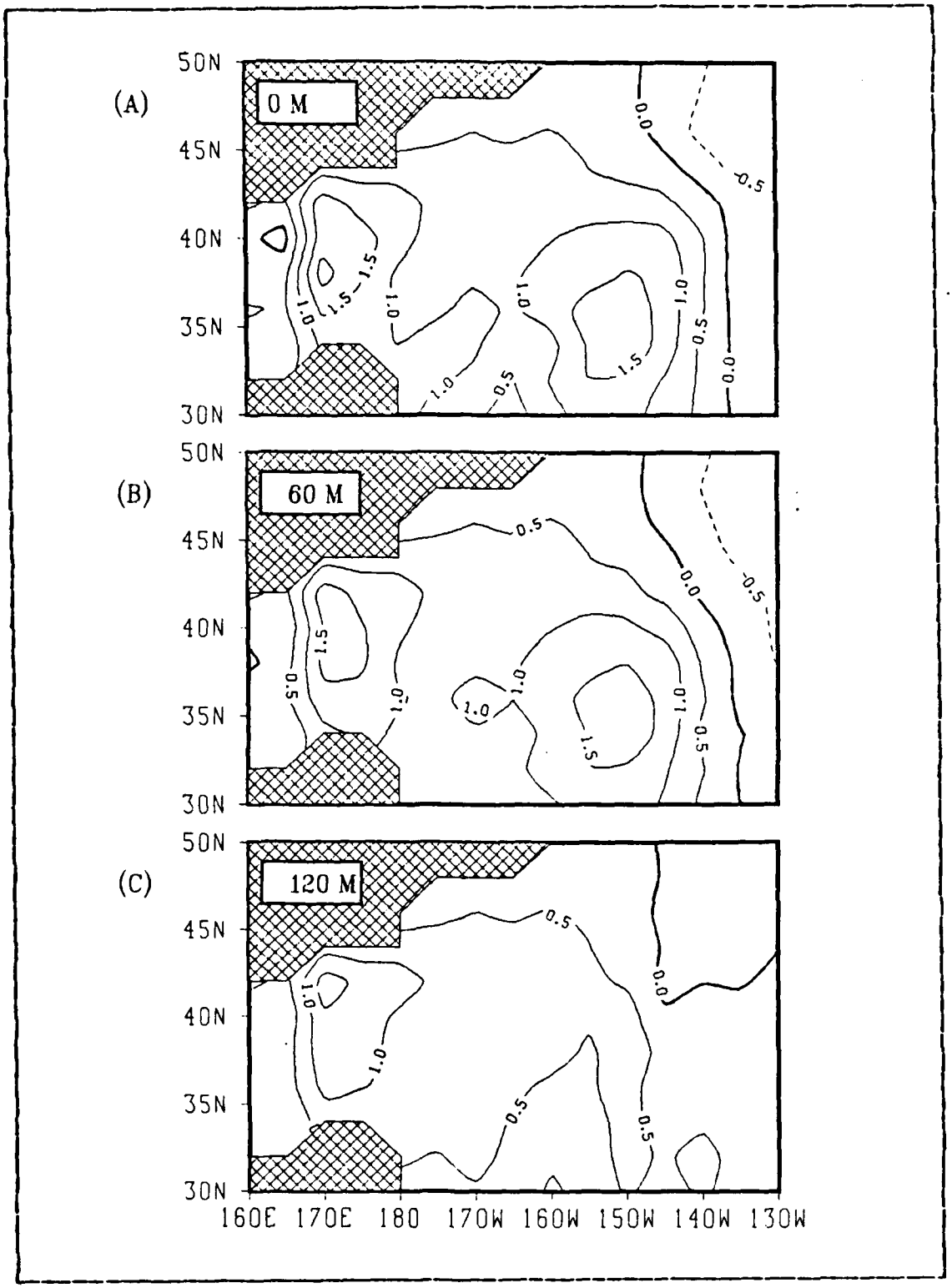

Figure 3.3 Similar to Figure 3.1 except for March 1976.

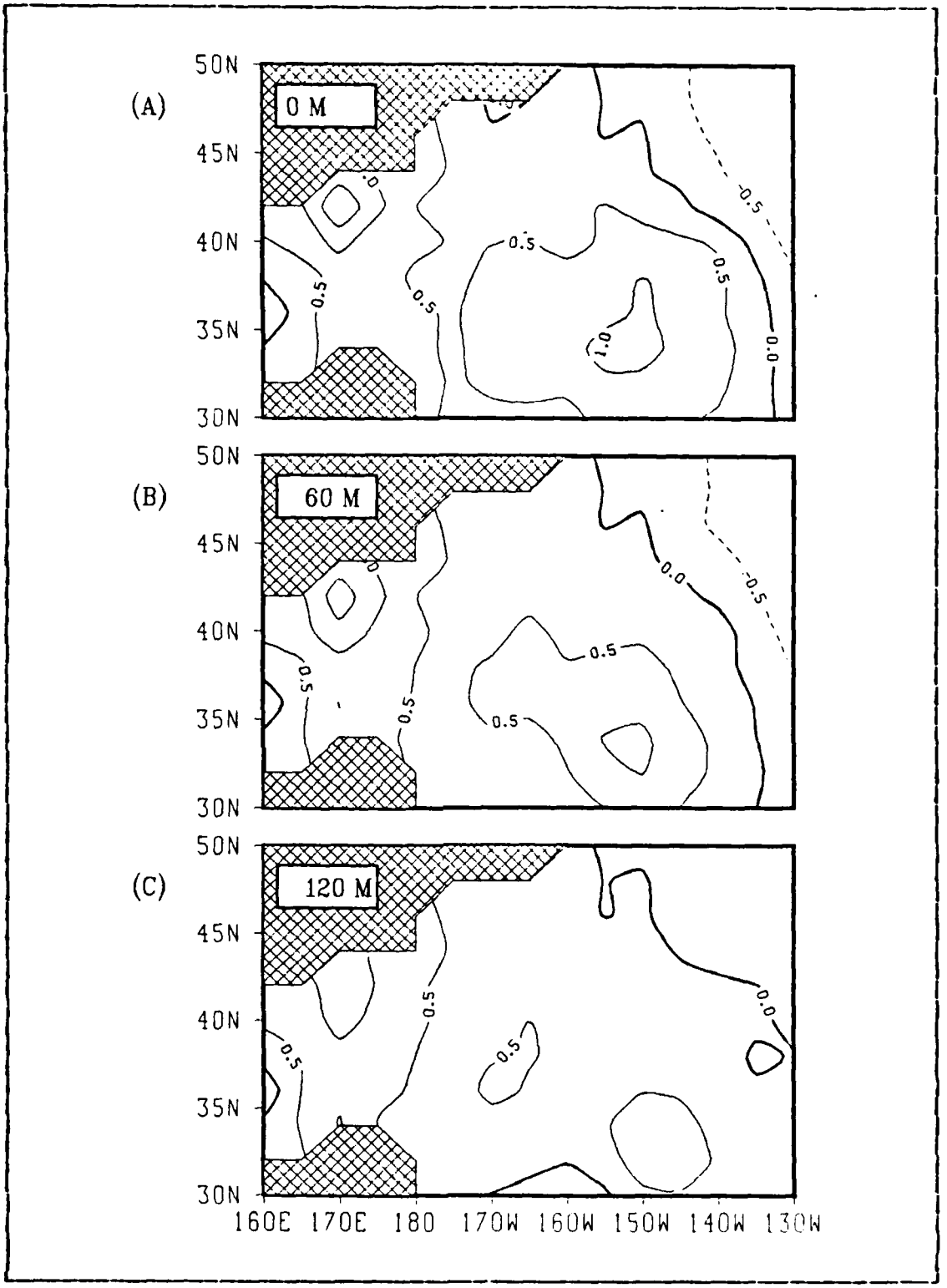

Figure 3.4 Similar to Figure 3.1 except for April 1976.

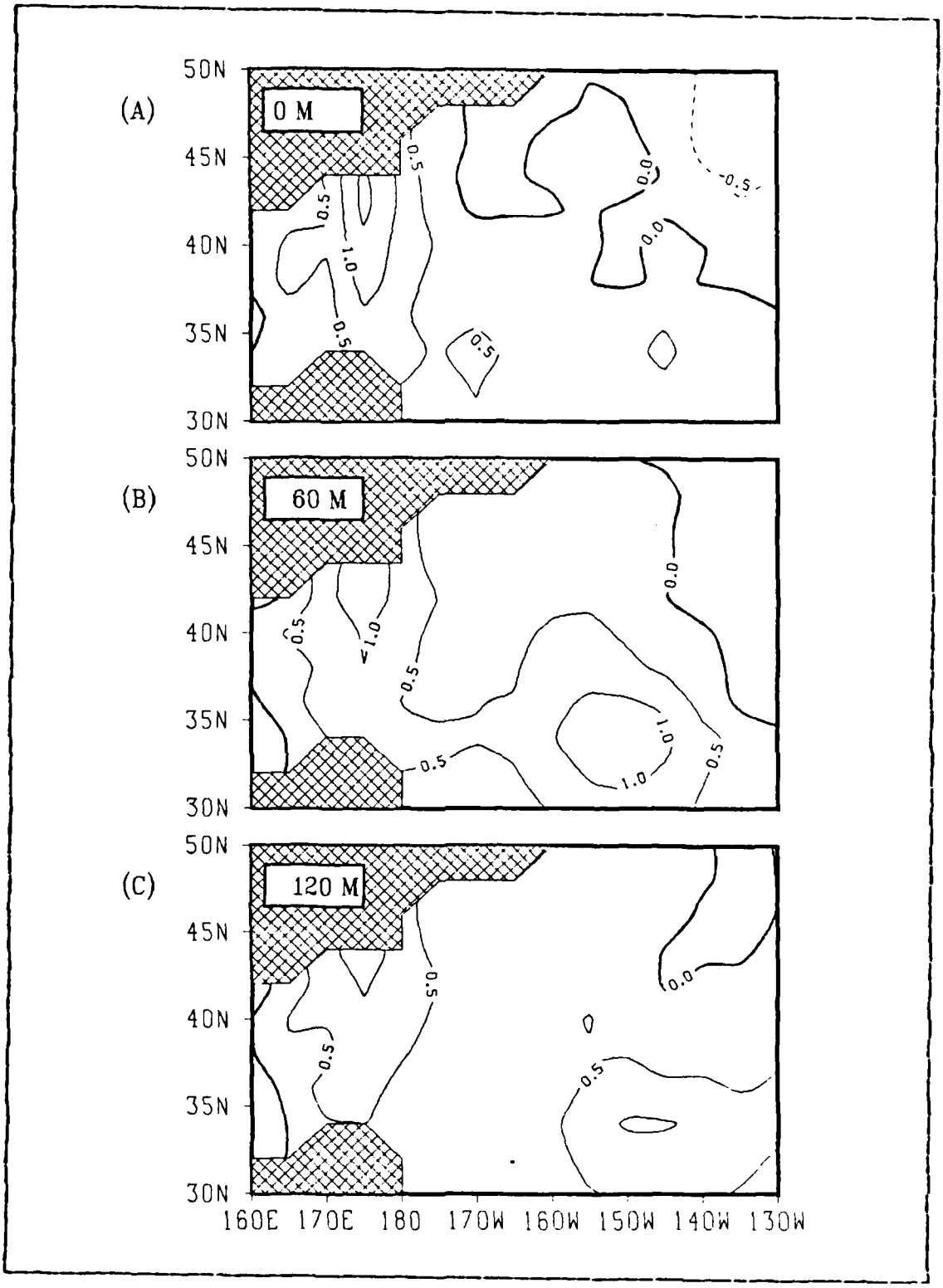

Figure 3.5 Similar to Figure 3.1 except for May 1976.

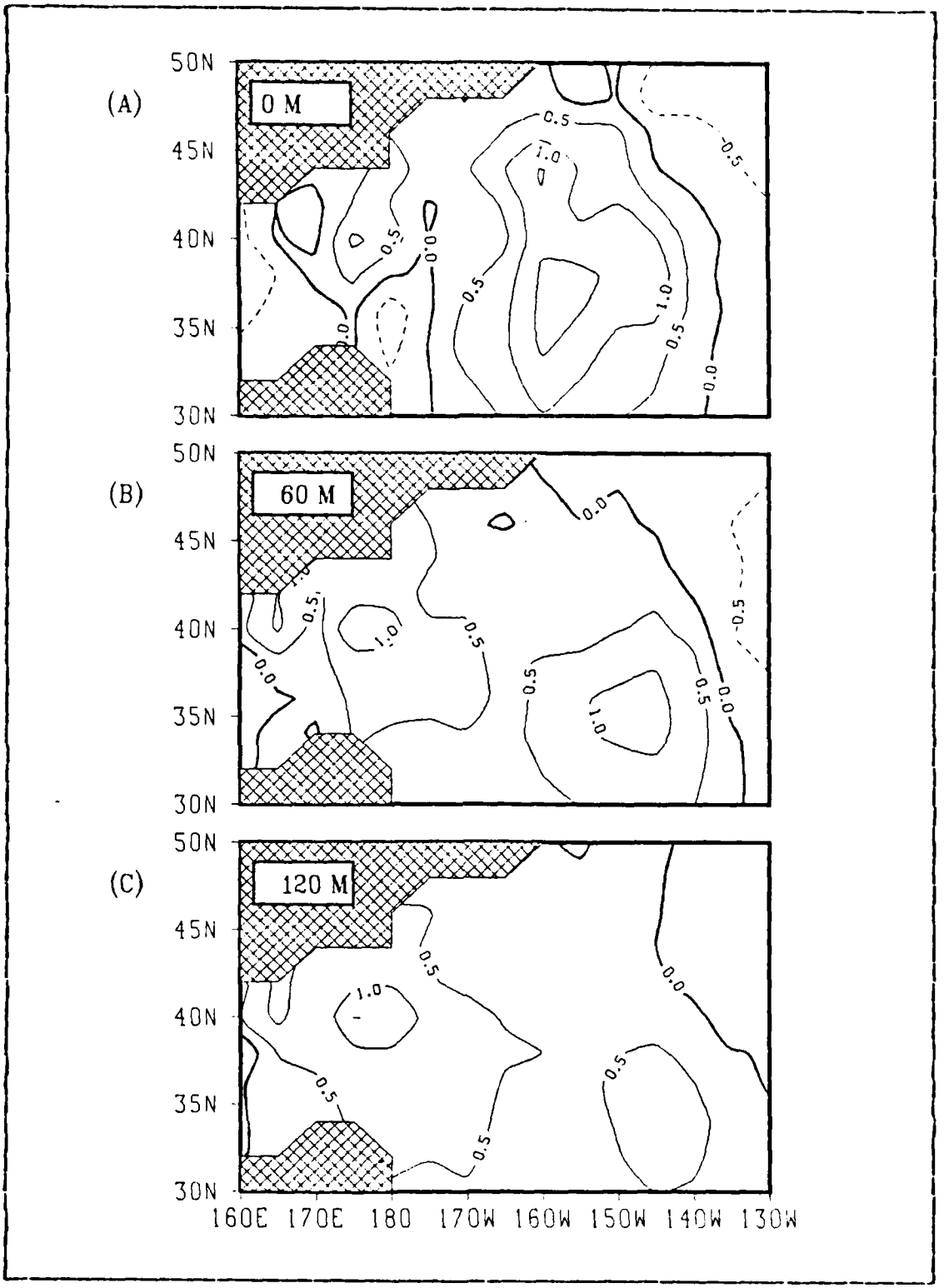

Figure 3.6 Similar to Figure 3.1 except for June 1976.

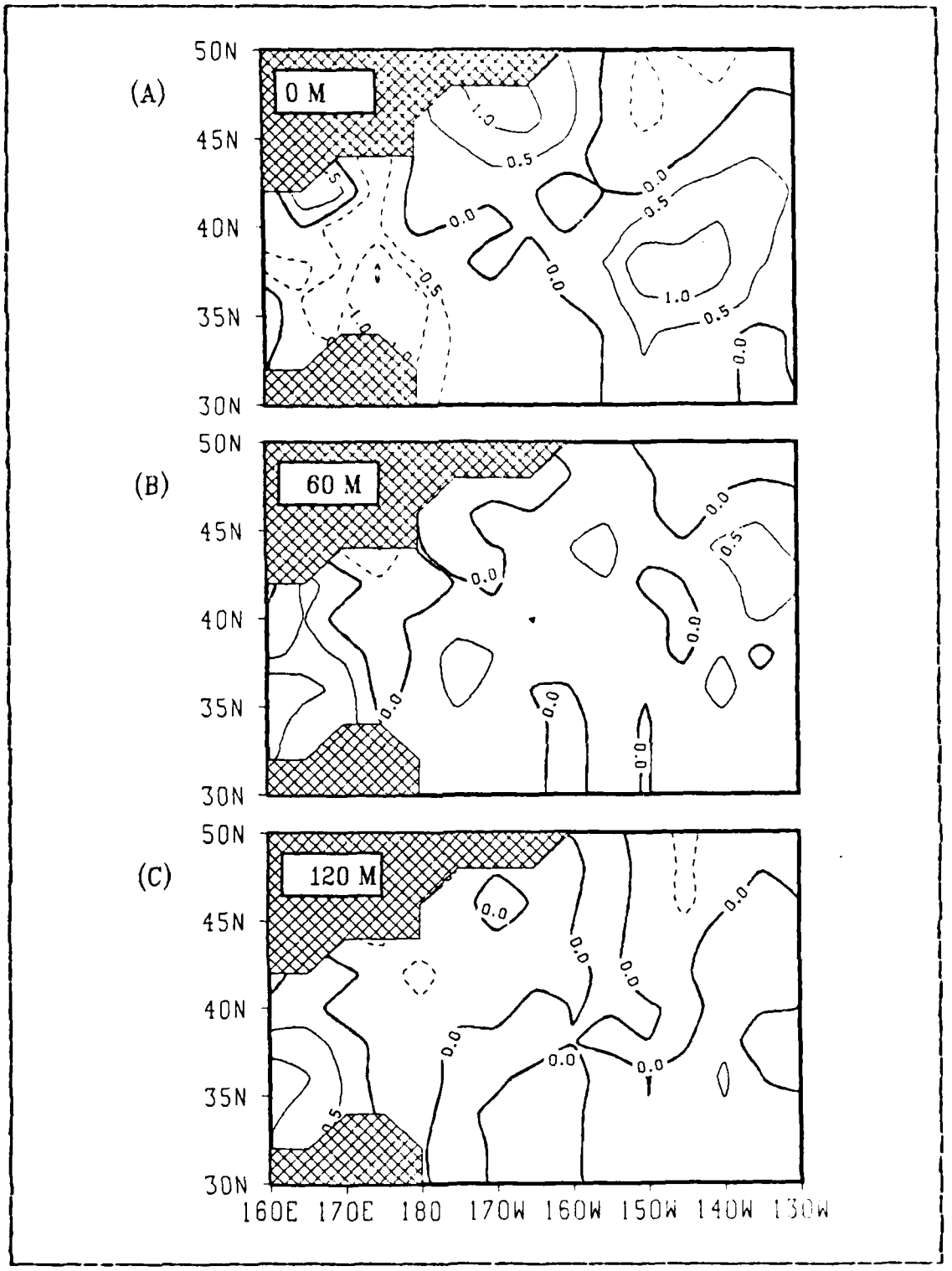

Figure 3.7 Temperature (C) anomaly WA 12-15 for July 1977 at (A) surface (B) 60m and (C) 120m.

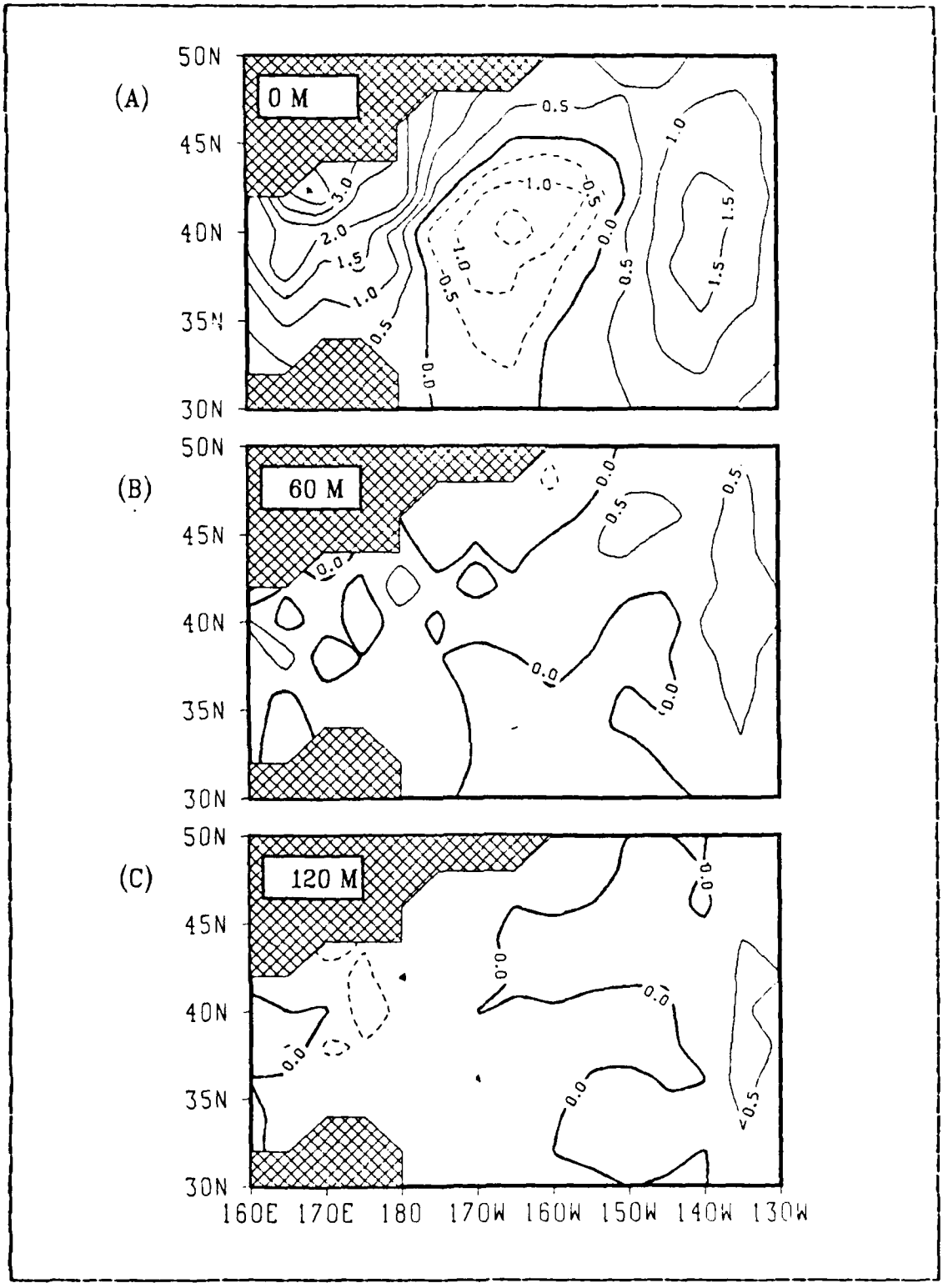

Figure 3.8 Similar to Figure 3.7 except for August 1977.

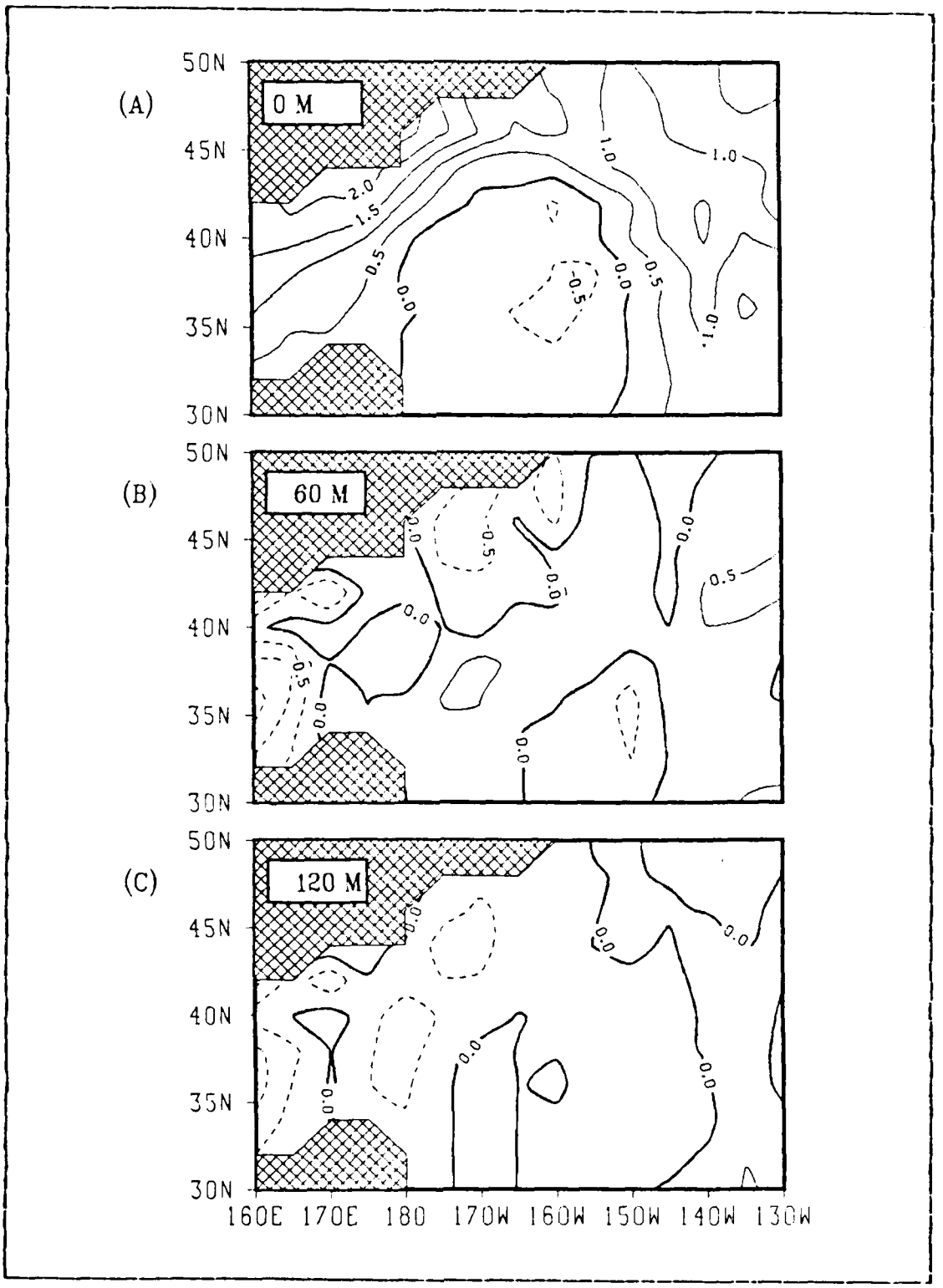

Figure 3.9 Similar to Figure 3.7 except for September 1977.

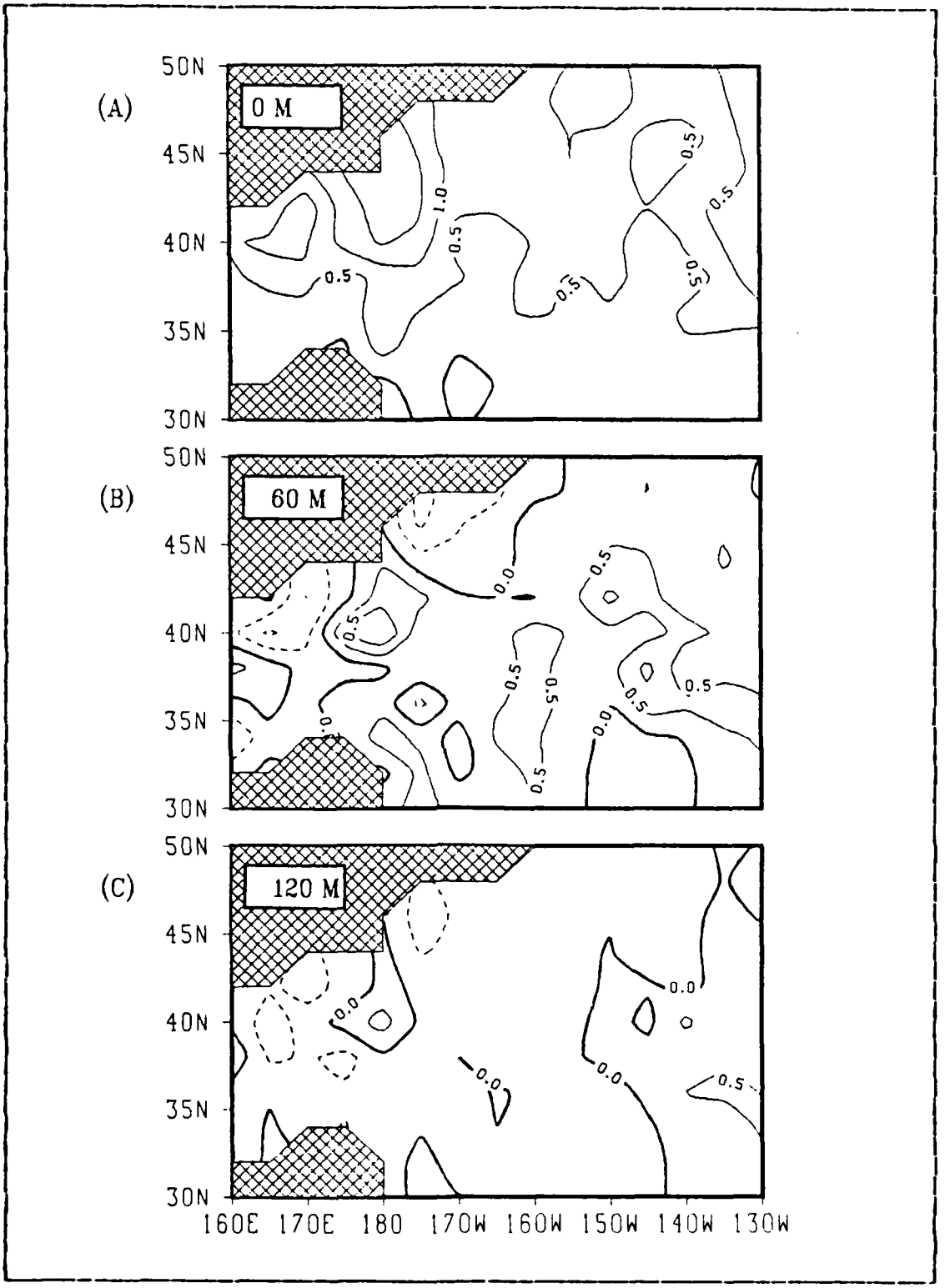

Figure 3.10 Similar to Figure 3.7 except for October 1977.

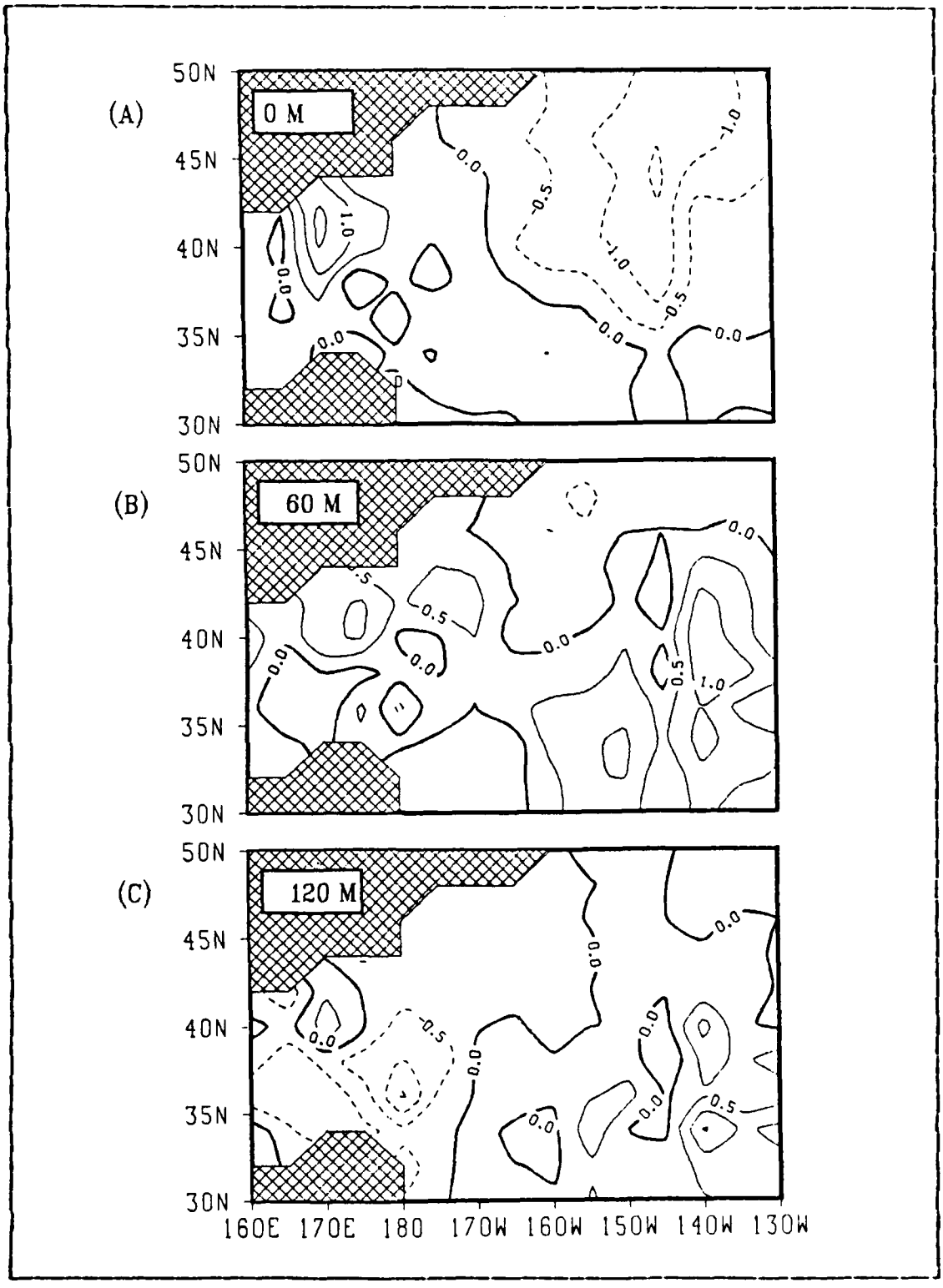

Figure 3.11 Similar to Figure 3.7 except for November 1977.

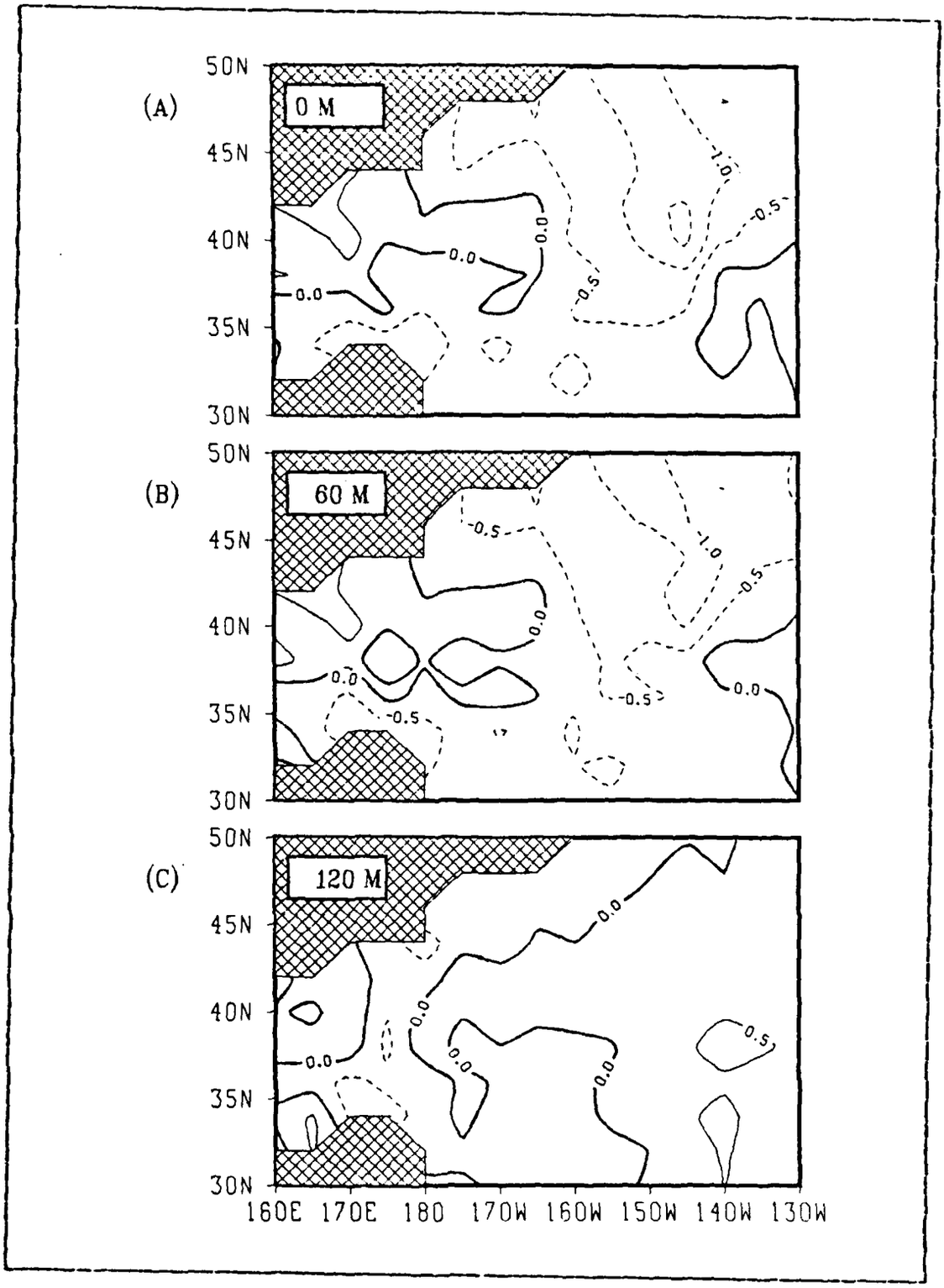

Figure 3.12 Similar to Figure 3.7 except for December 1977.

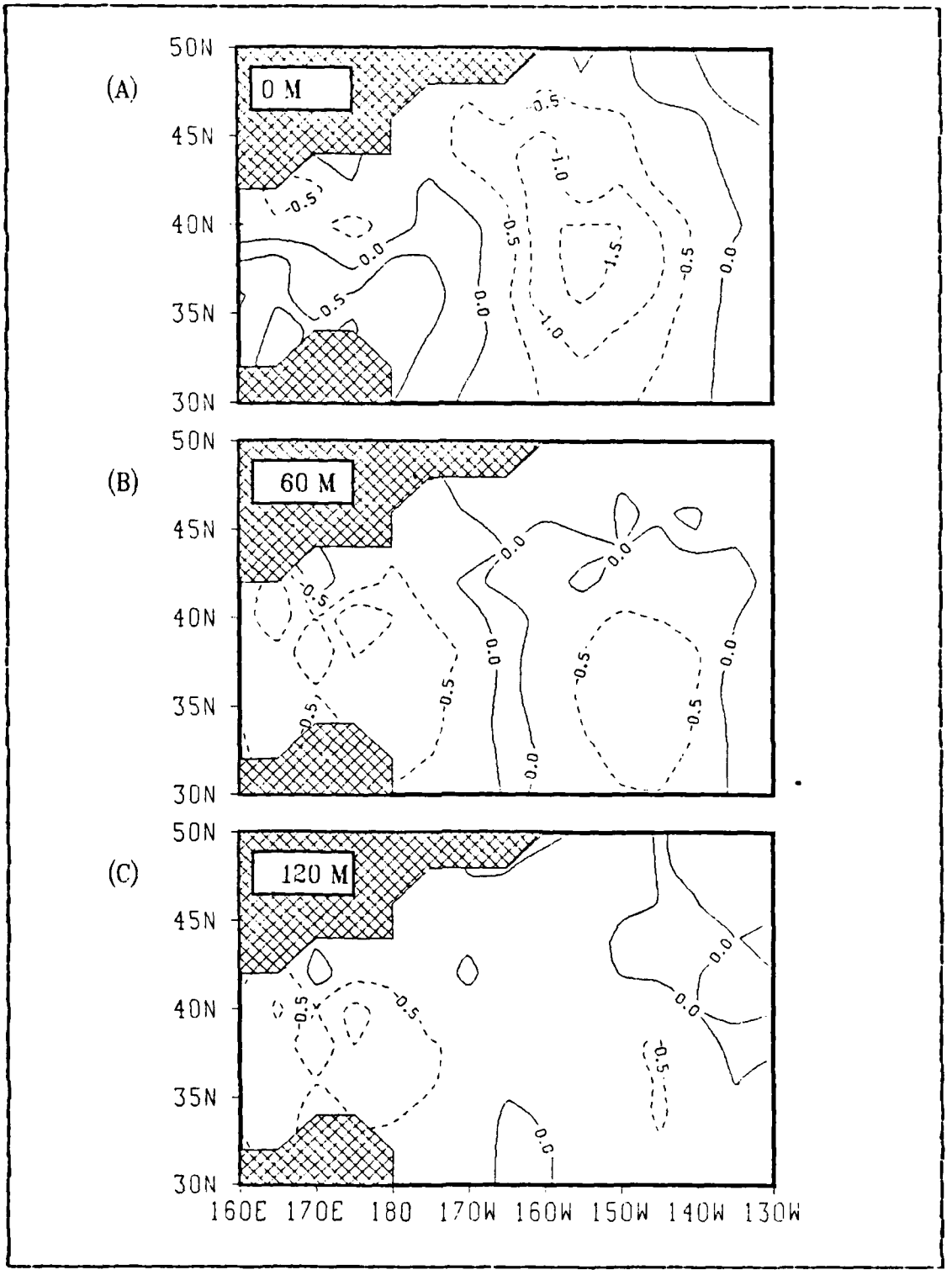

Figure 3.13 Temperature (C) anomaly WA 23 during June 1978 at (A) surface (B) 60m and (C) 120m.

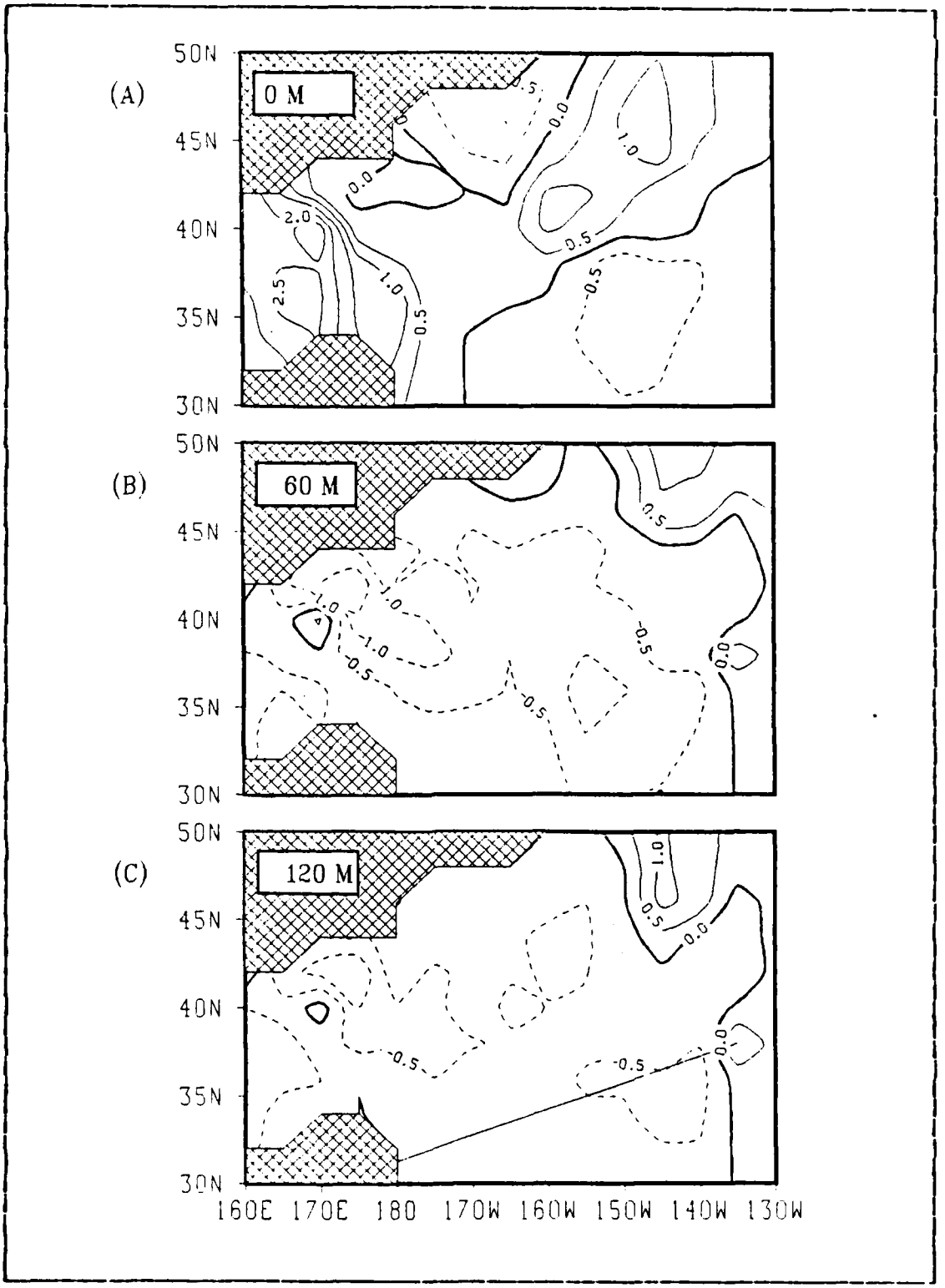

Figure 3.14 Similar to Figure 3.13 except for July 1978.

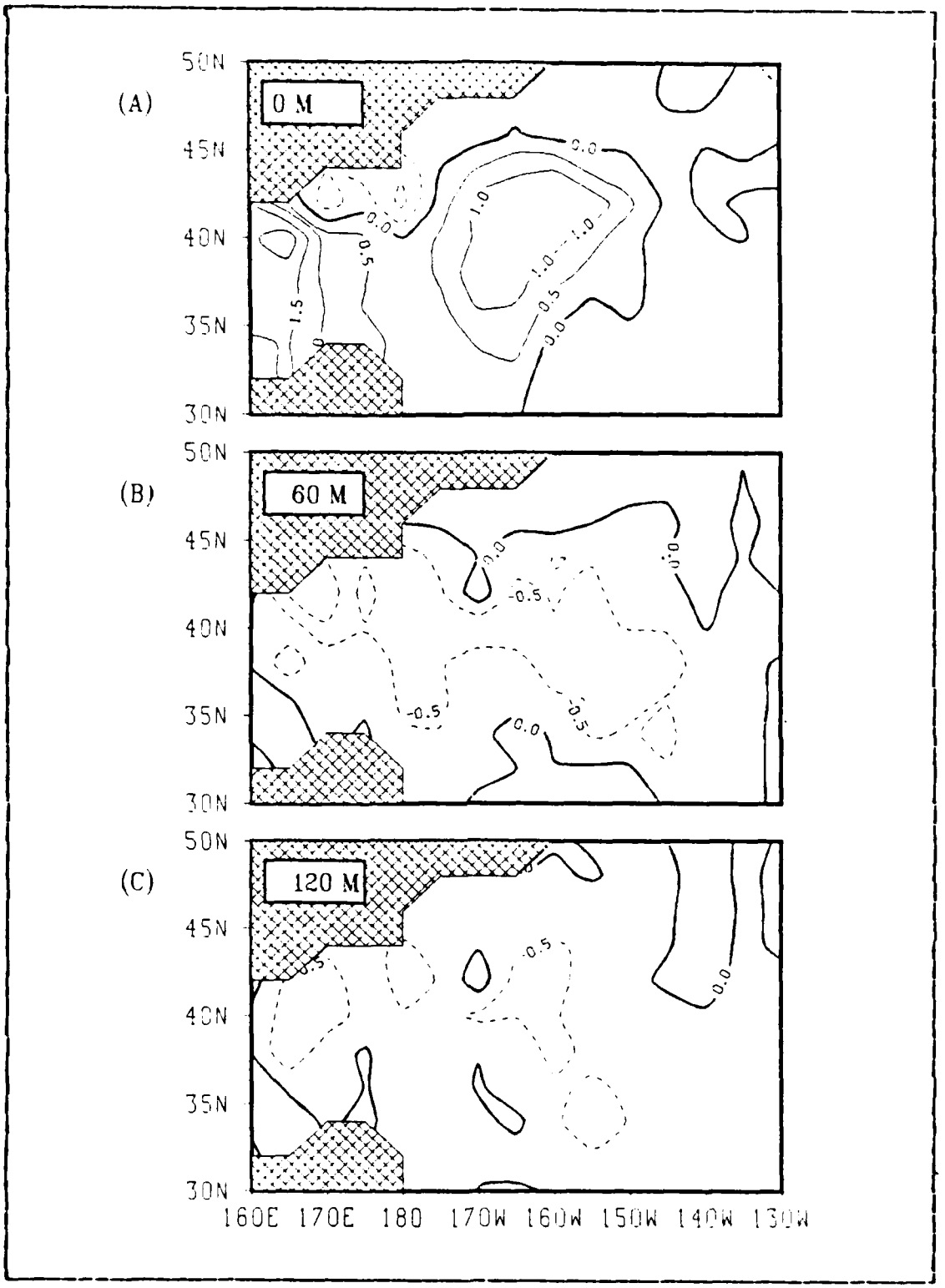

Figure 3.15 Similar to Figure 3.13 except for August 1978.

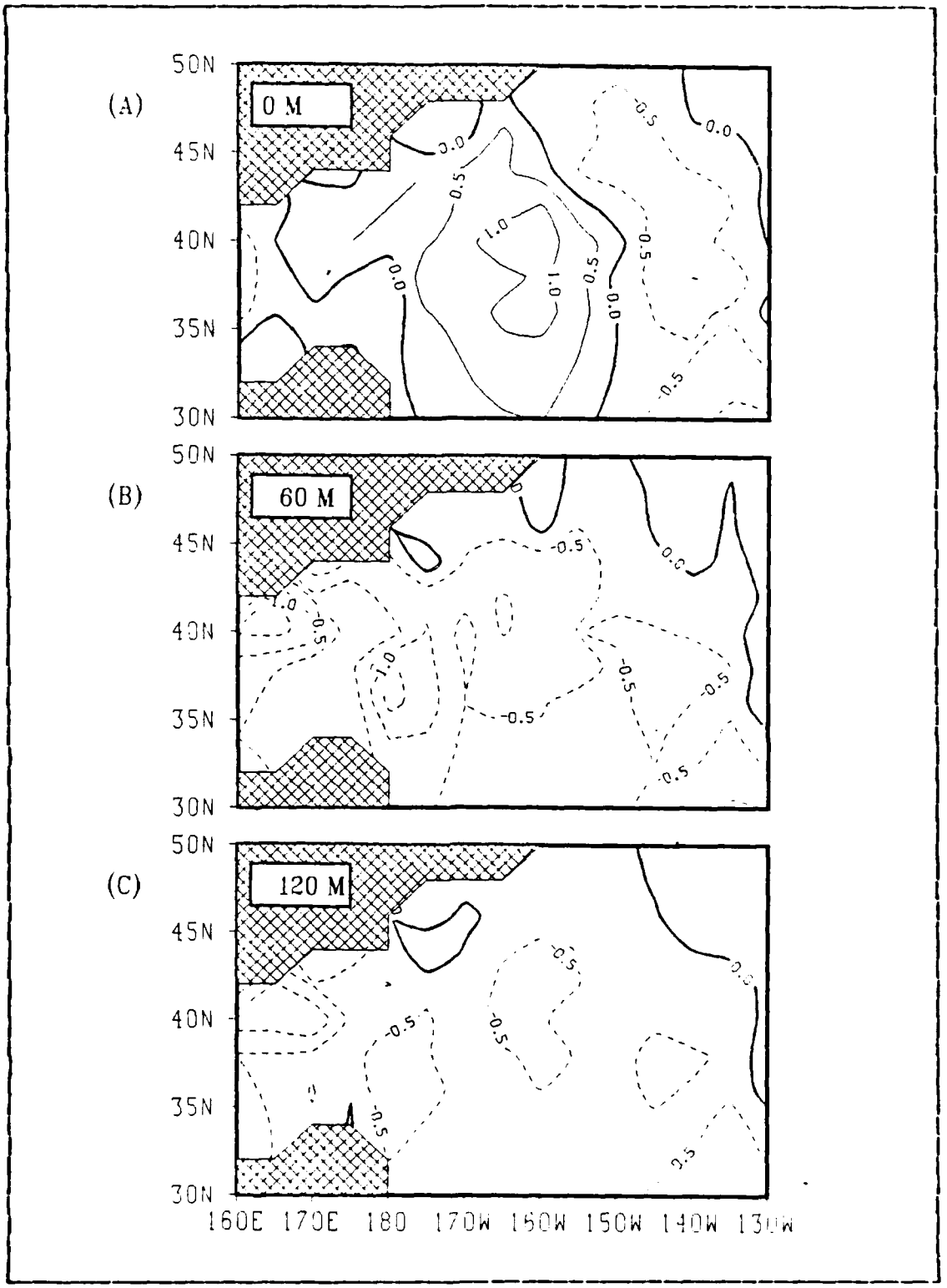

Figure 3.16 Similar to Figure 3.13 except for September 1978.

IV. MODEL HINDCASTS

A. INITIAL HINDCASTS

Several model integrations were conducted to test the hindcast ability of the Garwood model for the warm anomaly cases described earlier. The correction fields applied to the FNOC forcing fields were described in Elsberry et al (1982). The correction fields, which were derived by assuming a local heat balance during a 36-month period, consist of six bi-monthly fields which are to be added to the FNOC heat fluxes. The corrections are necessary for the heat fluxes to be used for one-dimensional ocean prediction. These corrections eliminate a bias of excessive upward surface heat flux found in the FNOC fields.

1. Model Hindcasts of WA 1/2

Generally, hindcasts of WA 1/2 were consistent with observations until April. Placement of the two major anomalies was reasonable and the overall structure for January through March was well simulated. This result is similar to that of Stringer (1983) for cold anomaly hindcasts prior to the spring transition. In April through July (Figures 4.1 through 4.4), the model hindcasts tended to be too warm. In April, a warm anomaly developed at approximately 37N, 170E with verified vertical structure to 200 m. The anomaly becomes more intense in May with a temperature of 4.5C at the western boundary. Between June and July, temperatures continued to increase unrealistically, especially in the western portion of the region. The anomalies did penetrate to 200 m, as is seen by the high subsurface temperatures.

Comparisons with Figures 3.4 through 3.7 show that there is good agreement in April at a depth of 60m, but the placement of the features at the surface and 200 m does not agree with the observations. Similar comparisons for May and June show even less agreement as the model continues to warm excessively.

An additional model hindcast was conducted using May as the initial month. Again, the hindcast was too warm, and the results very similar to the June initialization. To determine the effect of the correction to the forcing field, two model integrations were conducted from January through July and May through August without application of the correction field. Neither of these model hindcasts agreed with the observed anomaly fields in that both predicted a warm anomaly in the northwest area and a large area of anomalously low temperatures in the entire southern region from approximately 40N southward. Further studies with modified correction fields in space and time will be described in section C of this chapter.

2. Model Hindcasts of WA 12/13/15

Model hindcasts of WA 12/13/15 were generally cooler than observations over much of the area with a pronounced warm region in the southwest portion of the region. Using the June analysis to specify the initial conditions of the model (Figure 4.5), it is seen that July (Figure 4.6) is already much cooler than climatology in the northeast and much warmer in the southwest. Comparison with observations for July (Figure 3.7) shows very little correlation between the two plots. The August plot (Figure 4.7) maintains the same pattern developed in July and does not bear any resemblance to the observed July condition (Figure 3.8).

The model was then tested with initial conditions from March and May to determine if a relationship existed between initialization period and accuracy of model hindcasts. In both cases, the model predicted development of a general warm area in June, although by July there were cold anomalies in the northeastern portion of the area. By August, the size of the warm area was increasing (Figures 4.8 and 4.9). This was similar to the model output with a June initialization. Thus, time of initialization does not appear to affect the output as there are anomalously low temperatures as early as July. The model was also integrated without a correction to the forcing field. The output (not shown) for a model hindcast from June inital conditions showed the entire grid area was anomalously cool in July, and the temperatures continued to decrease as the period progressed. The different variations used to hindcast WA 12/13/15 did not significantly improve any of the hindcasts. Thus, the early summer period appears to pose serious problems for reliable model hindcasts.

3. Model Hindcasts of WA 23

Two model integrations for WA 23 were done with an initialization time of January and June. With an initialization of June (Figures 4.10 through 4.12), the model hindcasts produced a large anomalously cool area over most of the region with a small warm anomaly on the southern border. As the period progressed through August and September, the cold anomalies at the surface intensified and developed an unverified cold pattern. Comparison with observations (Figures 3.13 through 3.16) indicate a lack of agreement in feature placement or feature intensity during all months. Temperature structure with depth also did not agree favorably.

B. DISCUSSION

General results of each model hindcast showed that the model anomalies for WA 1/2 were hindcast well until April. However, the model tended to produce an anomalously warm condition throughout the remainder of the period. Model anomalies for WA 12/13/15 were hindcast as too cold as early as the second month of the model integration. Model anomalies for WA 23 were also hindcast as too cold throughout the period.

The three cases have at least one common factor in that they span the early summer months of June and July. During these months, changes in forcing (heat fluxes and wind speeds) are much more difficult to predict and can not be corrected by a bi-monthly average correction technique as previously done (Stringer, 1983) for cold anomaly studies. The variability in the total heat flux can cause the model to over-correct or under-correct in the quantity of heat necessary to simulate accurately the observed conditions for the early summer.

The importance of correctly determining the heat storage and heat input is discussed by Wyrtki and Ulrich (1982). They found that over a period of one month the observed change in heat storage can be computed to only an accuracy of +/- 100 W/m^2, which is as large as the net daily heat exchange. This uncertainty makes it difficult to account for contributions of advection or mixing over a monthly interval. If this magnitude of uncertainty is encountered in actual ocean estimates, then it is very possible that errors this large may exist in the FNOC short-term predictions used here for the forcing fields. Uncertainty in determining the heat storage and heat input can also adversely affect the depth of the mixed layer as predicted by the model. For a shallowing mixed layer depth with no

entrainment, the mixed layer depth, h, is related to the total heat flux, Q_o, by the relationship:

$$h = L \simeq u^{*3} / \{\alpha g Q_o / (\rho C_p)\} \text{ where}$$

L=Obukhov length scale

u^*=Friction velocity

C_p=Specific heat of water

Q_o=Heat flux

α=Specific volume

ρ=Density

g=Gravity

The corresponding temperature change is given by

$$dT/dt = (Q_o / \rho C_p) / h.$$

The heat flux may be expressed as

$$Q_c = Q_o \text{ (correct)} + Q_o \text{ (error)} = Q_c + Q_E = Q_c (1+E), \text{ where}$$

E is an error bias equal to Q_E / Q_c. This now gives

$$h = \rho C_p u^{*3} / \{\alpha g Q_c (1+E)\} = h_c / (1+E)$$

and with the expression for Q_c yields

$$dT/dt = Q_c^2 \{1+E\}^2 \alpha g / \{(\rho C_p)^2 u^{*3}\}$$

$$dT/dt = \{(1+E)^2\} \{dT/dt\}_c$$

This expression demonstrates that a net flux error, Q, contributes as a square because it also contributes to an incorrect mixed layer depth.

The heat flux corrections by Elsberry et al. (1982) were computed on a bi-monthly basis and were averaged over three years. This average correction field does not appear to accurately modify the forcing field in the proper amounts for the early summer. To study this problem further, the correction field for WA 1/2 was modified, and a different source of heat flux values was used to improve model hindcasts.

C. WA 1/2 DETAILED STUDY

1. One-Dimensional Heat Budget Correction Field

Previous case studies of cold anomalies by Stringer (1983) and the initial model hindcasts for warm anomalies in this study indicated that the model hindcasts are degraded by boundary condition (surface heat flux) errors in the late spring and early summer. Since the bi-monthly average correction field derived by the method of Elsberry et al. (1982) did not correctly modify the forcing fields for late spring and early summer cases, a new correction field was derived. This correction field exactly accounts for the difference between the heat content in the water column to a depth of 200 m and the integrated surface heat at a given geographical location. The correction is formed from the following:

$$I = \int_{t_1}^{t_2} Q_T(t)\,dt$$

$$H = \rho C_p \int_{0}^{D} \{T(z) - T(200\,m)\}\,dz$$

I is the integrated surface heat flux, H is the heat content, Q_T is the surface heat flux, t is time, t_1 is the 15th of one month and t_2 is the 15th of the following month. This yields the unfiltered exact correction ($\mathcal{E}$);

$$\mathcal{E} = \{H(t_1) - H(t_2)\} - I_{t_1}^{t_2} / (t_2 - t_1)\ \text{hours}$$

This field was then filtered using the same procedureas in the original correction field.

The one-dimensional heat budget correction field was used in model hindcasts for May through August 1976. These hindcasts were compared with monthly temperature change fields. This comparison emphasizes model temperature changes and is not dependent on climatology as in the anomaly comparisons above.

For June to May model temperature fields (Figure 4.13) are close to the observed fields (Figure 4.16). In overall structure, the field shows some similarity to the observed pattern, especially in the warming of approximately 2C in the eastern third of the region.

The July to June model plot (Figure 4.14) shows two distinct warm features at 42N,175E and 32N,165W which deviate greatly from the observed fields (Figure 4.17). Larger temperature difference gradients are more evident in the model plot. Locations of maximum warming and cooling do not correspond to similar features in the observed field, and it appears that the model is generating temperatures too high for the entire region during July.

The August to July (Figure 4.15) model output appears to have even less correlation with the observed field (Figure 4.18) than during the previous two months. The two general areas with large deviations noted previously again appear. The overall pattern of large gradients in both warming and cooling constitutes an unverified hindcast.

To determine what caused the model to deviate so greatly from observations in July and August, observed and model temperature profiles at 42N,175E were analysed (Figures 4.19 and 4.20). It is seen from the June and July observed temperature profiles that a large amount of heat is added in the water column during this two-month period. Calculations of the heat storage show that approximately 3.0×10^4 cal/cm^2 is added, which is abnormally large when compared to surrounding values. Analysis of the surface heat flux field shows a value of 1.0×10^4 cal/cm^2 which is in good agreement with surrounding points. Therefore, it appears that the large heat content influenced the correction and caused the model to over-correct by adding too much heat. The reason for such a large heat content could be horizontal advection of warmer water, downward vertical velocities, or

possible observational error. Whatever caused this heat excess is not handled well by the model, and must be better understood to be corrected. Use of the one-dimensional heat budget correction field is not sufficient for the model to produce acceptable hindcasts for all points.

2. Correction to the One-Dimensional Heat Budget Correction Field

In an attempt to correct the large deviations seen in the model using the exact correction field, a correction method applied to a specific area was devised. The point (42N, 175E) was chosen for this test since there is a large temperature difference between July and June and the model temperature profile is greatly exaggerated for July. The point correction, ε_p, was derived by removing the amount of heat in the mixed layer during the two-month period and using the residual heat content as an additional correction factor to the correction field at that point. For (42N, 175E) the following calculations were used:

$$\varepsilon_p = \Delta H_{200} - \Delta H_{mL} \; / \tau = 28.13 \text{ cal/cm}^2\text{-hr}$$

where $\Delta H_{200} = 3 \times 10^4$ cal/cm^2 and $\Delta H_{mL} = 1.0 \times 10^3$ cal/cm^2 and $\tau = 720$ hours.

This correction was then applied to the one-dimensional heat budget correction field at that point, and the model was integrated again. The resulting model temperature profiles (Figure 4.21) are much closer to the observed temperature profiles. The July profile is within 0.5C at the surface and is in close agreement down to 80 m. The August model profile still shows a large amount of heat in the column and requires some additional correction to reproduce the observed temperature profile.

Although this procedure did improve the July temperature profile, it would not be useful to apply a similar correction at every point without a better understanding of

the cause of the error (i.e., neglect of advection or observational error). A better method for deriving either the correction field or the initial forcing field is needed to make better use of the model as a prediction tool.

3. Average Climatological Surface Heat Flux

The solar flux values used in the above model hindcasts were derived from the FNOC short-term predictions. The above attempts to correct for uncertainties in this field and using variations of exact corrections did not produce overall favorable hindcasts. A climatological solar flux estimate will now be used to determine if model performance could be improved.

Climatological heat flux values developed by Wyrtki (1967) provide an alternate source for monthly-averaged surface heat flux values in the North Pacific. Values for the months of May through September were extracted from the available graphs and then interpolated in time as required by the model.

Monthly climatological heat flux and the average heat flux fields from FNOC are compared in Figures 4.22 through 4.29. It is apparent that the FNOC heat fluxes contain larger gradients and more zonal structure. The FNOC values tend to be larger when compared to climatology. This large deviation from climatology was unexpected and it may help explain the difficulty in deriving an objective correction to this field, as was seen in the earlier model hindcasts.

Three model integrations were made using this climatology. Case I used the total heat flux field, and it neglected the absorption of shortwave radiation below the surface. That is, all solar radiation was assumed to be absorbed at the surface. In Case II, the solar radiation

was added as a separate field that was also derived from the climatological charts of Wyrtki. Thus, below-surface absorption was considered in Case II. Case III was similar to Case II, except it included the diurnal cycle for the radiation.

Case I: Plots of monthly temperature changes for June to May (Figure 4.30) were much smoother than the previous results using the FNOC heat fluxes (Figure 4.13) and temperature magnitudes were much closer to the observed values (Figure 4.16). The region has a general warming pattern increasing from west to east and north to south with a small temperature change maximum in the southeast corner. The July to June plot (Figure 4.31) shows a larger gradient from north to south with a much more intense warming area situated at approximately 32N,170W. The pattern tends to be warmer than observations (Figure 4.17) with the largest temperature changes shifted slightly south and east of a similar but lower temperature change maximum in the observation. The August to July plot (Figure 4.32) also has a smoother field and shows a slight decrease in temperature change. The bull's-eye pattern apparent in the previous plot has been modified and appears as a broad warm area in the southwestern part of the grid. These temperatures are slightly lower than observations (Figure 4.18). General warming throughout the entire region is still evident.

Although placement of features is not completely consistent with observations, the general overall warming pattern is verified. Temperature change magnitudes are close to observed values. Temperature patterns produced by the model tend to be somewhat zonal due to the zonal pattern of the climatological heat flux fields.

Case II: Inclusion of a separate solar radiation field did modify the temperatures compared to Case I. The June to May plot (Figure4.33) is very similar to that in

Case I with a reduction of the temperature magnitudes by approximately 1.0C. The July to June plot (Figure 4.34) shows a similar trend, with temperatures reduced again by approximately 1.0C. The August to July plot (Figure 4.35) also shows a pattern similar to that seen in Case I with slightly smaller temperature changes.

Overall, the inclusion of a separate solar radiation field produced patterns very similar to that in Case I. The gradients of temperature difference were much smaller, but the observed general warming trend is correctly simulated.

Case III: The diurnal variation to the solar radiation field further modified the temperature difference pattern seen in Case II. All three plots (Figures 4.36 through 4.38) are very similar in structure to the Case II plots previously discussed. The July to June plot shows the greatest modification with an additional decrease of 0.5C in the area of the bull's-eye described earlier. The general warming pattern is still apparent and, even with the modification of temperatures and weaker gradients, a pattern similar to that of the observations is predicted.

Climatological heat flux fields do aid the model in producing patterns which are closer to observations than the previous attempts using FNOC heat flux fields. However, placement of features seen in the observations is still not handled well by the use of climatology for the heat flux forcing.

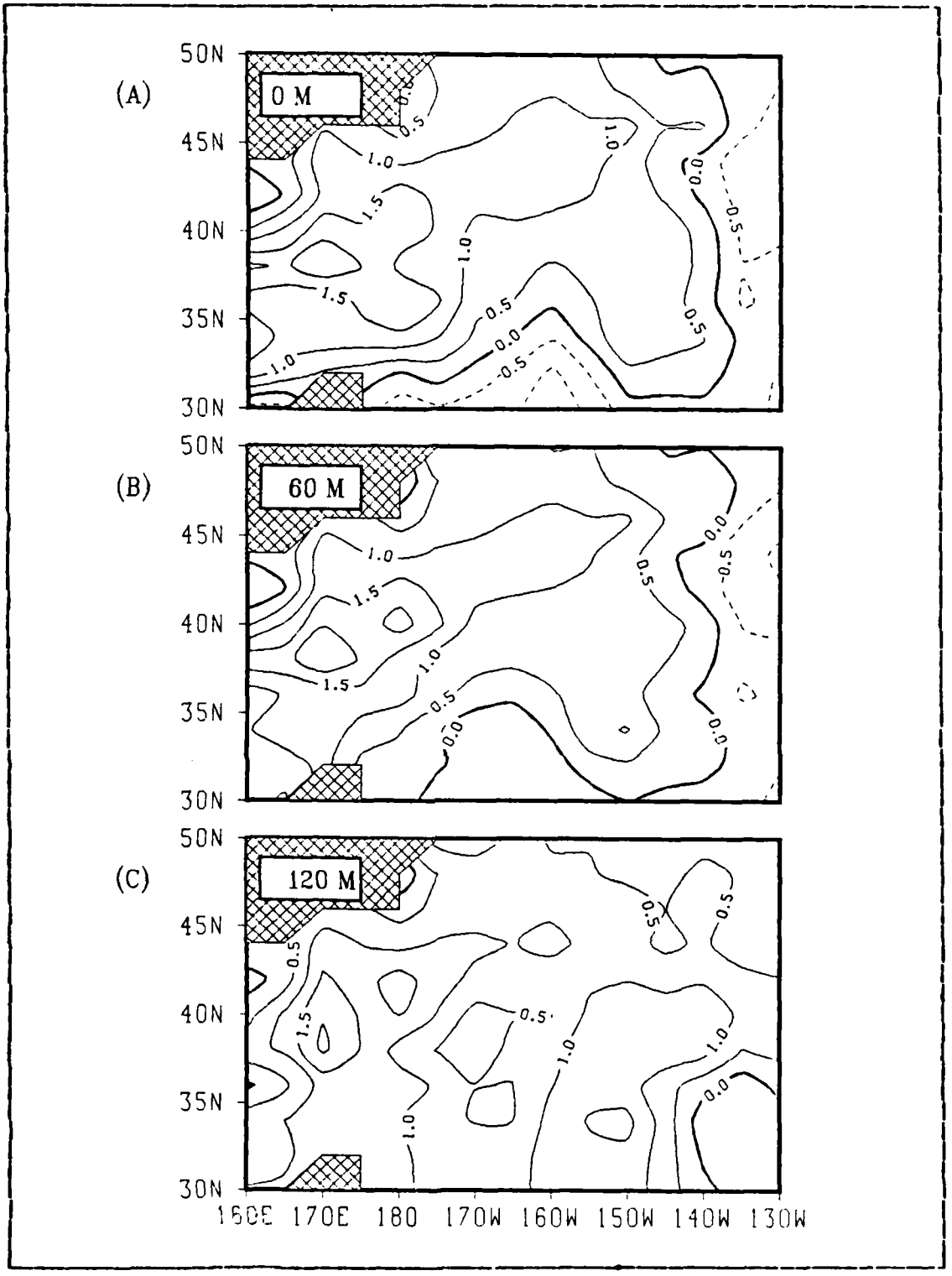

Figure 4.1 Model temperature anomaly MA 1/2 during April 1976 at (A) surface, (B) 60m, and (C) 120m.

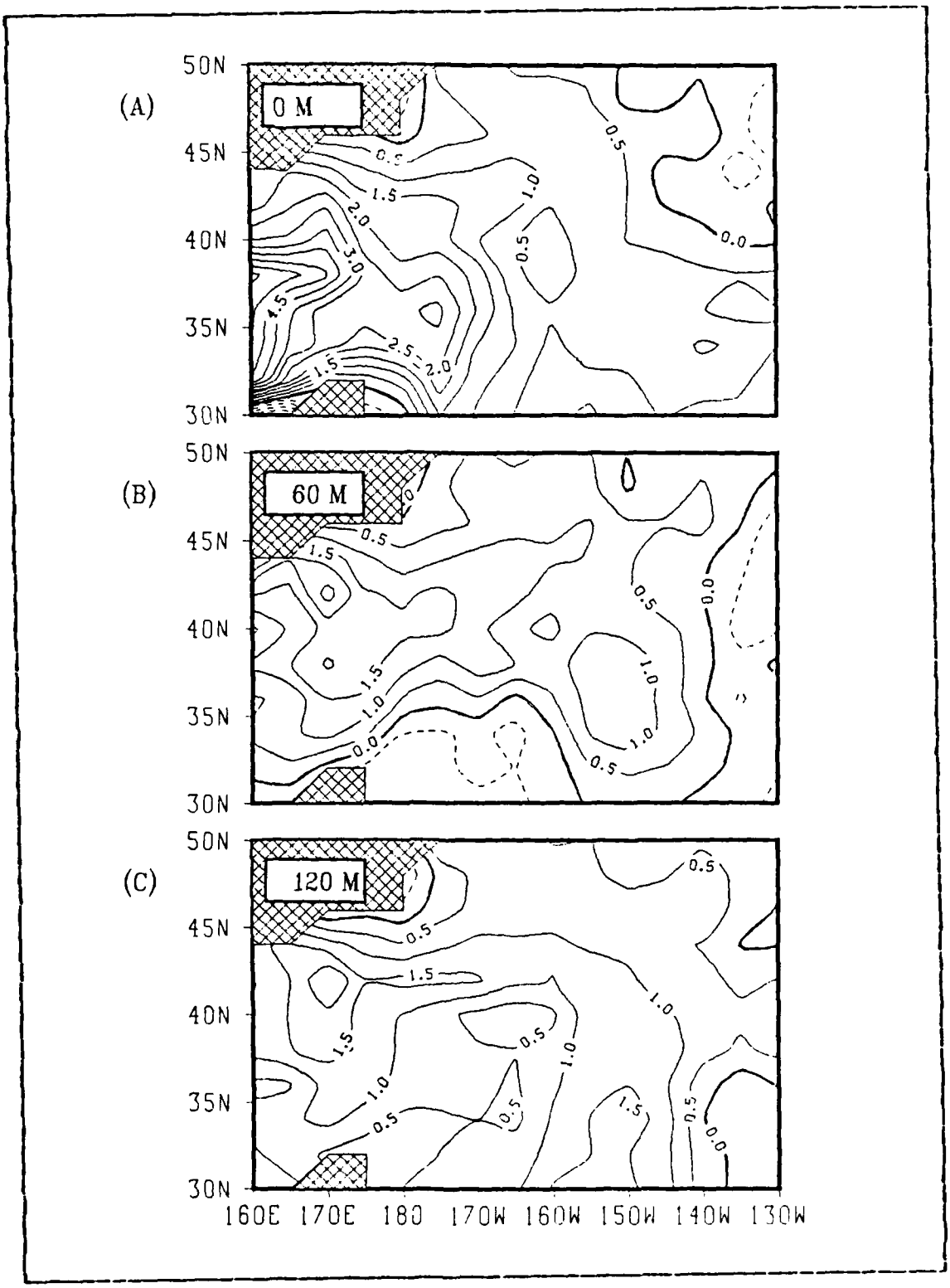

Figure 4.2 Similar to Figure 4.1 except for May 1976.

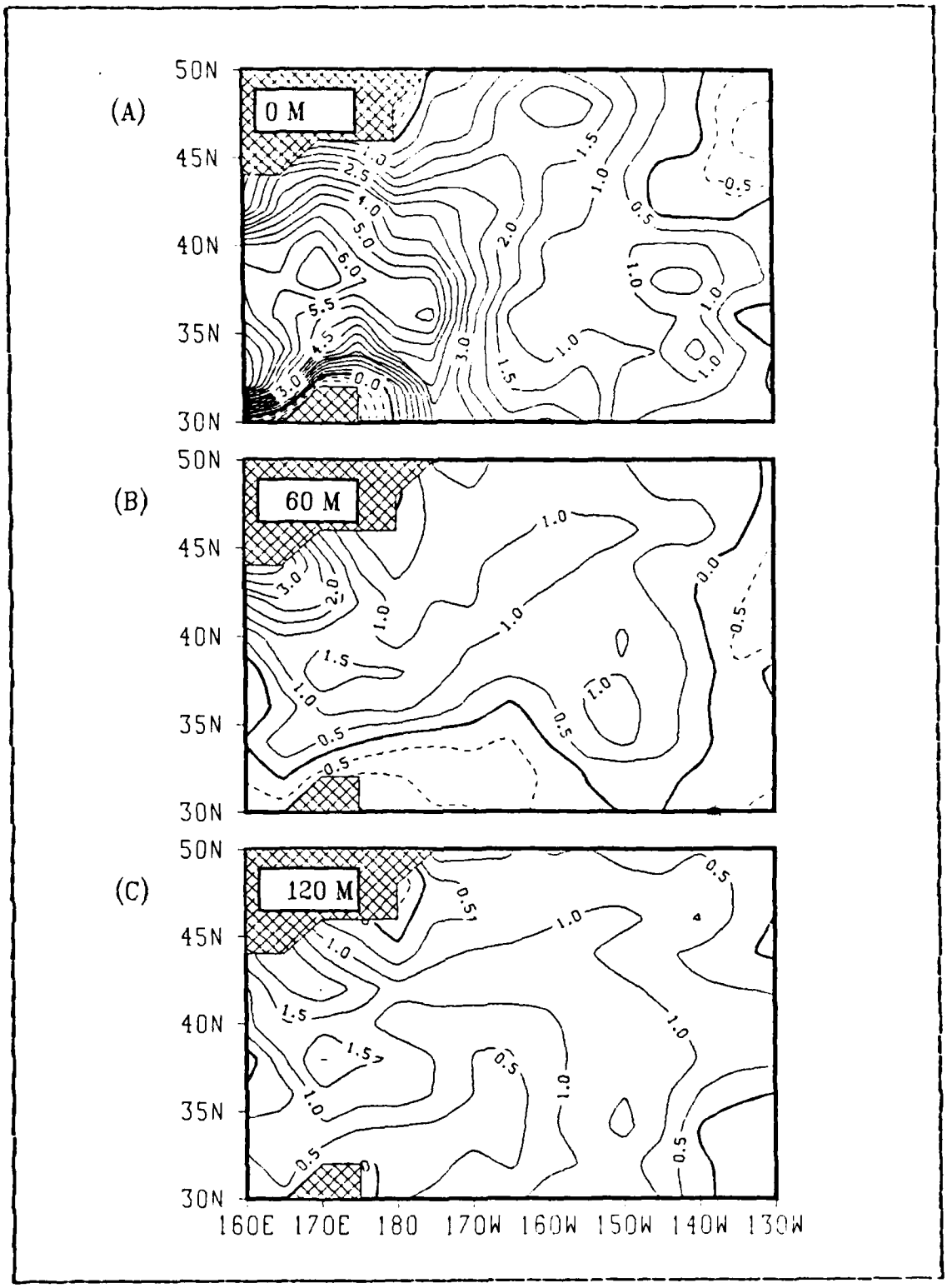

Figure 4.3 Similar to Figure 4.1 except for June 1976.

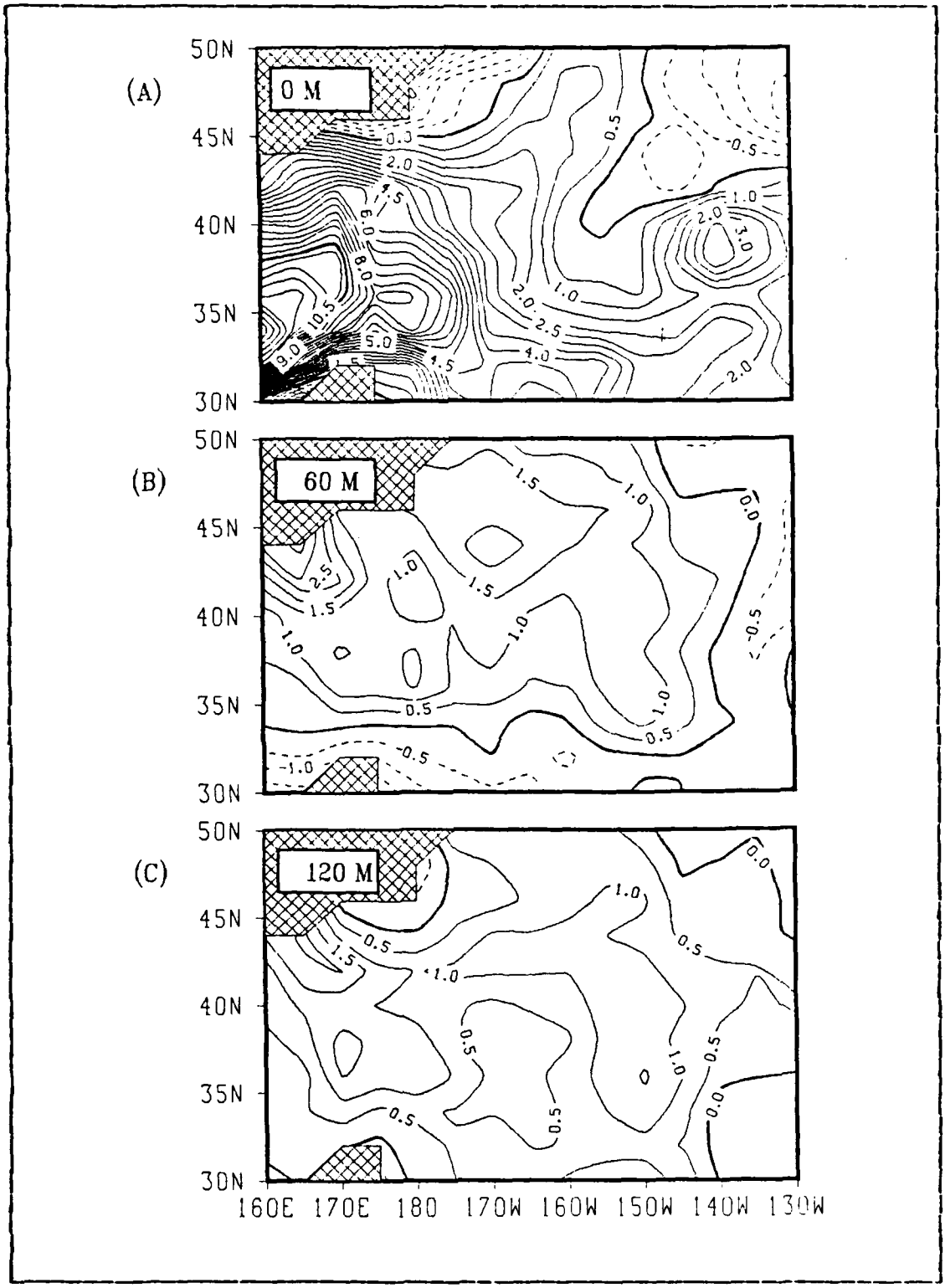

Figure 4.4 Similar to Figure 4.1 except for July 1976.

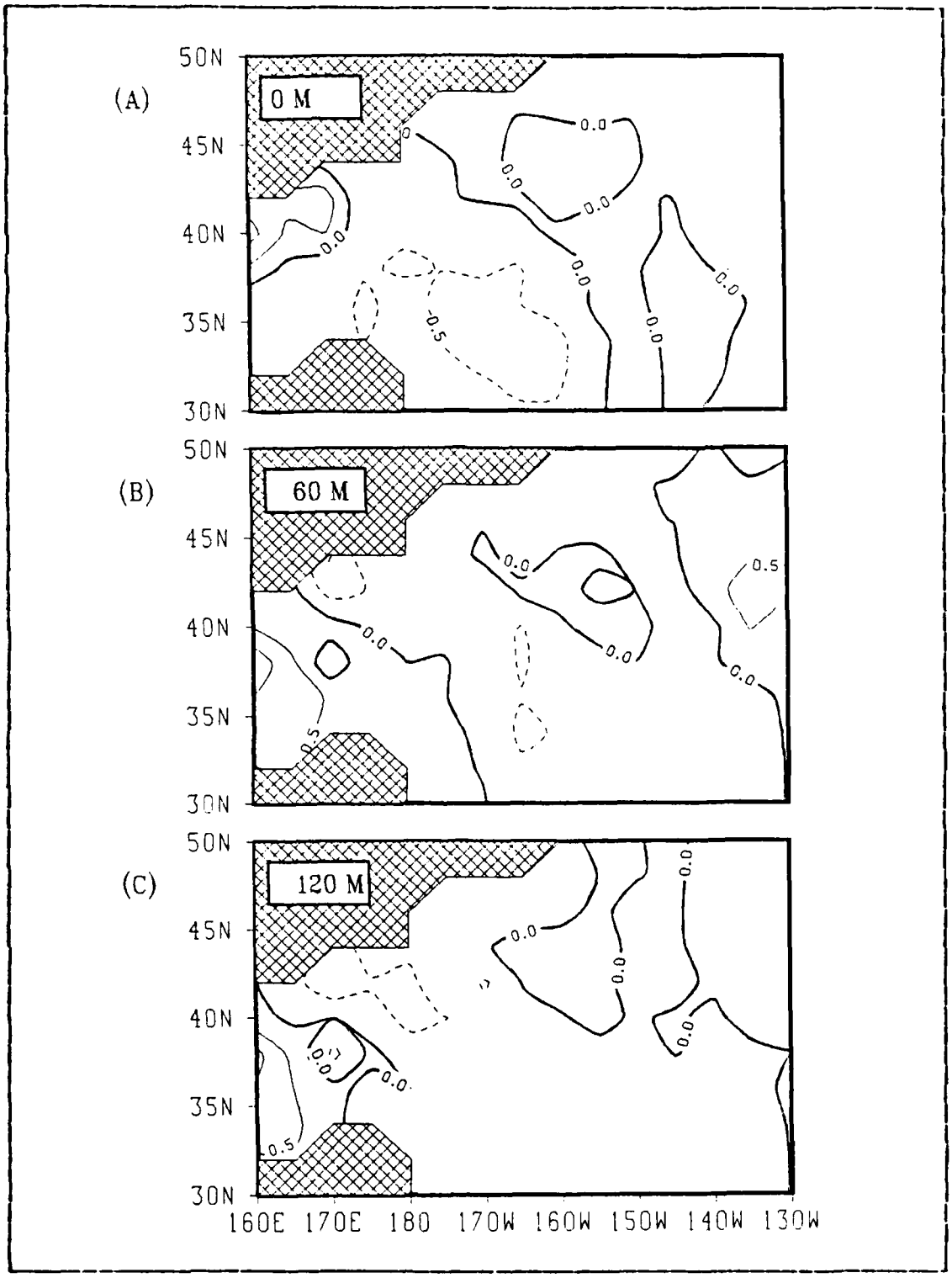

Figure 4.5 Model temperature anomaly MA 12-15 during June 1977 at (A) surface, (B) 60m, and (C) 120m.

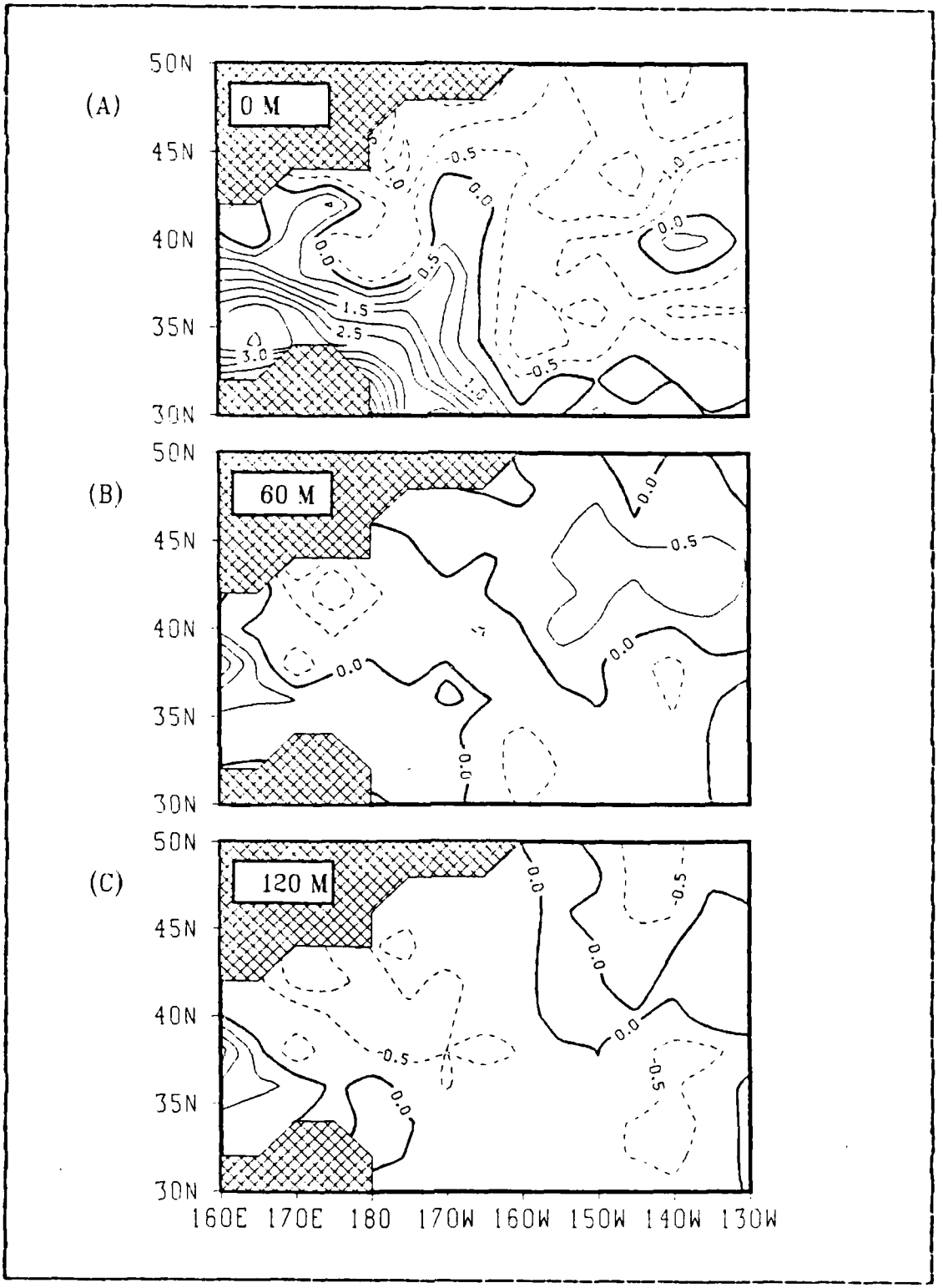

Figure 4.6 Similar to Figure 4.5 except for July 1977.

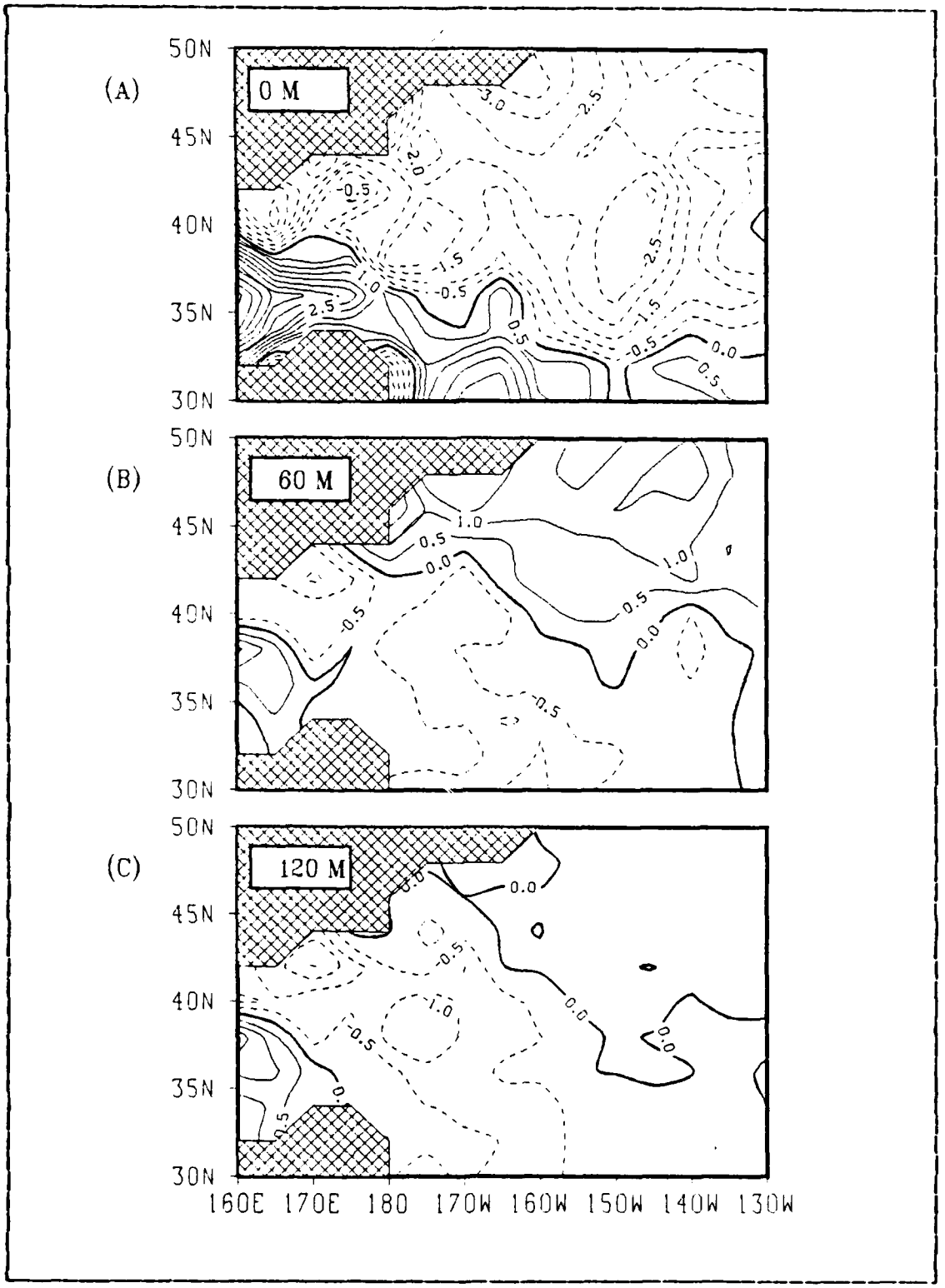

Figure 4.7 Similar to Figure 4.5 except for August 1977.

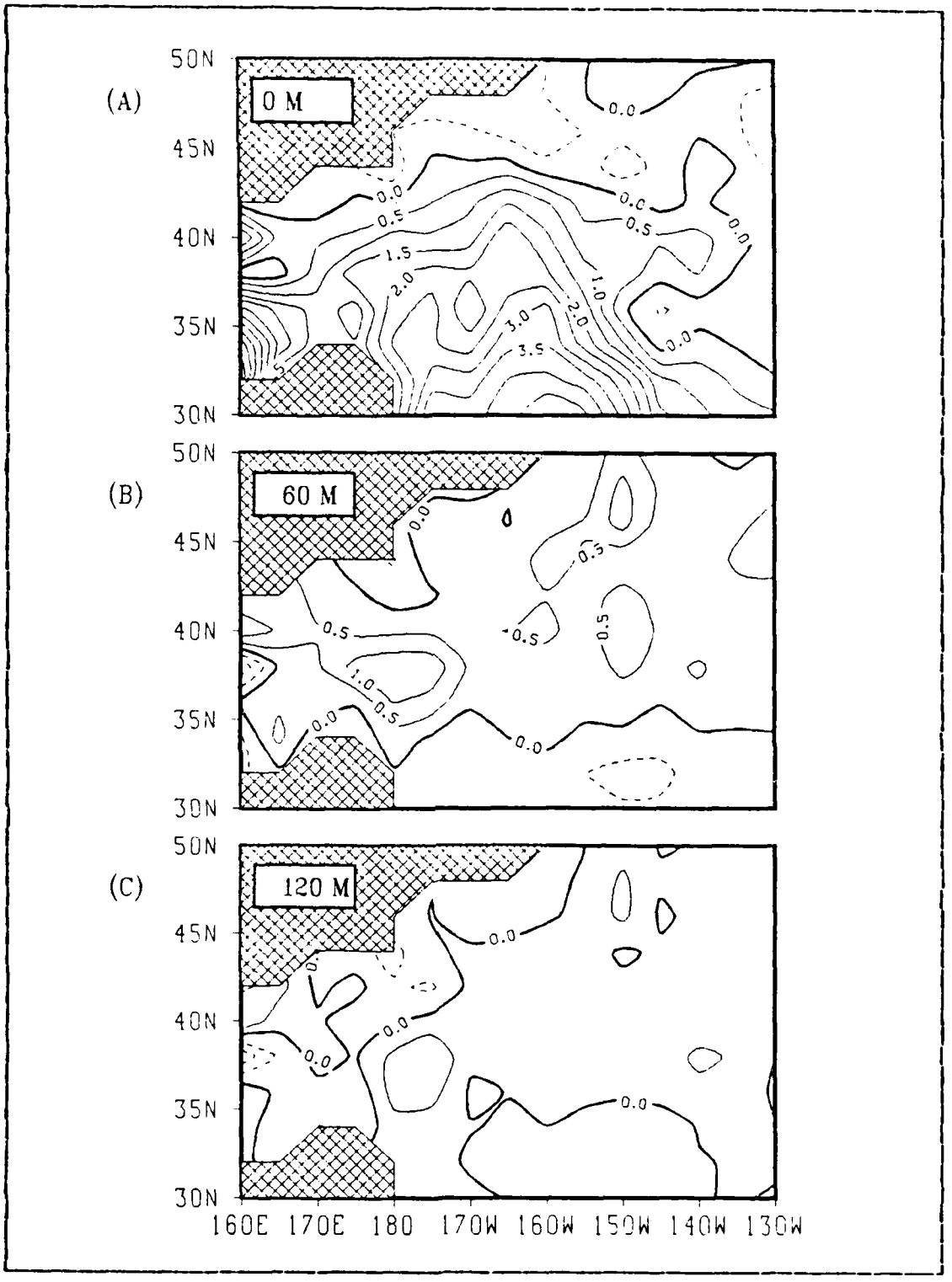

Figure 4.8 Similar to Figure 4.5 except for model initialization in May 1977.

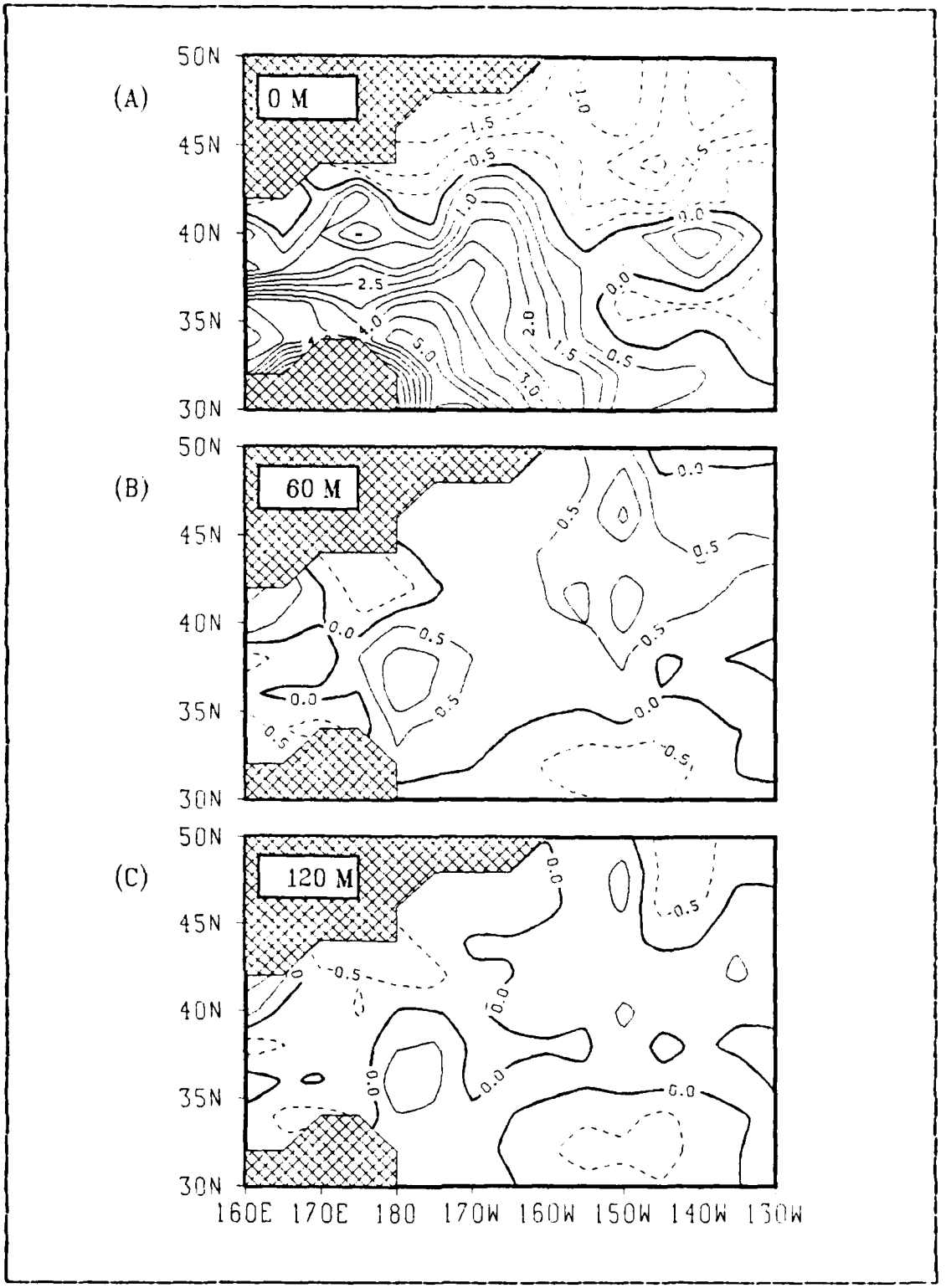

Figure 4.9 Similar to Figure 4.8 except for July 1977.

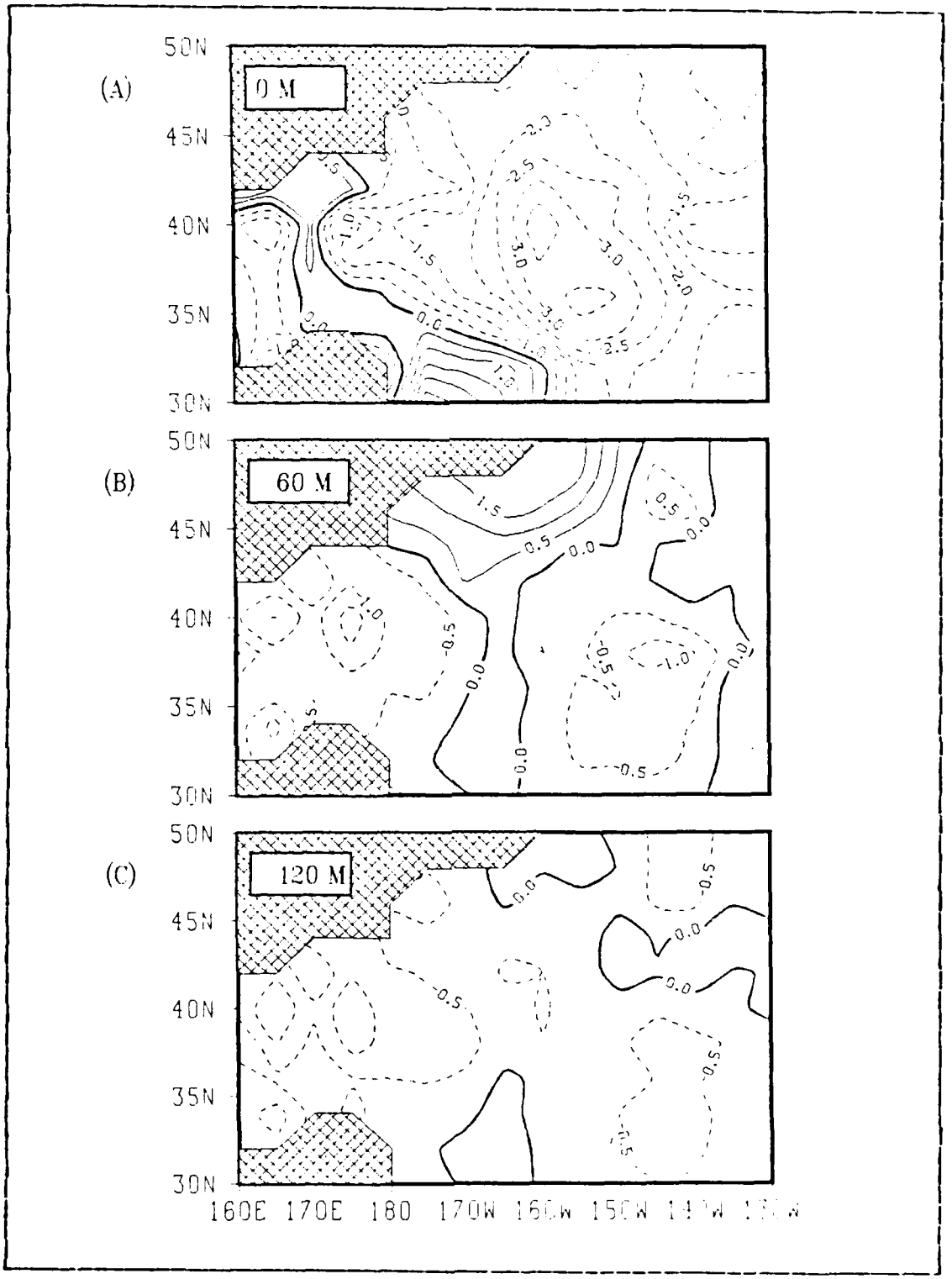

Figure 4.10 Model temperature anomaly MA 23 during July 1978 at (A) surface, (B) 60m, and (C) 120m.

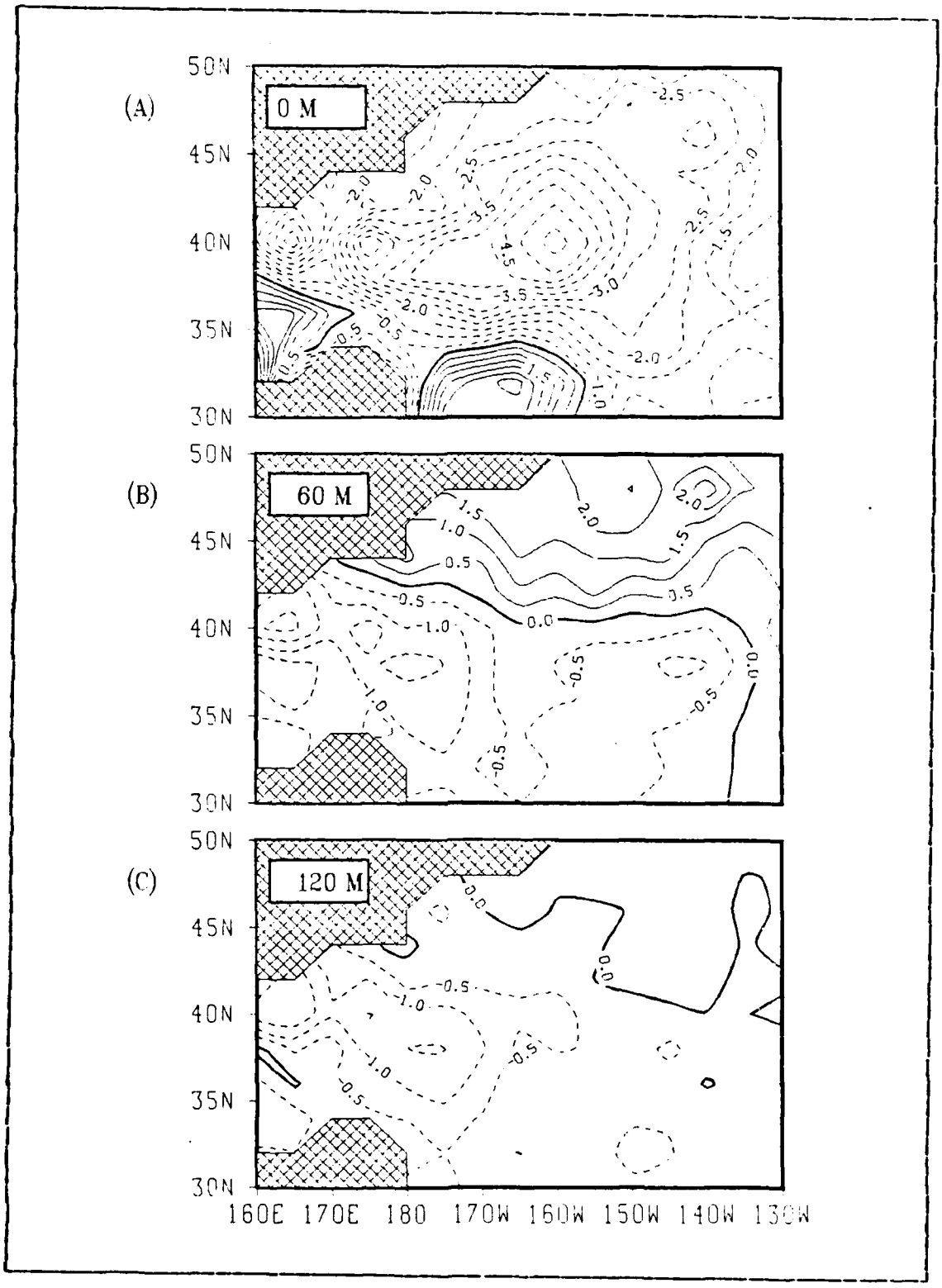

Figure 4.11 Similar to Figure 4.10 except for August 1978.

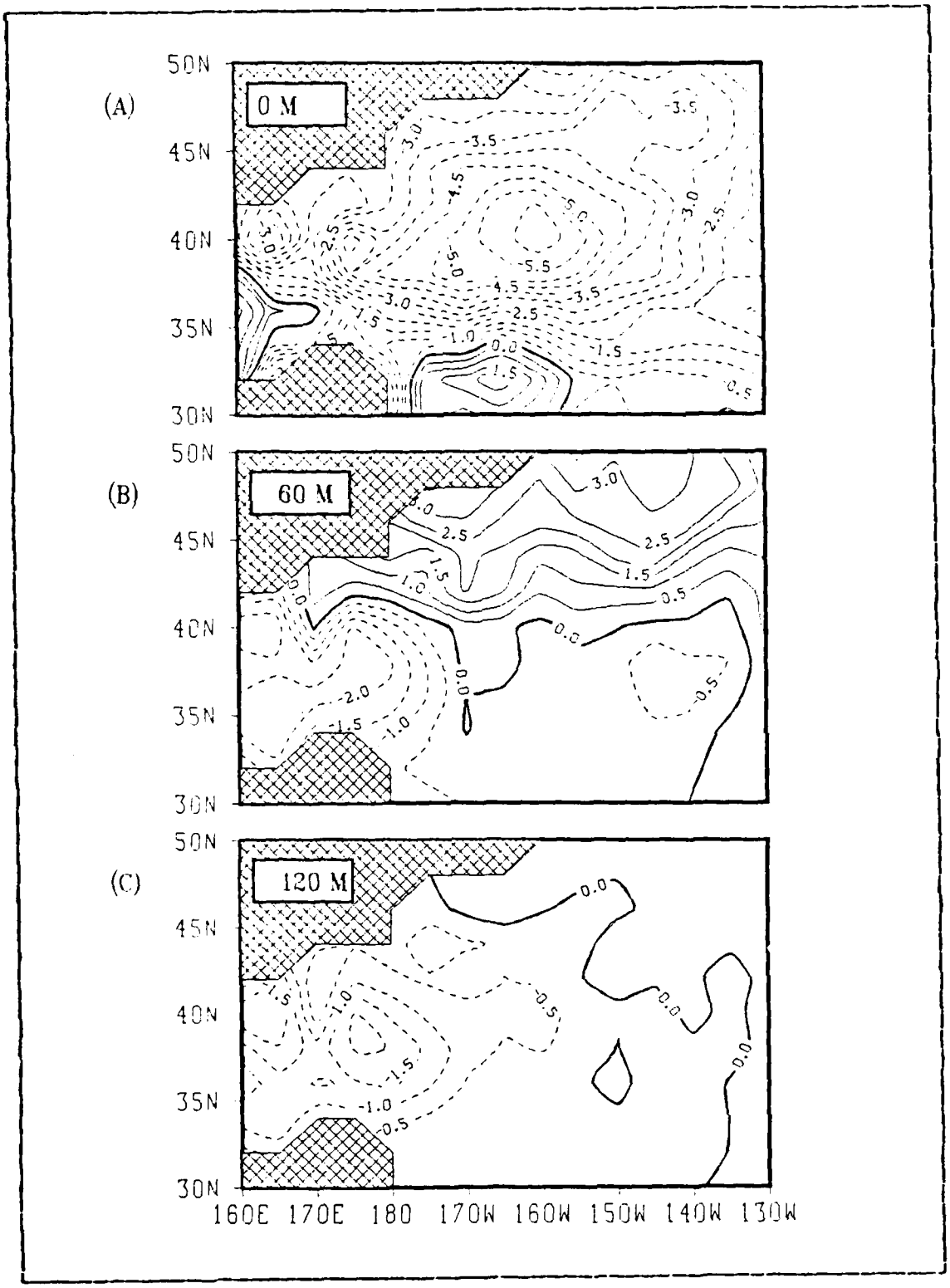

Figure 4.12 Similar to Figure 4.10 except for September 1978.

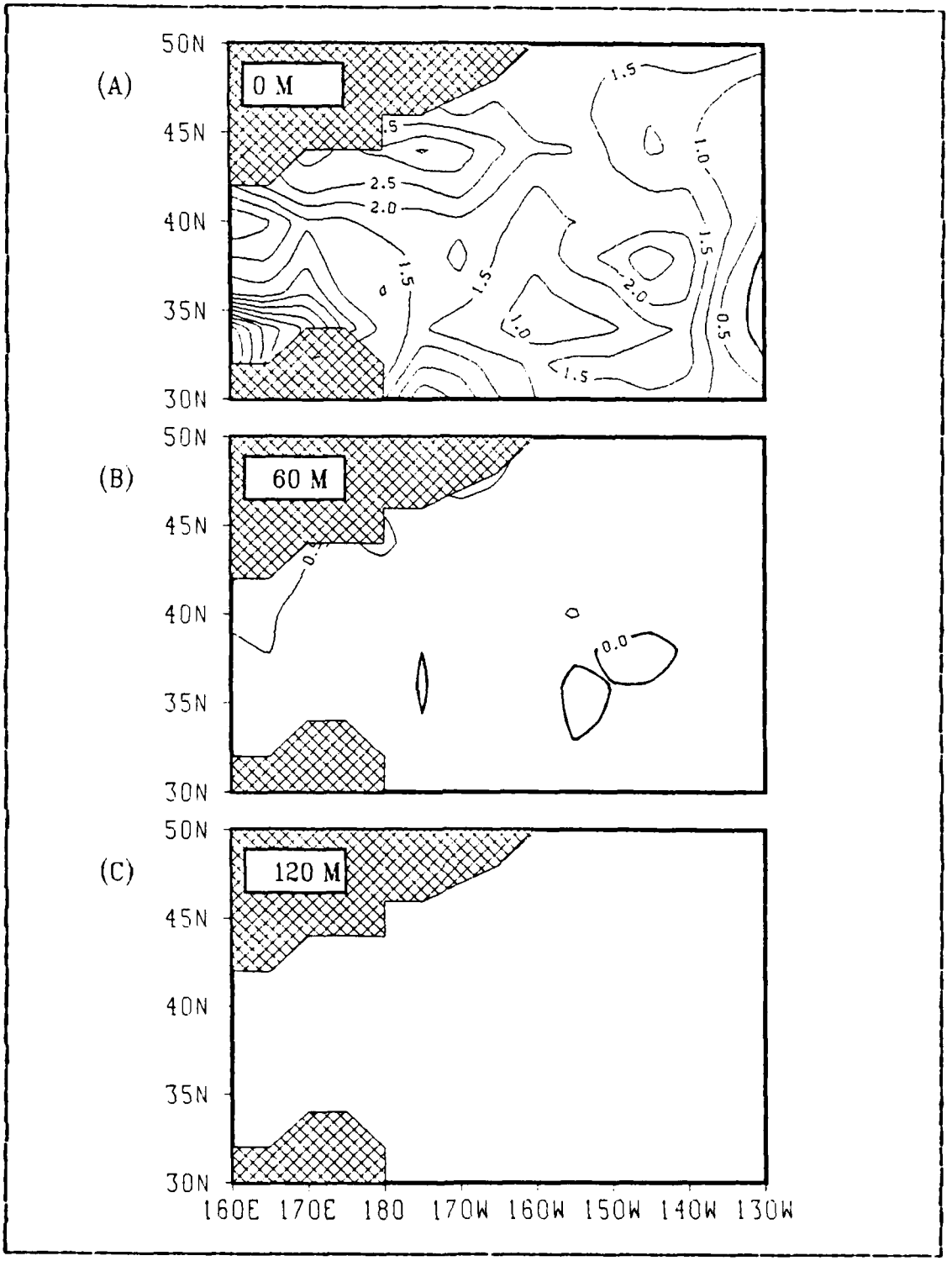

Figure 4.13 Model monthly temperature difference MA 1/2 for June to May with the one-dimensional heat budget correction field.

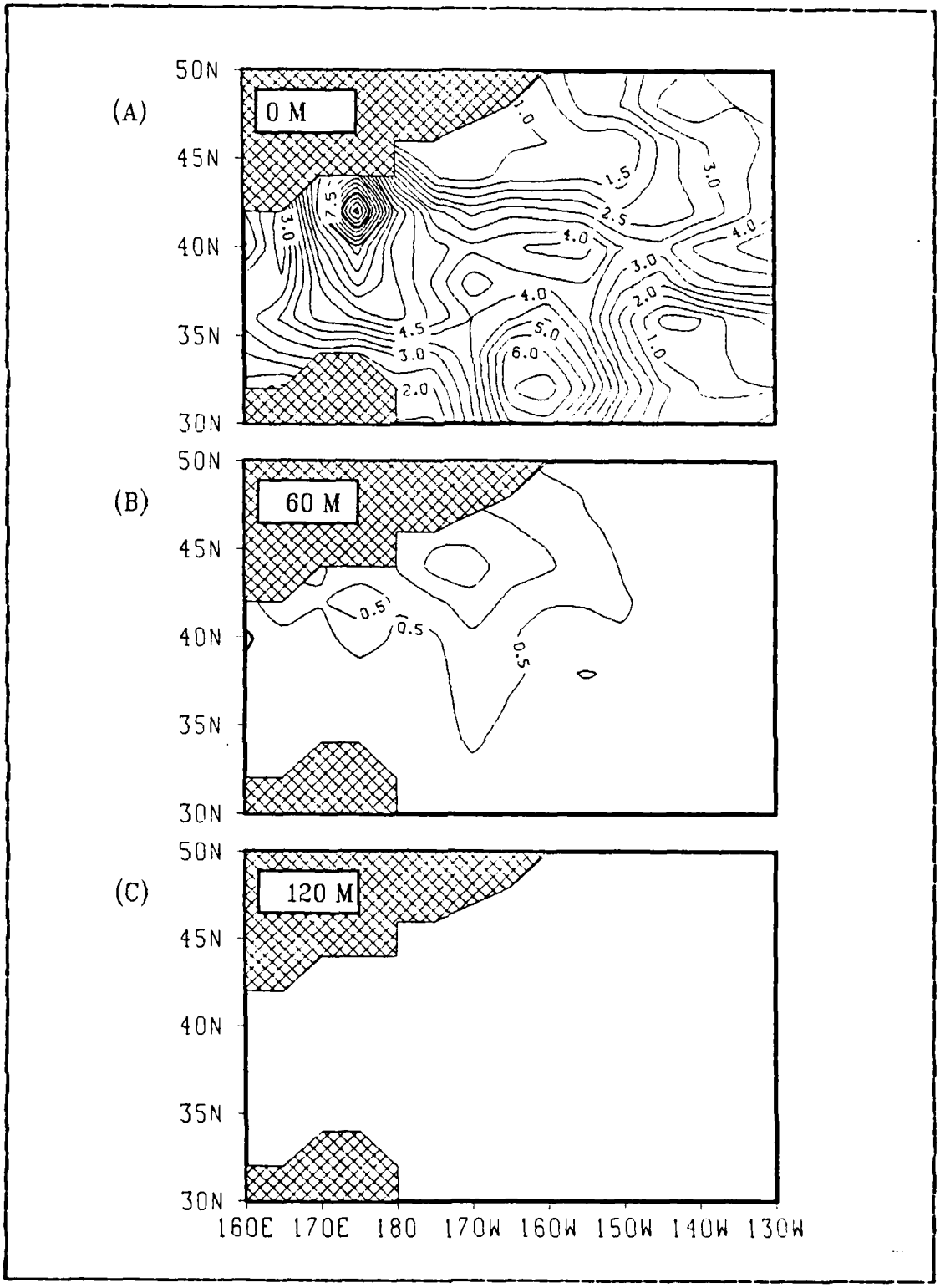

Figure 4.14 Similar to Figure 4.13 except for July to June.

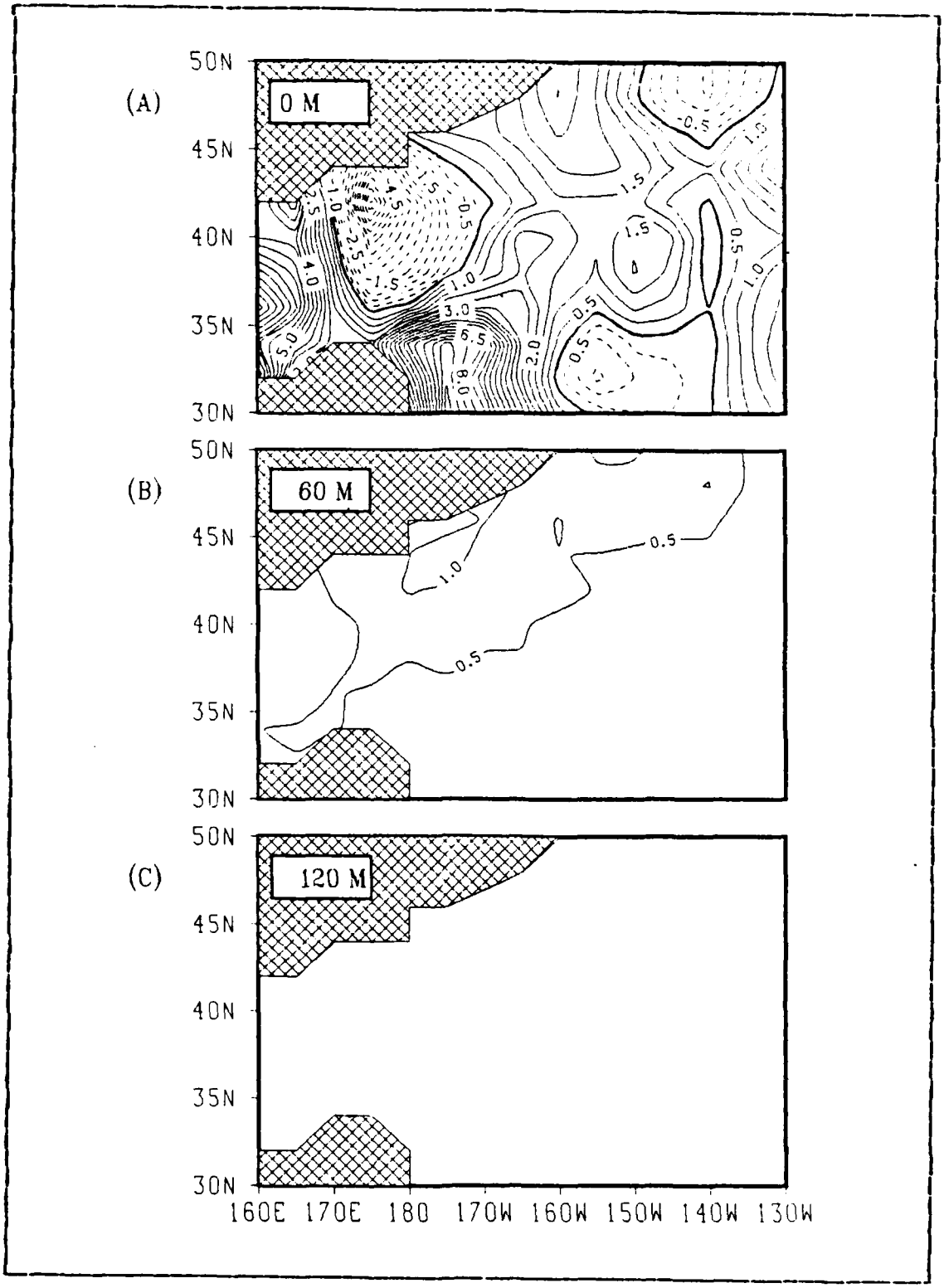

Figure 4.15 Similar to Figure 4.13 except for August to July.

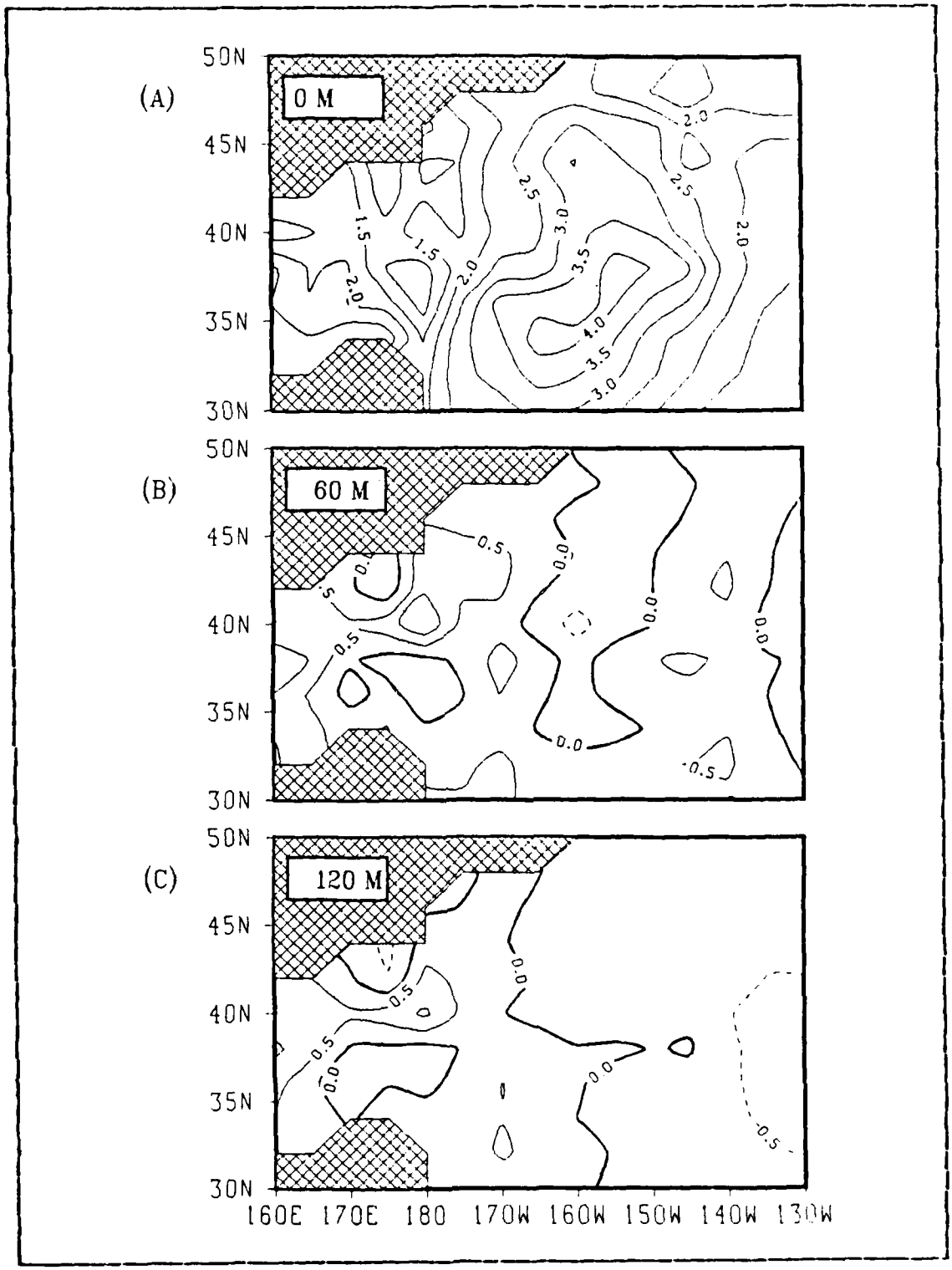

Figure 4.16 Observed monthly temperature difference WA 1/2 for June to May.

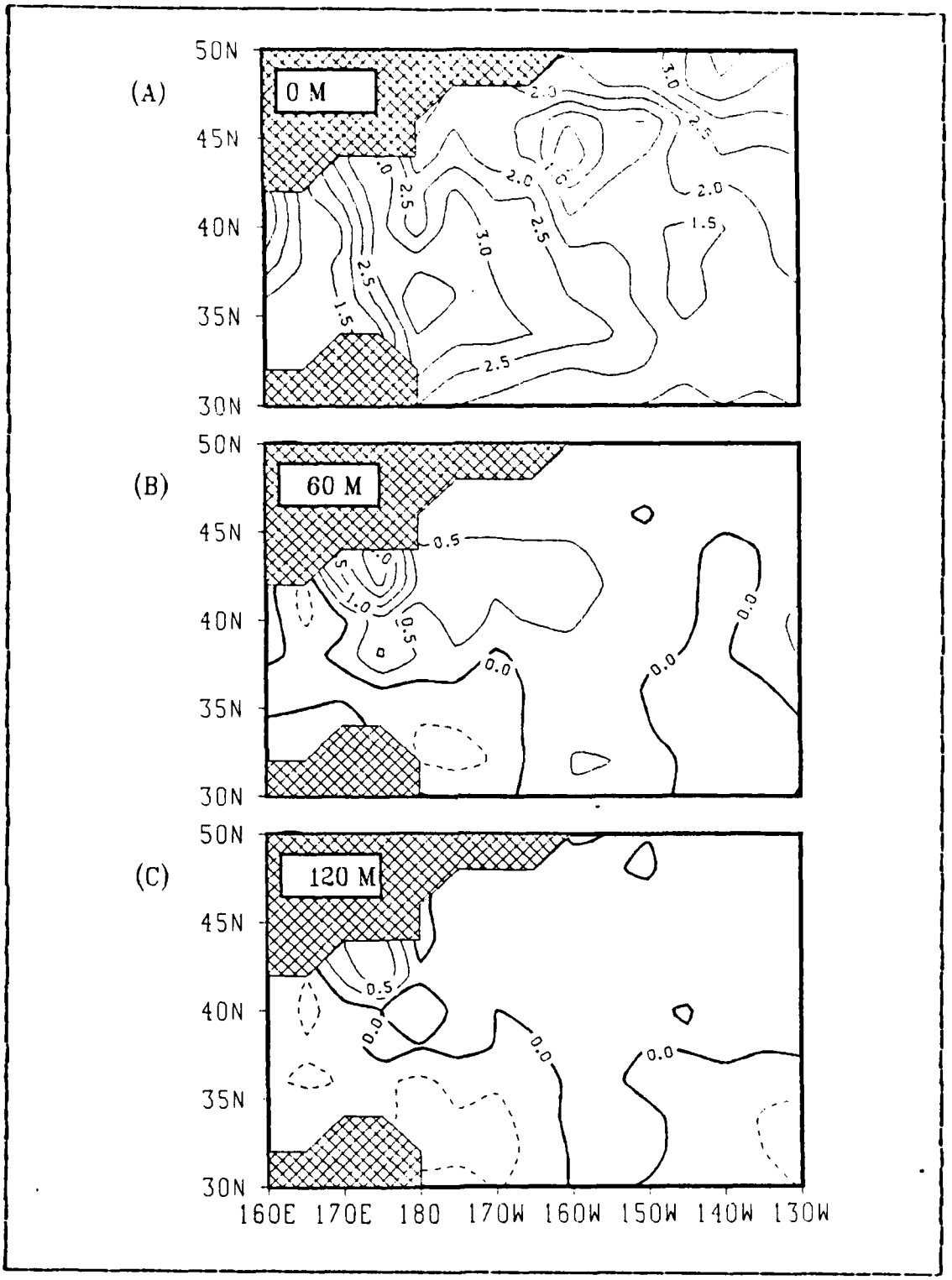

Figure 4.17 Similar to Figure 4.16 except for July to June.

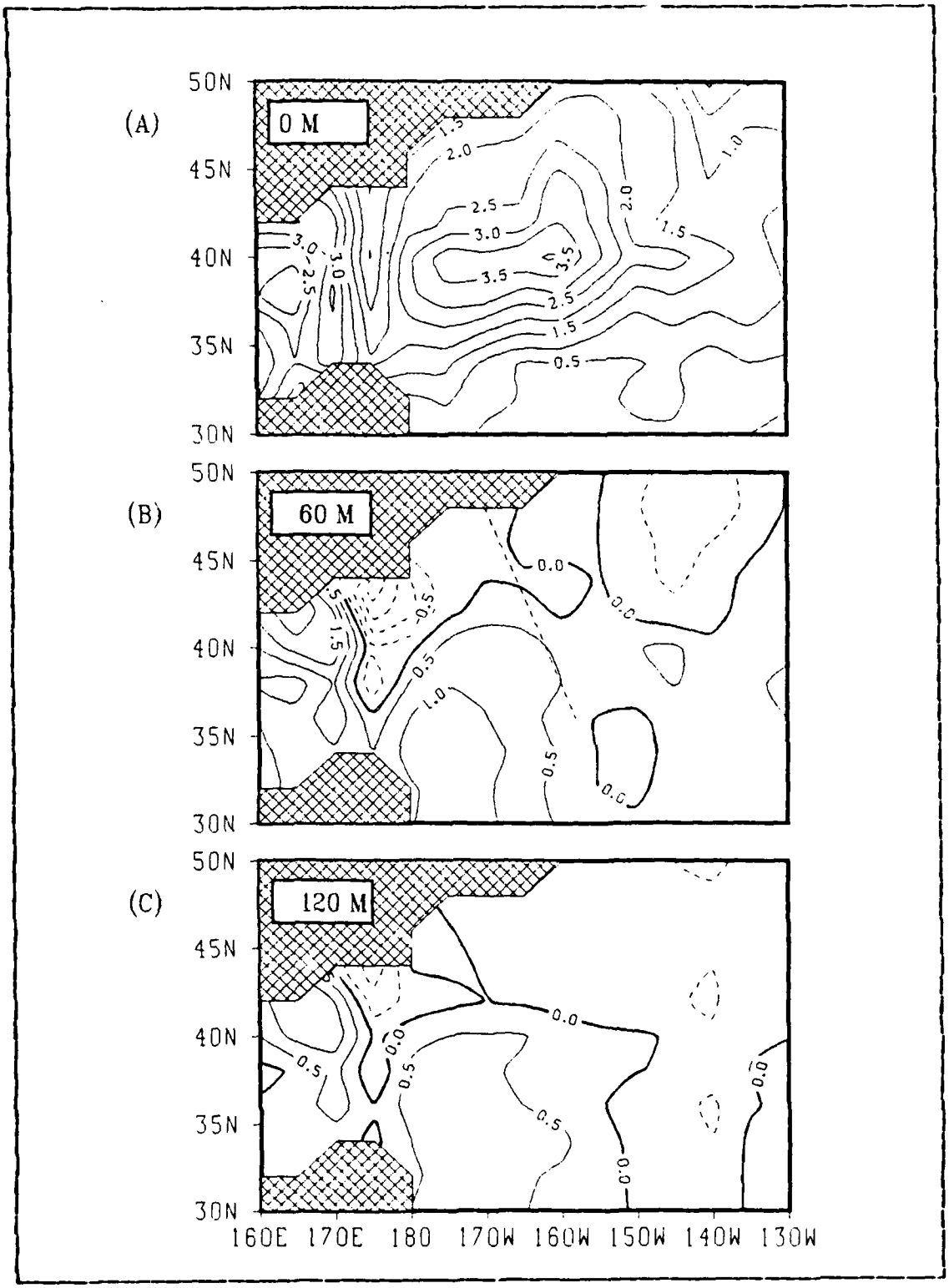

Figure 4.18 Similar to Figure 4.16 except for August to July.

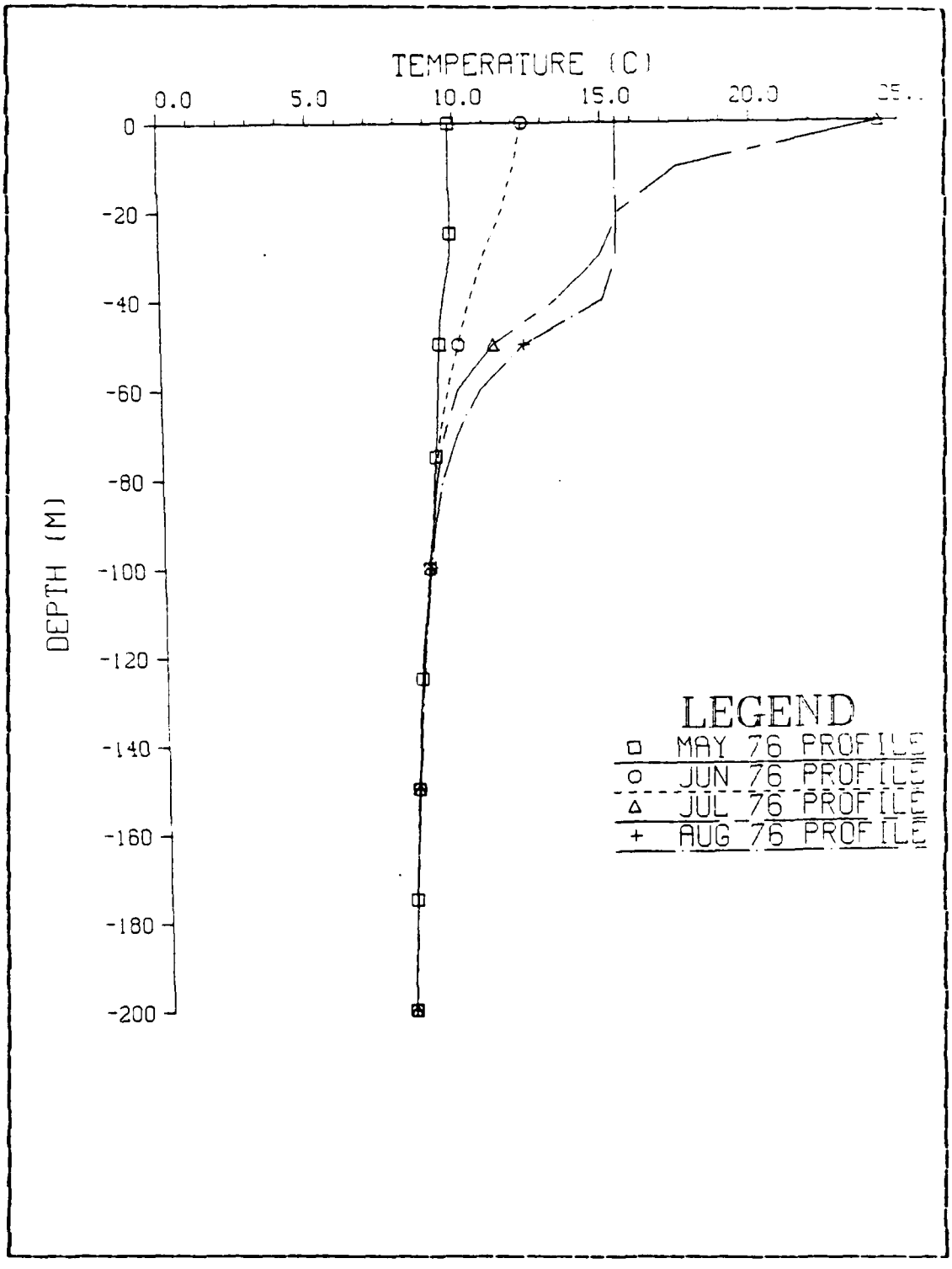

Figure 4.19 Model temperature profiles for May through August 1976 at 42N, 175E with one-dimensional heat budget correction.

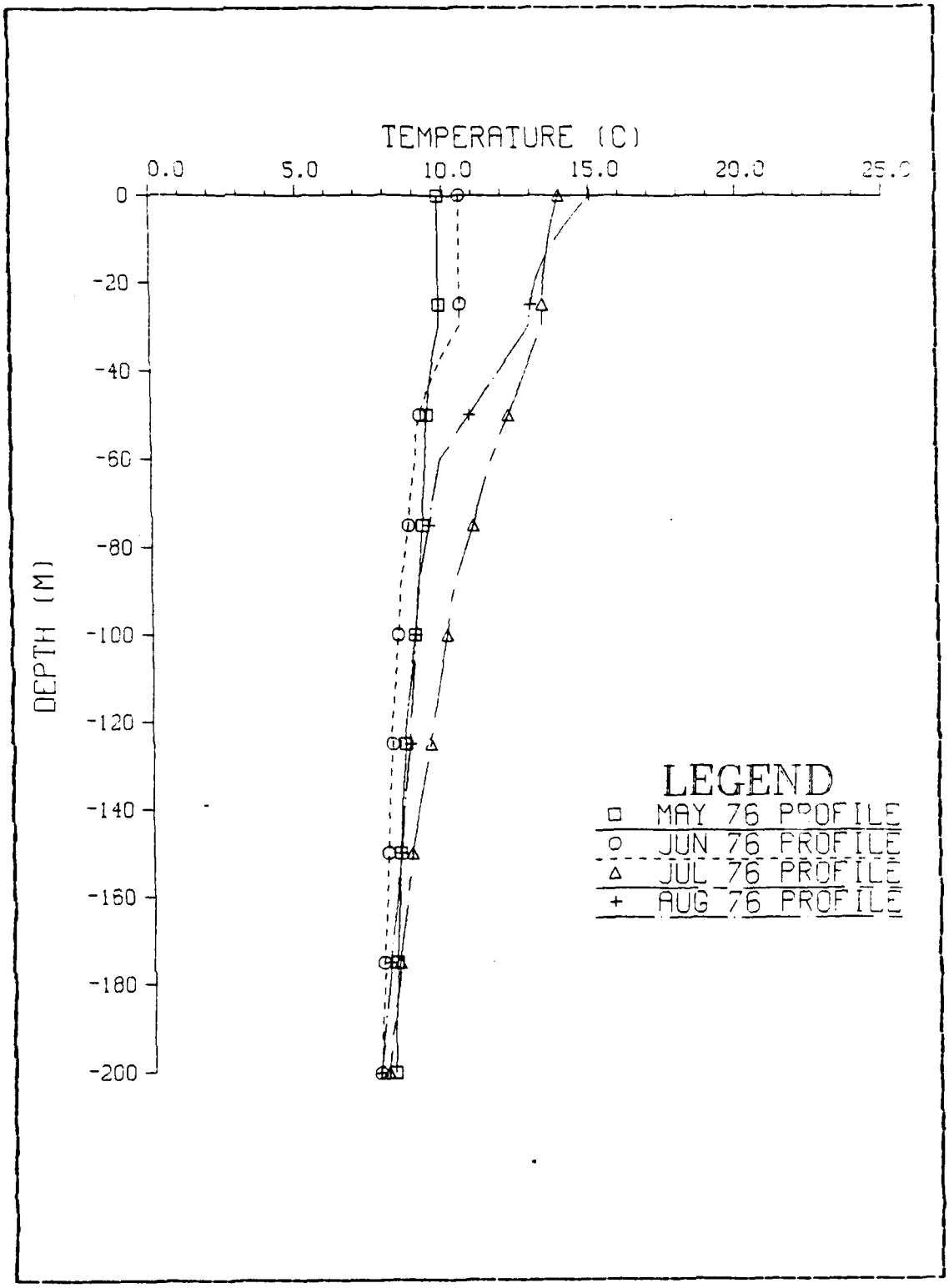

Figure 4.20 Similar to Figure 4.19 except for observed values.

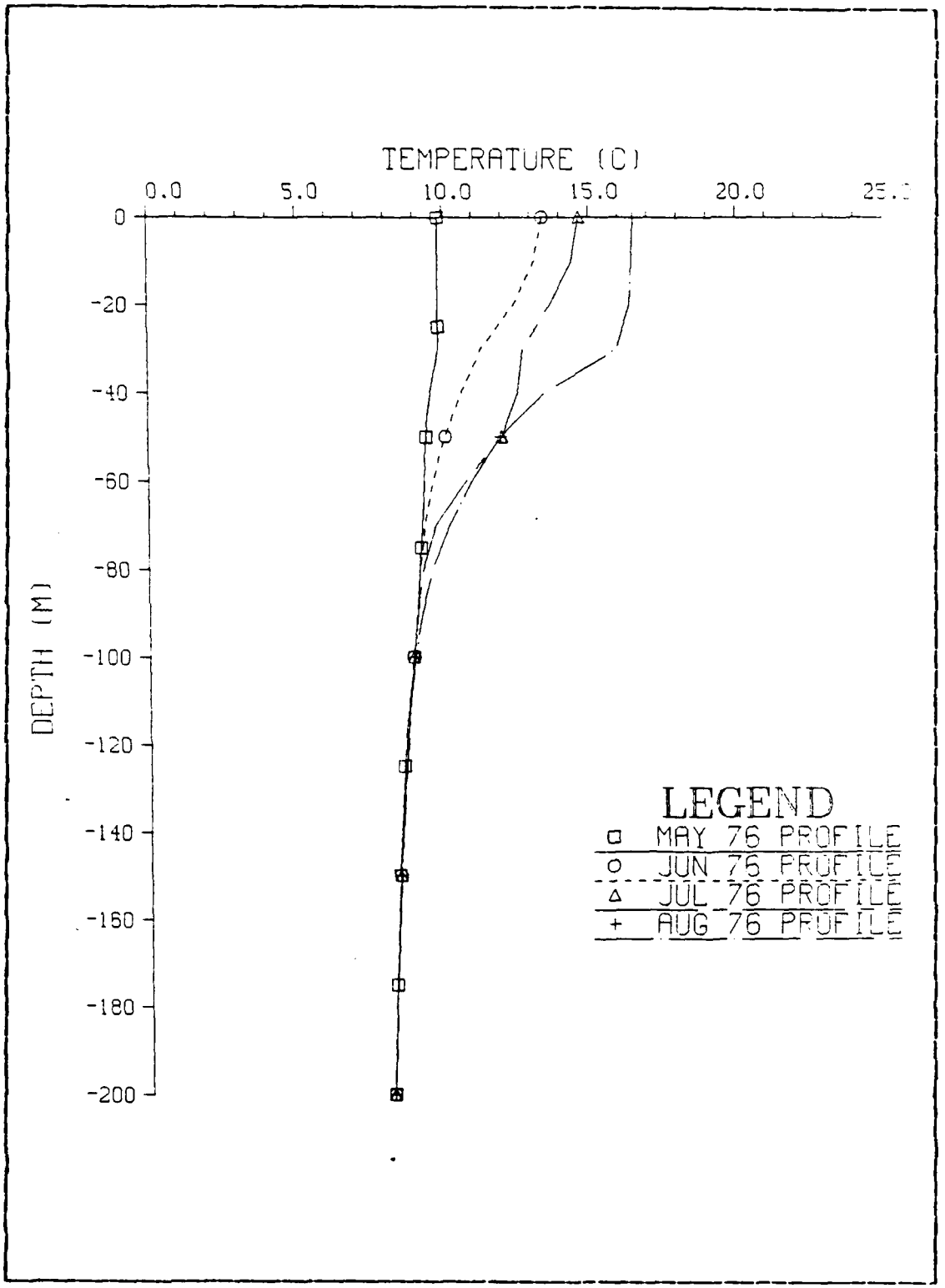

Figure 4.21 Similar to Figure 4.19 except with added corrections.

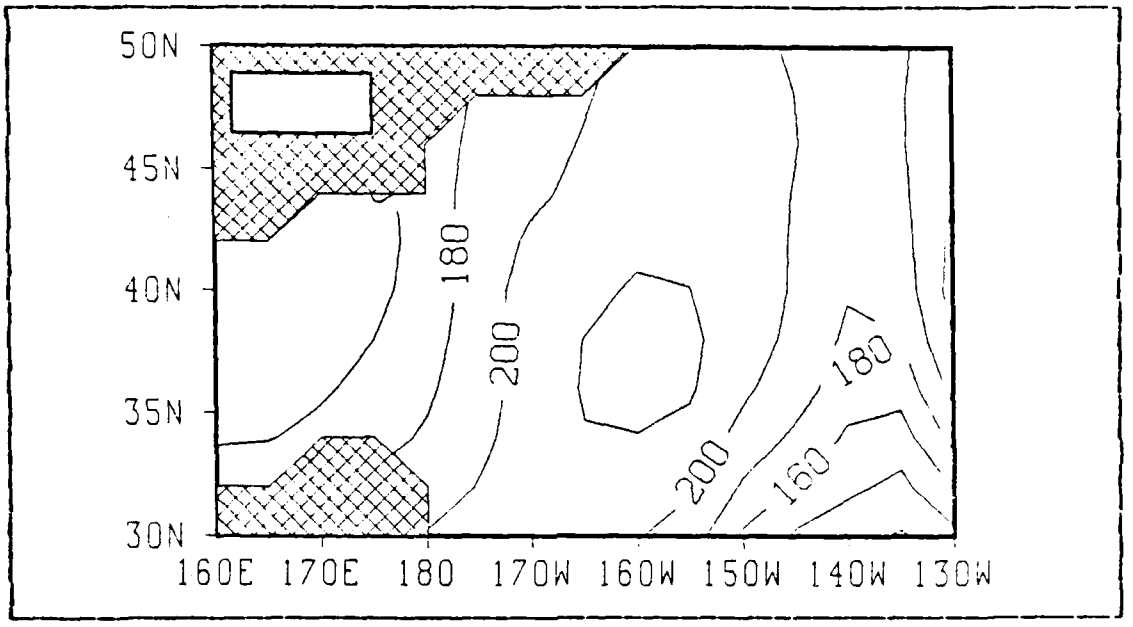

Figure 4.22 Climatological total heat flux for May.

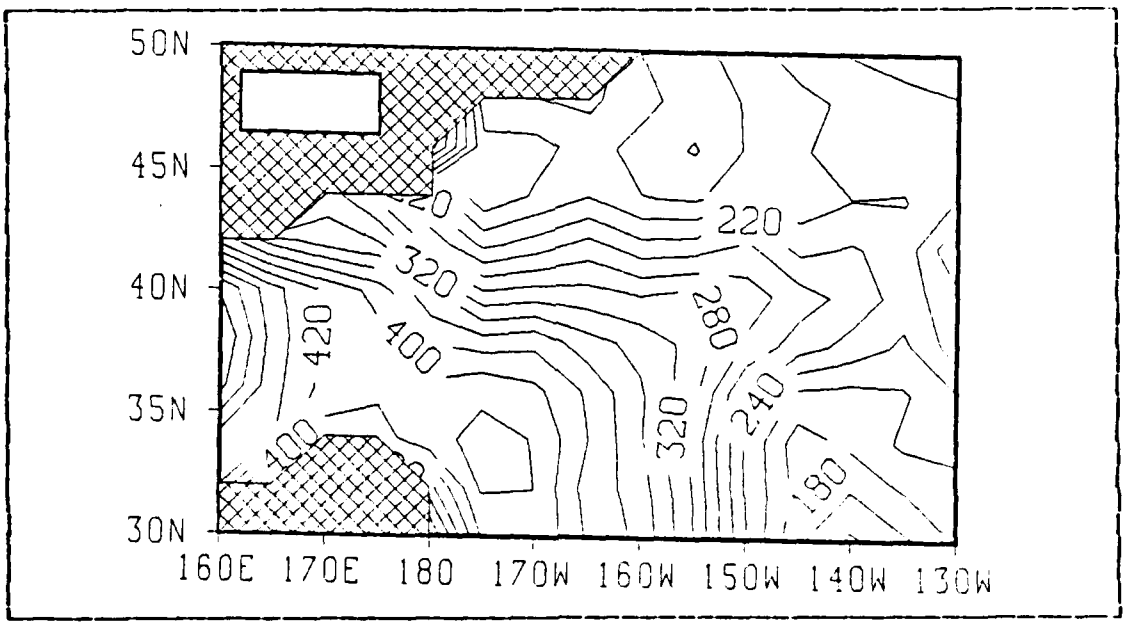

Figure 4.23 FNOC average total heat flux for May.

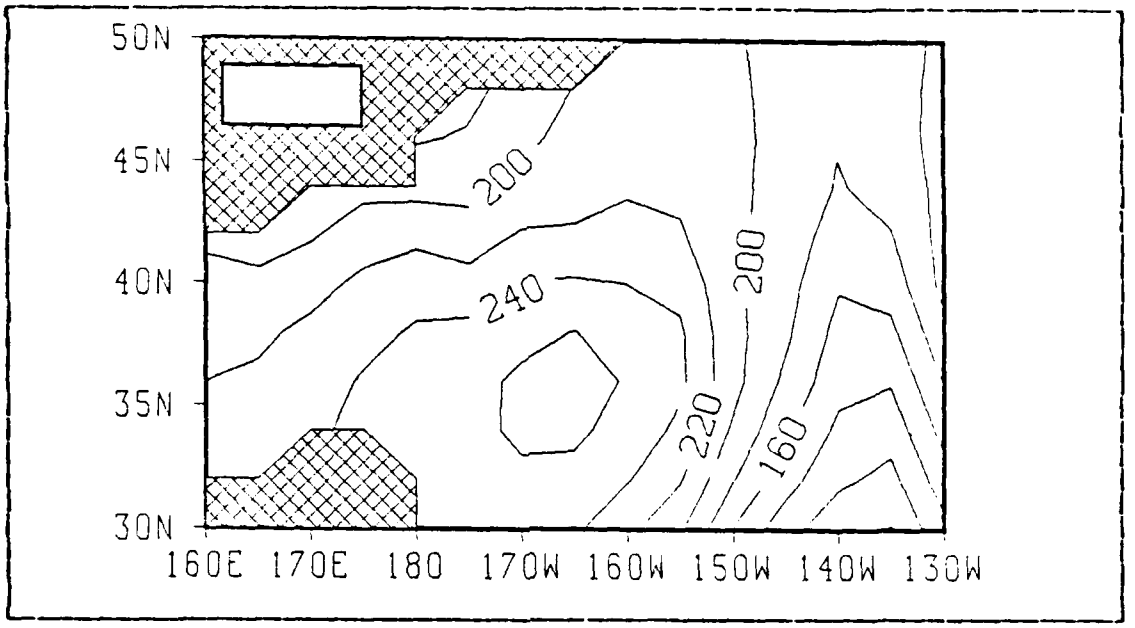

Figure 4.24 Similar to Figure 4.22 except for June.

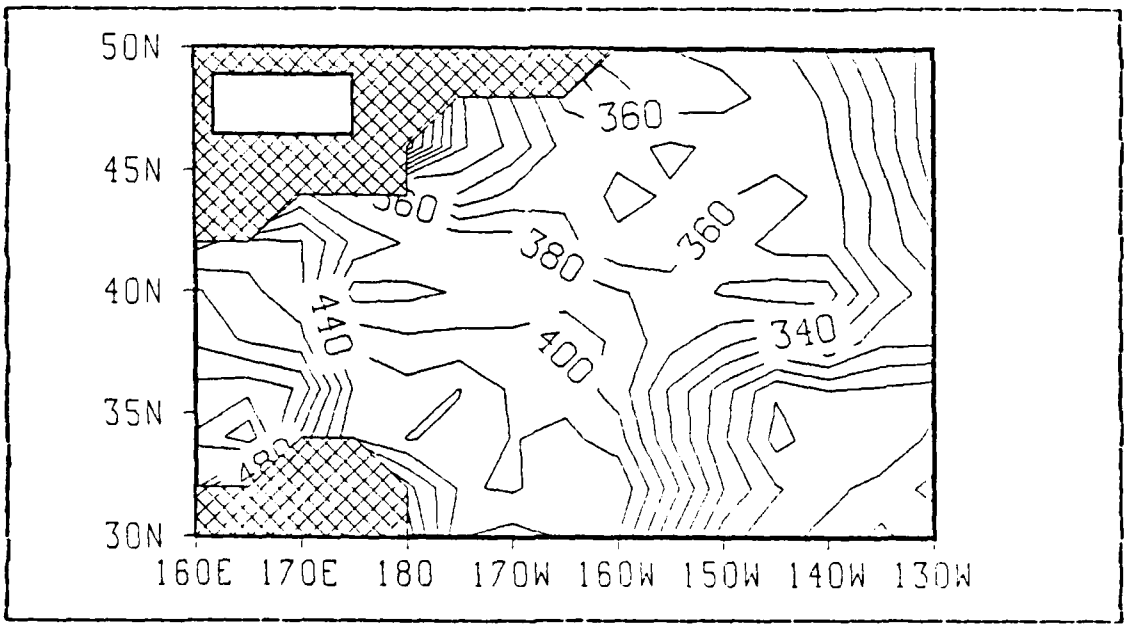

Figure 4.25 Similar to Figure 4.23 except for June.

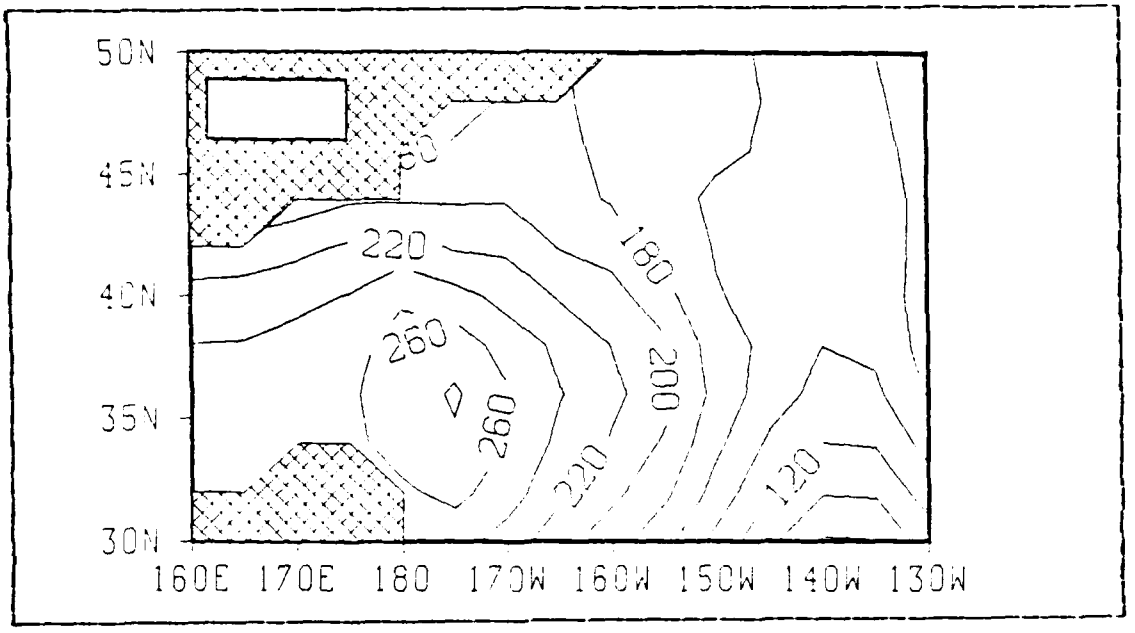

Figure 4.26 Similar to Figure 4.22 except for July.

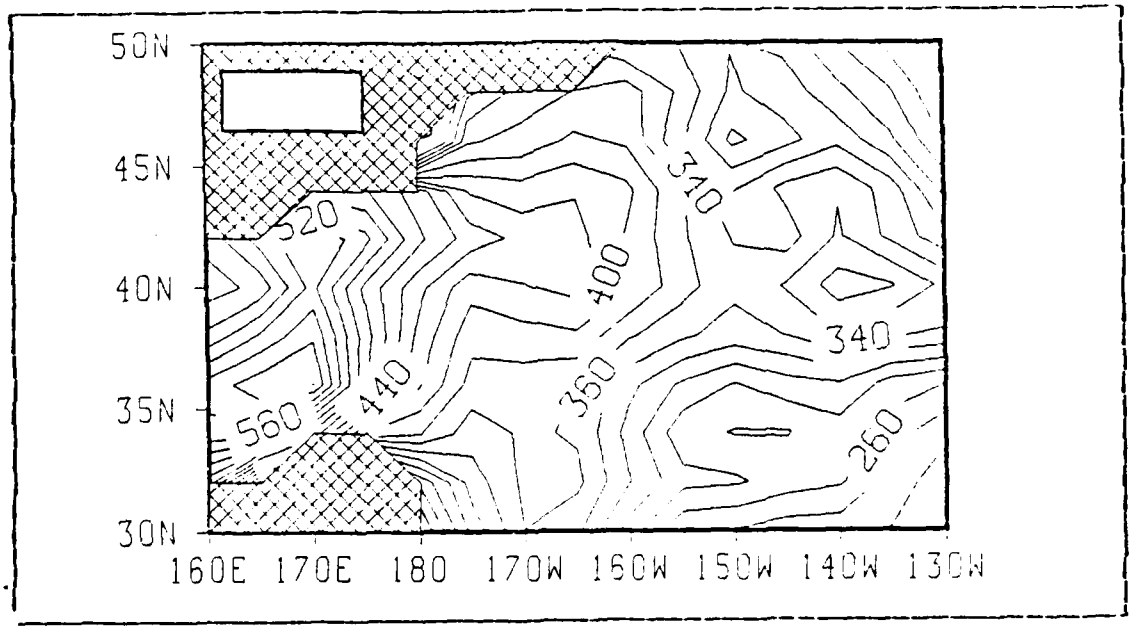

Figure 4.27 Similar to Figure 4.23 except for July.

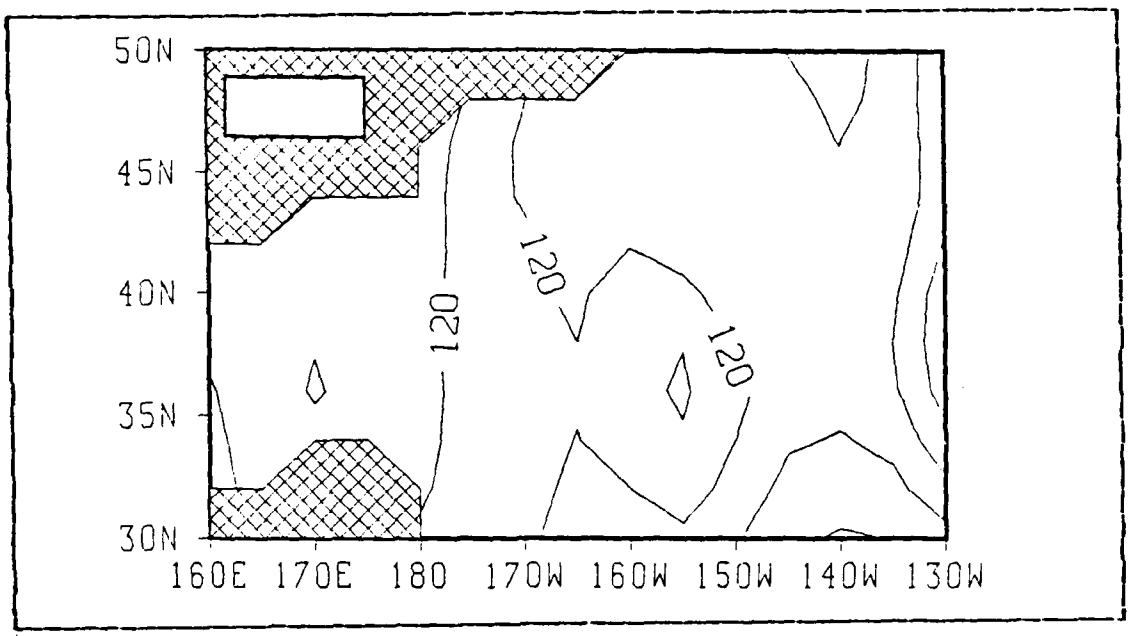

Figure 4.28 Similar to Figure 4.22 except for August.

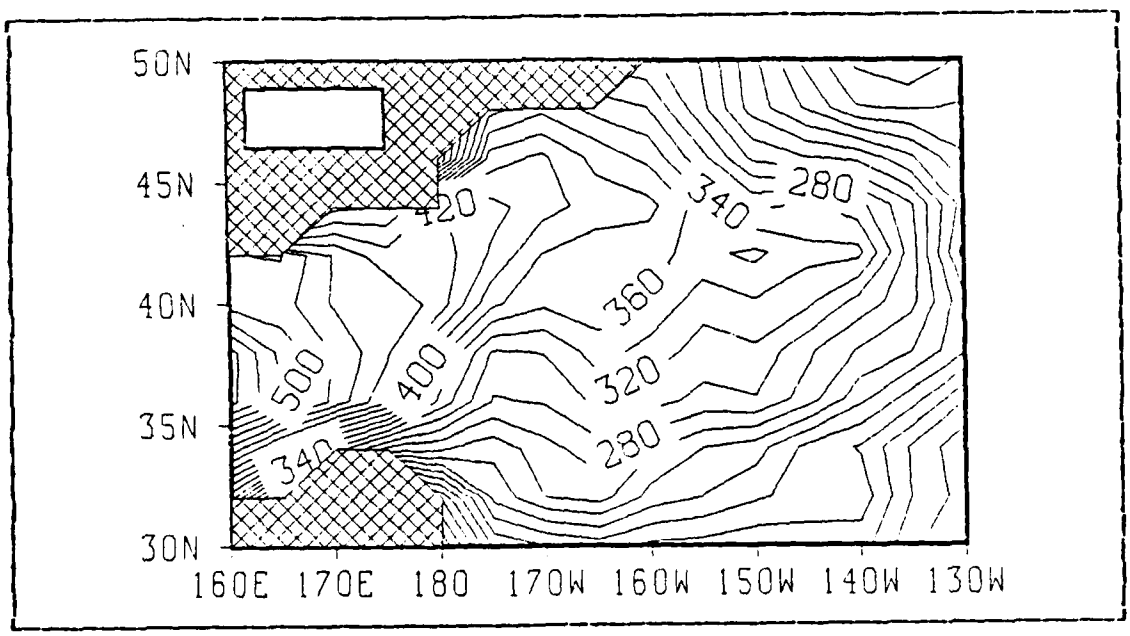

Figure 4.29 Similar to Figure 4.23 except for August.

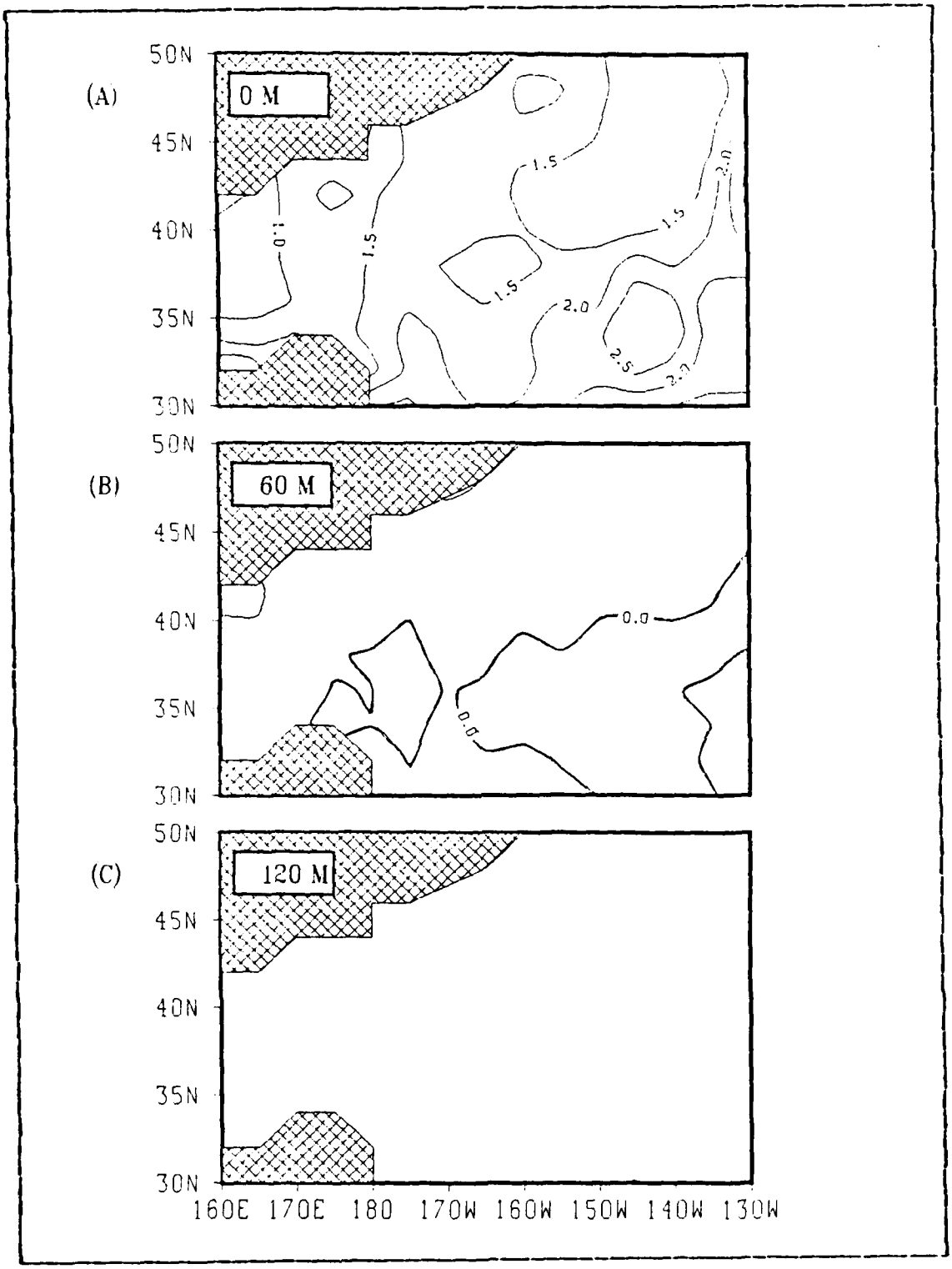

Figure 4.30 Model monthly temperature difference MA 1/2 for June to May with climatological heat flux field (Case I).

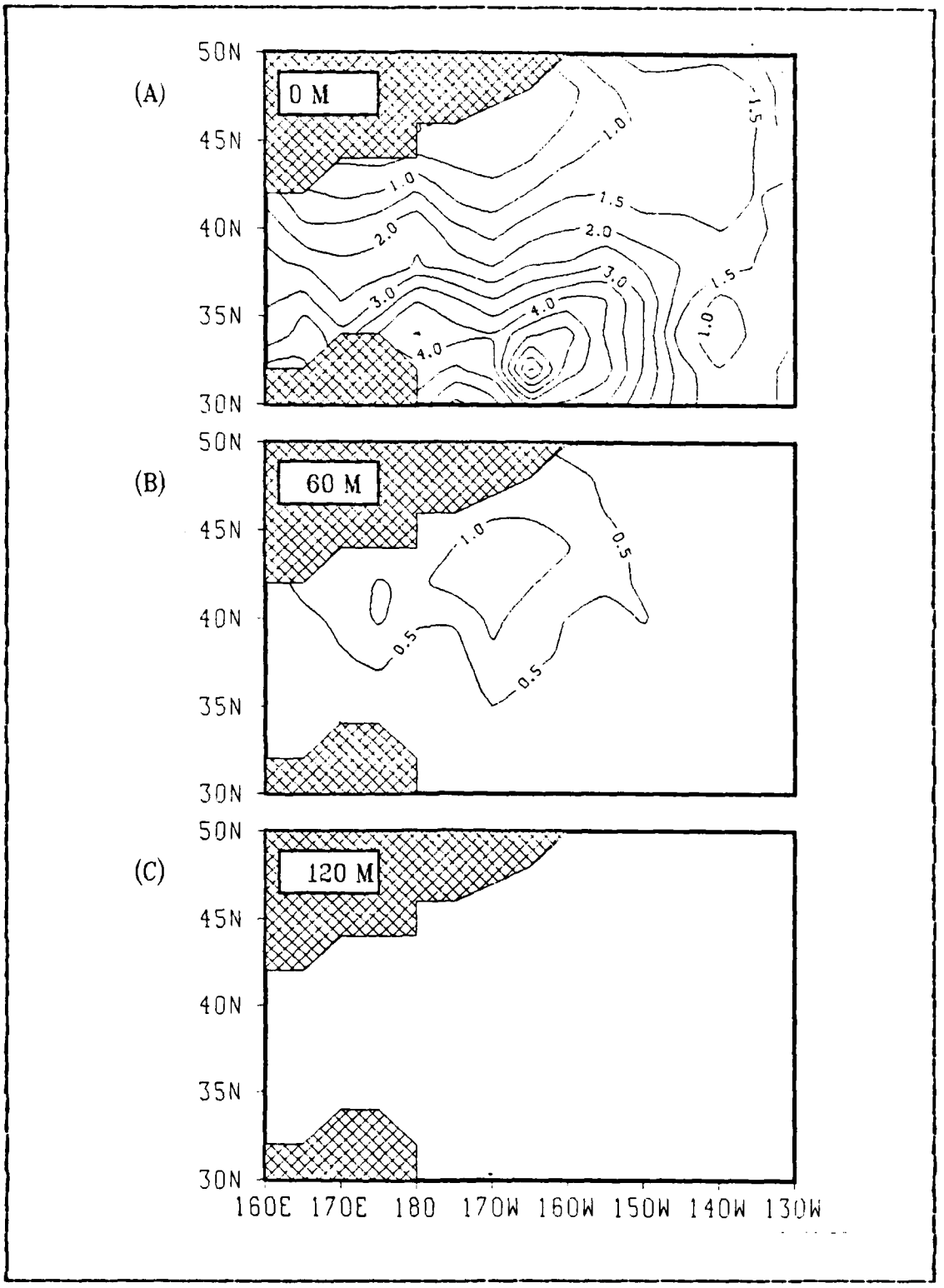

Figure 4.31 Similar to Figure 4.30 except for July to June.

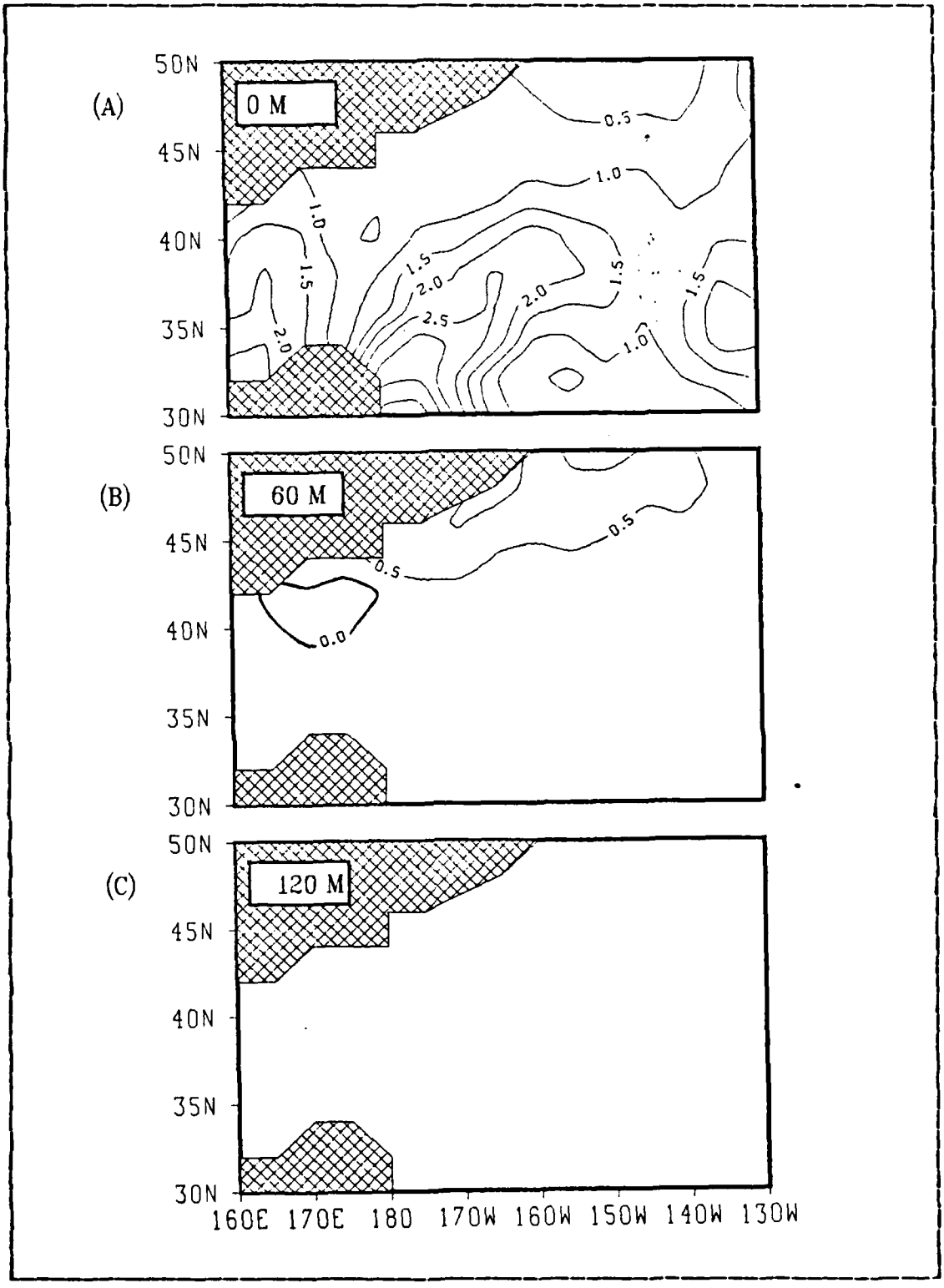

Figure 4.32 Similar to Figure 4.30 except for August to July.

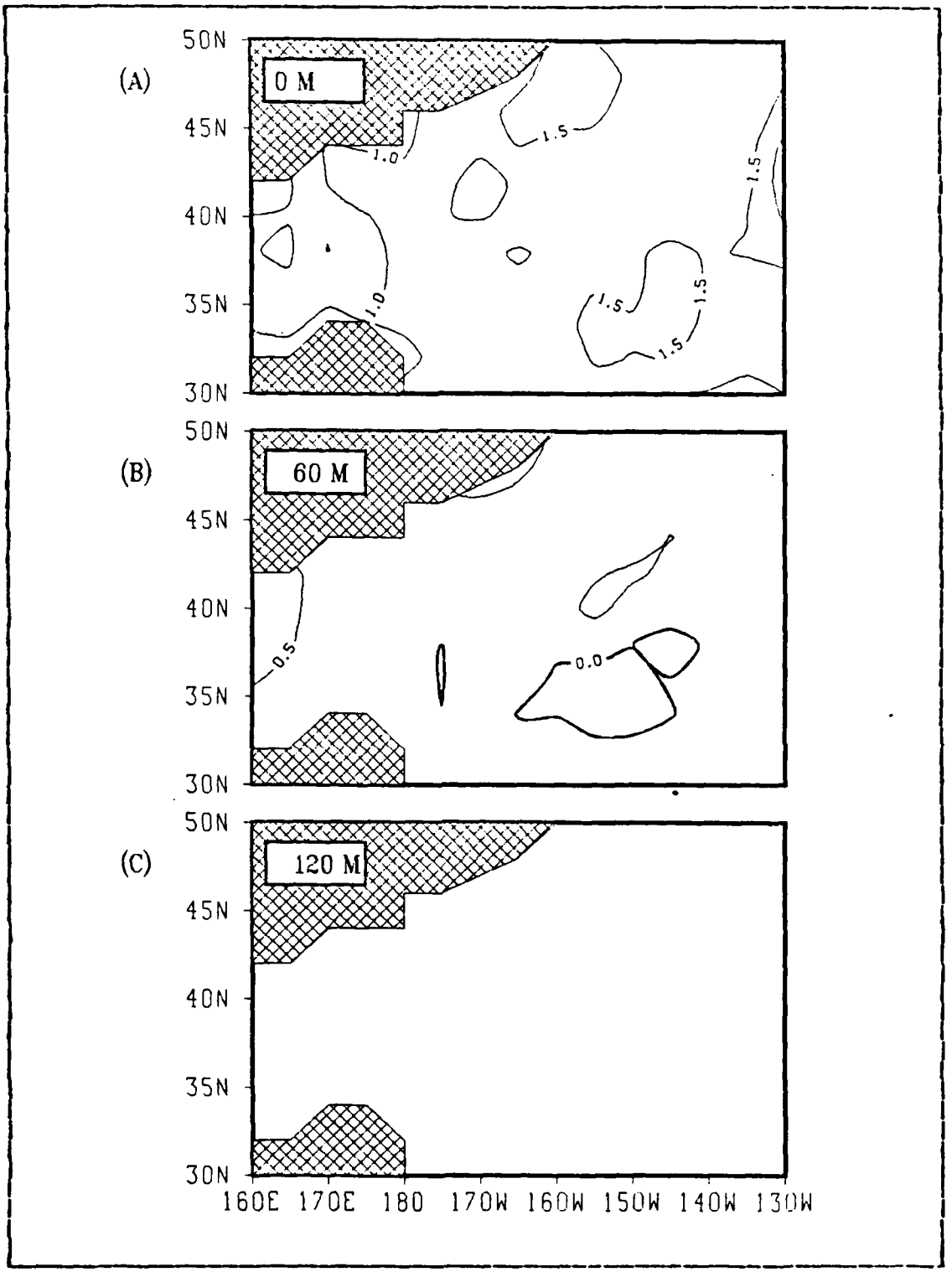

Figure 4.33 Similar to Figure 4.30 except with a climatological radiation field (Case II).

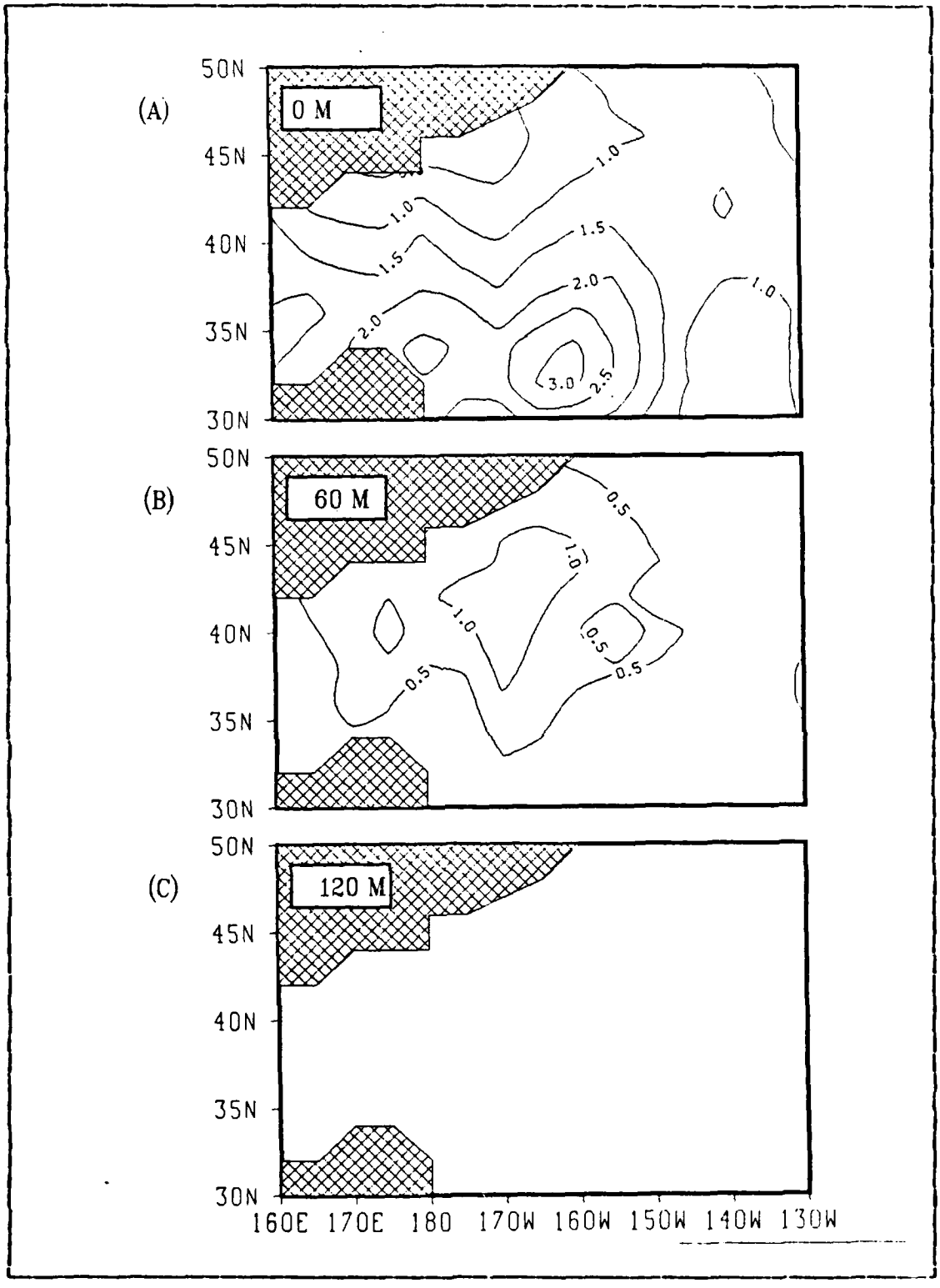

Figure 4.34 Similar to Figure 4.33 except for July to June.

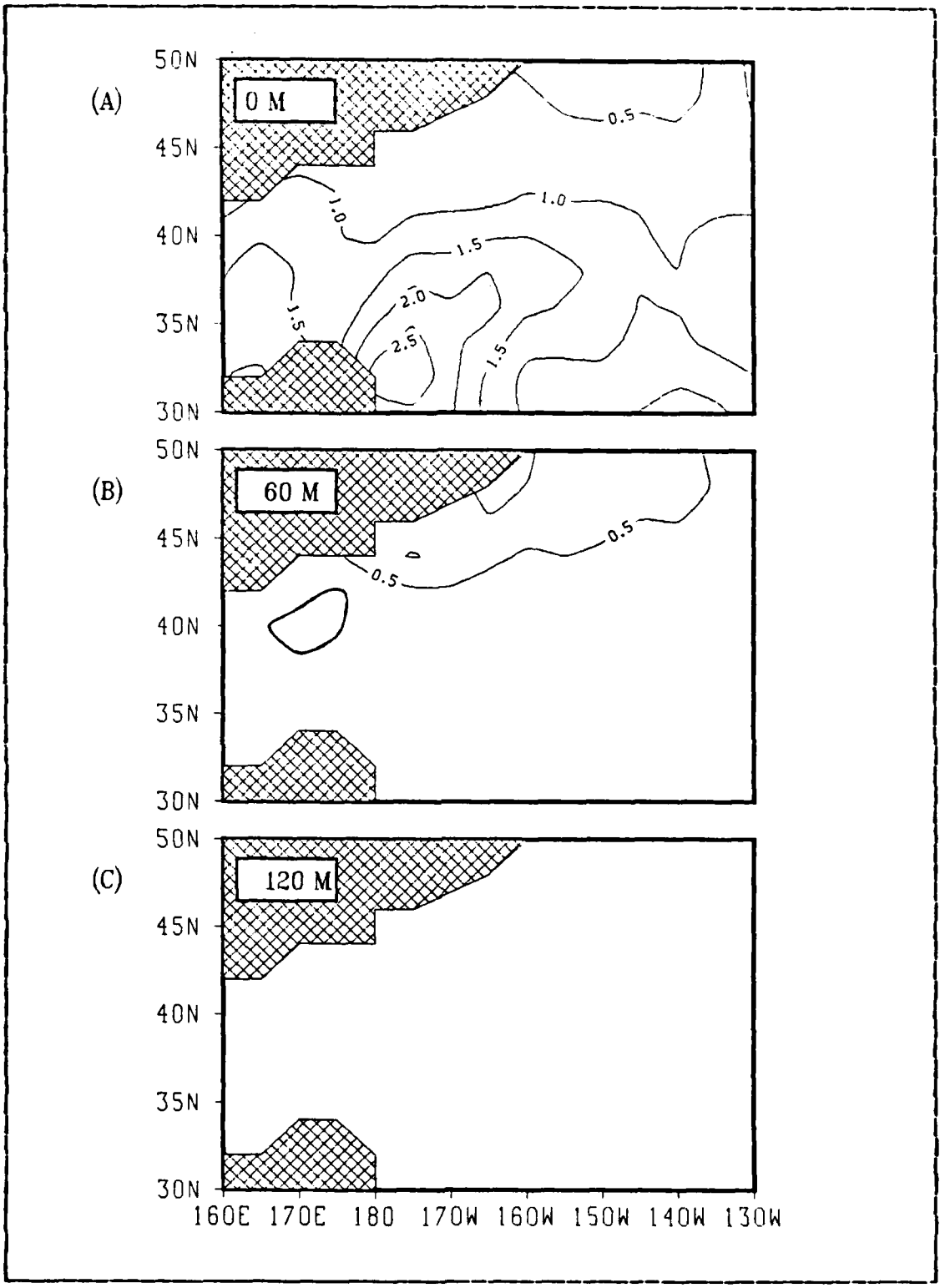

Figure 4.35 Similar to Figure 4.33 except for August to July.

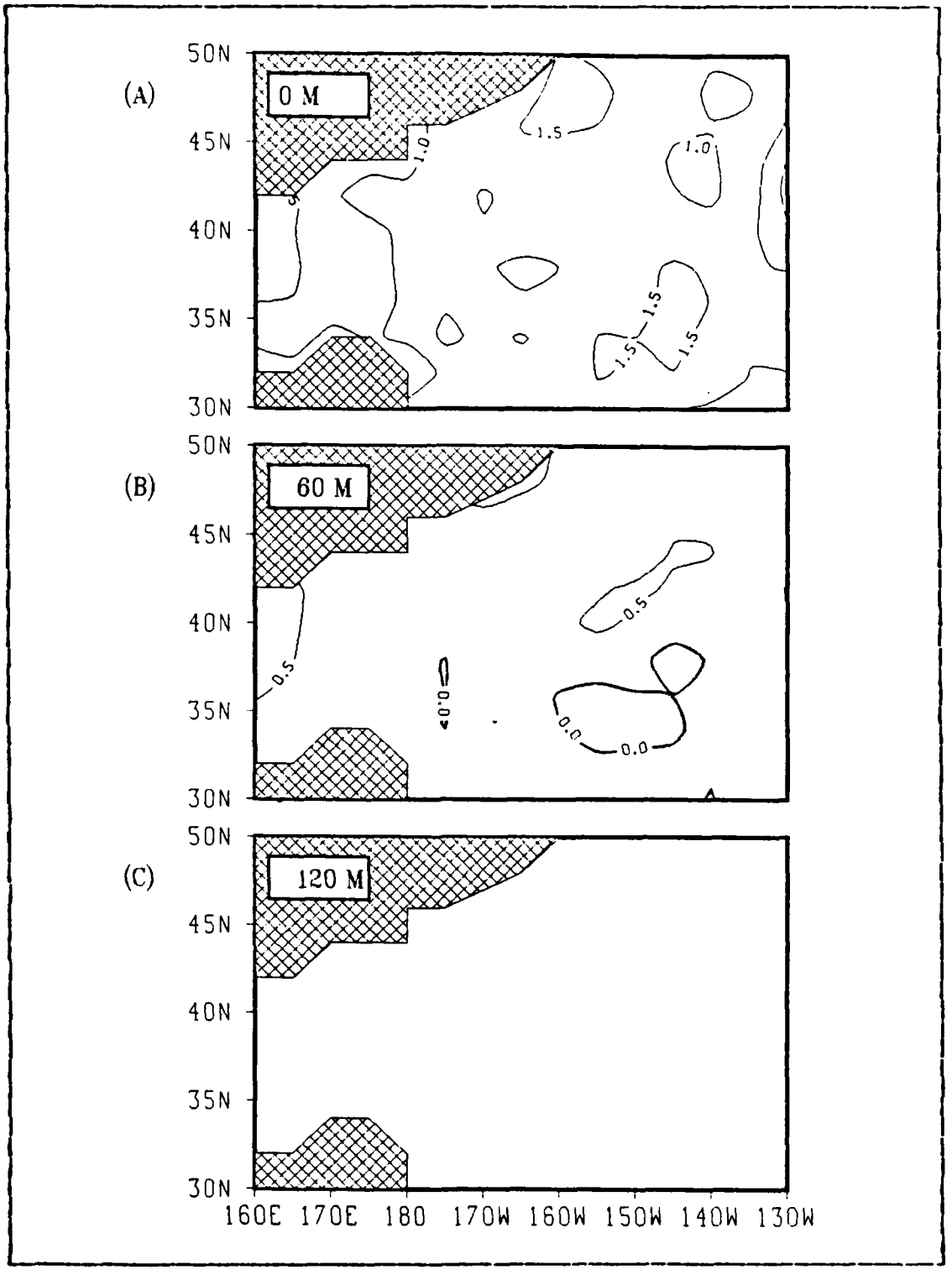

Figure 4.36 Similar to Figure 4.30 except with a diurnal radiation field(Case III).

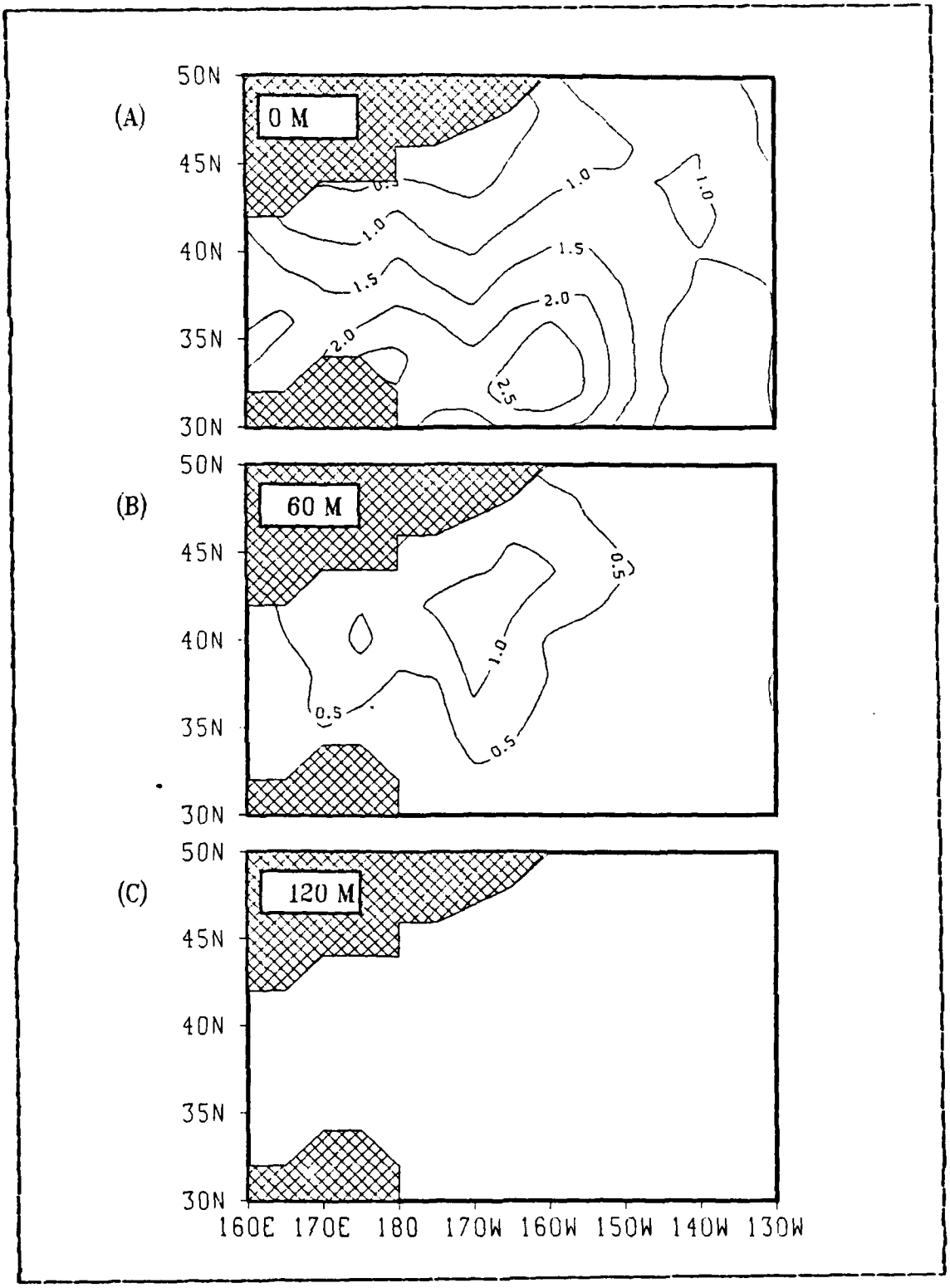

Figure 4.37 Similar to Figure 4.36 except for July to June.

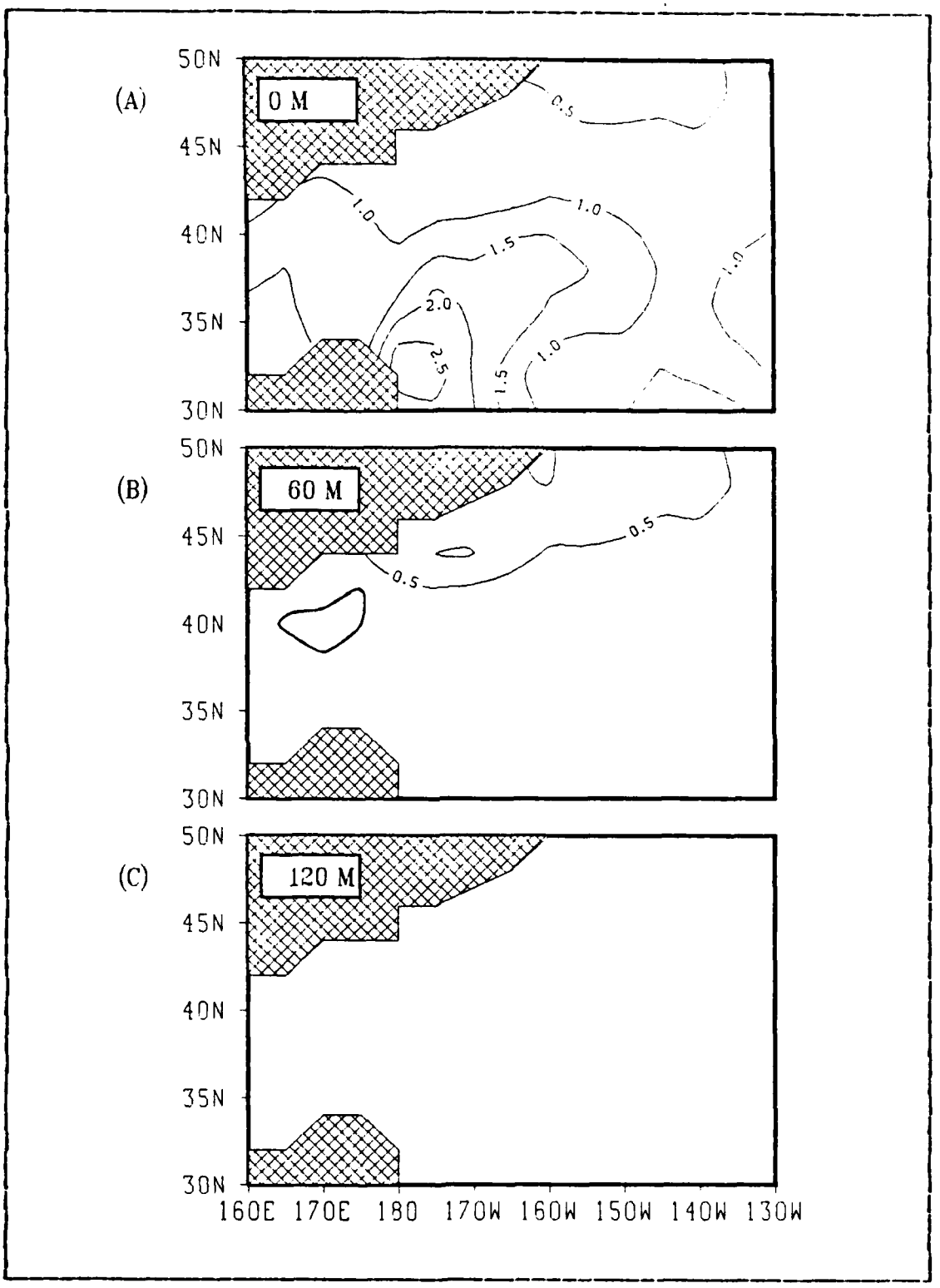

Figure 4.38 Similar to Figure 4.36 except for August to July.

V. SUMMARY AND CONCLUSIONS

None of the three warm anomaly (WA) periods chosen for this study were hindcast well by the Garwood one-dimensional model using heat fluxes derived from FNOC. Since all three hindcasts seemed to develop difficulties during the early summer, one case (WA 1/2) in 1976 was selected for further study.

A detailed examination of the FNOC surface heat flux fields used in previous studies of cold anomalies (Stringer, 1983) revealed that the early summer can not be corrected by a seasonally varying heat flux correction. Corrections to the average heat flux fields did not prove as successful for warm anomalies as for the earlier cold anomaly studies. A local heat budget correction field did not significantly improve hindcasts. Some improvement in specific problem areas was seen when selective corrections were done, but this procedure would be of little value in real-time predictions. For research purposes, however, selective correction is a useful method to diagnose potential model difficulties in the hindcast mode of operation.

Use of climatological heat flux fields in conjunction with FNOC winds produced a better result than did the use of FNOC's heat fluxes. FNOC heat fluxes and winds and the various forms used in this study produced general patterns which more closely resembled observations. Whenever temperature anomalies are primarily attributable to anomalous wind-mixing, the use of climatological heat fluxes with actual winds (synoptically varying) may provide reasonable hindcasts of thermal structure. However, this climatology, as used in this study, still does not account for the mixed layer dynamics attributable to synoptic variability in the

heat fluxes. Horizontal and vertical advection are also neglected, and may account for some of the differences between the observations and the model simulations. Also, the one month resolution afforded by the observations is not adequate to verify a model which is most sensitive to synoptic variability in the atmospheric forcing.

This study has shown that it is possible to hindcast warm temperature anomalies for the mid-latitudes. The importance of using a reasonably correct heat flux field was shown dramatically. This study indicates a need for much additional research to improve the surface heat fluxes. Only then will the model be able to predict (hindcast) specific features that are related to the surface thermodynamic boundary conditions. Future three-dimensional modelling will include the advective processes neglected here, but the largest difficulty and potential source of error still appears to be the specification of the surface heat flux.

LIST OF REFERENCES

Elsberry,R.L., 1984: A synoptic case study of the ocean temperature anomalies in the Central Pacific region during 1976-79. Naval Postgraduate School Tech. Rep. NPS 63-84-003, 75 pp.

Elsberry,R.L., P.C Gallacher, A.A. Bird, and R.W. Garwood, Jr., 1982: Deriving corrections to FNOC surface heat flux estimates for use in North Pacific ocean predictions. Naval Postgraduate School Tech. Rep. NPS 63-82-005, 67 pp.

Gallacher, P.C., 1979: Preparation of ocean model forcing parameters from FNWC atmospheric analysis and model predictions. Naval Postgraduate School Tech. Rep. NPS 63-79-005, 24 pp.

Garwood, R.W. Jr., 1977: An ocean mixed layer model capable of simulating cyclic states. J. Phys. Oceanogr., 7, 455-468.

Stringer, G.L., 1983: One-dimensional model hindcasts of cold anomalies in the North Pacific ocean. M.S. Thesis, Naval Postgraduate School, 136 pp.

White, W.B., and R.L. Bernstein, 1979: Design of an oceanographic network in the midlatitude North Pacific. J. Phys. Oceangr.,9 592-606.

Wyrtki, K., 1966: Seasonal variation of heat exchange and surface temperature in the North Pacific. Hawaii Inst. Geophys. Rep. HIG-66-3, 8 pp.

Wyrtki, K., and L. Uhrich, 1982: On the accuracy of heat storage computations. J. Phys. Oceanogr., 12, 1411-1416.

INITIAL DISTRIEUTION LIST

No.		Copies
1.	Defense Technical Information Center Cameron Station Alexandria, VA 22314	2
2.	Library, Code 0142 Naval Postgraduate School Monterey, CA 93943	2
3.	Professor Robert J. Renard, Code 63Rd Department of Meteorology Naval Postgraduate School Monterey, CA 93943	1
4.	Professor Christopher N. K. Mooers, Code 68Mr Department of Oceanography Naval Postgraduate School Monterey, CA 93943	1
5.	Professor Roland W. Garwood, Code 68Gd Department of Oceanography Naval Postgraduate School Monterey, CA 93943	1
6.	Professor Russell L. Elsberry, Code 63 Es Department of Meteorology Naval Postgraduate School Monterey, CA 93943	1
7.	Mr. Patrick C. Gallacher, Code 63 Department of Meteorology Naval Postgraduate School Monterey, CA 93943	1
8.	ICDR Bernardino J. Jaramillo Naval Oceanography Command Center Box 31, Rota, Spain FPO New York 09540	2
9.	Directory Naval Oceanography Division Naval Observatory 34th and Massachusetts Avenue NW Washington, D.C. 20390	1
10.	Commander Naval Oceanography Command NSTL Station Bay St. Louis, MS 39522	1
11.	Commanding Officer Naval Oceanographic Office NSTL Station Bay ST. Louis, MS 39522	1
12.	Commanding Officer Fleet Numerical Oceanography Center Monterey, CA 93943	1

13. Commanding Officer 1
Naval Ocean Research and Development Activity
NSTL Station
Bay ST. Louis, MS 39522

14. Commanding Officer 1
Naval Environmental Prediction Research Facility
Monterey, CA 93943

15. Chairman, Oceanography Department 1
U.S. Naval Academy
Annapolis, MD 21402

16. Chief of Naval Research 1
800 N. Quincy Street
Arlington, VA 22217

17. Office of Naval Research (Code 420) 1
Naval Ocean Research and Development Activity
800 N. Quincy Street
Arlington, VA 22217

18. Scientific Liaison Office 1
Office of Naval Research
Scripps Institution of Oceanography
La Jolla, CA 92037

19. Library 1
Scripps Institution of Oceanography
P.O. Box 2367
La Jolla, CA 92037

20. Library 1
Department of Oceanography
University of Washington
Seattle, WA 98105

21. Library 1
School of Oceanography
Oregon State University
Corvallis, OR 97331

22. Commander 1
Oceanographic Systems Pacific
Box 1390
Pearl Harbor, HI 96860

END

FILMED

7-85

DTIC